Price: 10 EUR

HUNGARIAN GROUP OF *fib*

CONCRETE STRUCTURES

ANNUAL TECHNICAL JOURNAL

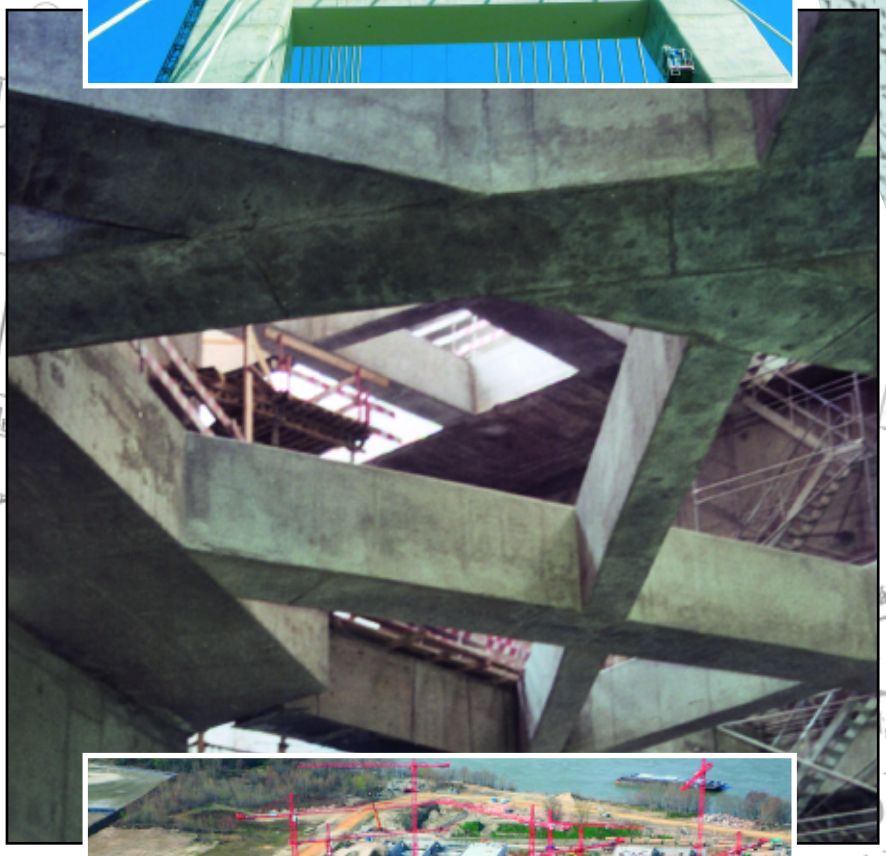

2010

Vol. 11

CONCRETE STRUCTURES
Journal of the Hungarian Group of *fib*

Editor-in-chief:
Prof. György L. Balázs

Editors:
Prof. Géza Tassi
Dr. Herbert Träger

Founded by: Hungarian Group of *fib*
Publisher: Hungarian Group of *fib*
(*fib* = International Federation for Structural Concrete)

Editorial office:
Budapest University of Technology and Economics (BME)
Department of Construction Materials and Engineering Geology
Műegyetem rkp. 3., H-1111 Budapest
Phone: +36-1-463 4068
Fax: +36-1-463 3450
WEB http://www.fib.bme.hu
Editing of online version:
László Bene

Price: 10 EUR
Printed in 1000 copies

ISSN 1419-6441
online ISSN: 1586-0361

Cover photos:
Selected structures from Hungary

CONTENT

Sponsors:
Railway Bridges Foundation, ÉMI Nonprofit Ltd., HÍDÉPÍTŐ Co., Holcim Hungary Co., MÁV Co., MSC Consulting Co., Lábatlani Vasbetonipari Co., Pont-*TERV* Co., UVATERV Co., MÉLYÉPTERV KOMPLEX Engineering Co., SW Umwelttechnik Hungary Ltd., Betonmix Consulting Ltd., BVM Épelem Ltd., CAEC Ltd., Pannon Freyssinet Ltd., STABIL PLAN Ltd., UNION PLAN Ltd., DCB Consulting Ltd., BME Dept. of Structural Engineering, BME Dept. of Construction Materials and Engineering Geology

THE CABLE-STAYED MEGYER BRIDGE ON THE DANUBE AT BUDAPEST – SUBSTRUCTURES AND PYLONS

Sándor Kisbán

The three span fan-shaped cable-stayed bridge has a symmetric arrangement with a 300 m long middle span and 145 m long side spans. The deck is suspended by two inclined cable planes, each having 44 stay cables, onto two typical, "A"-shaped pylons. The paper summarizes the main characteristics of the substructures and the pylons of the bridge. The arrangement of the 100 m high pylons, the specialities of pylon erection, the auxiliary constructional elements and the solution for tying the applied tower crane to the pylon leg will be introduced. The applied geodetic system implemented to control the full pylon erection process and accounting for the consequences of the inclined pylon legs with box-shaped cross section will be thoroughly detailed. The arrangement of deck supports made of special hydraulic devices will also be discussed. The paper ends with the description of the architectural features and the applied glass cover of the pylon heads.

Keywords: cable-stayed bridge, river bed substructure, concrete frame pylon, climbing formwork technology

1. INTRODUCTION

The 1862 m long Northern Danube Bridge on the M0 motorway as the longest river bridge in Hungary is situated at the northern border of Budapest, bridging both Danube branches and the southern part of the Szentendre Island, and consists of five statically independent, consecutive bridge structures. The history of design and the general description of the bridge as well as the structures included in the authorization plan is introduced in ref. Hunyadi, 2008.

In the main Danube branch on the Vác side, a three span cable-stayed bridge has been built. River bridge with a cable-stayed main structural system has not built in Hungary so far. The bridge includes two concrete pylons, onto which the steel deck is suspended by two inclined, fan-shaped cable planes at every 12 m (*Fig. 1*). The spans are 145+300+145 m that results in a total length of 590 m. The adjacent structures both on the Pest side (left bank flood-bridge) of the main Danube branch and above the Szentendre Island as well as on the Buda side (right bank flood-bridge) of the Szentendre Danube branch are continuous, post-tensioned concrete bridges with box-girder superstructures. The adjacent flood-bridges are discussed in ref. Pusztai and Skultéty, 2008.

The M0 motorway running through this bridge includes 2×2 traffic lanes with hard shoulders. The hard shoulders are wider than specified giving the possibility to extend the carriageway width up to 2×3 traffic lanes without any structural modification if the future traffic expansion will make it necessary. On the

Fig. 1: The completed cable-stayed bridge

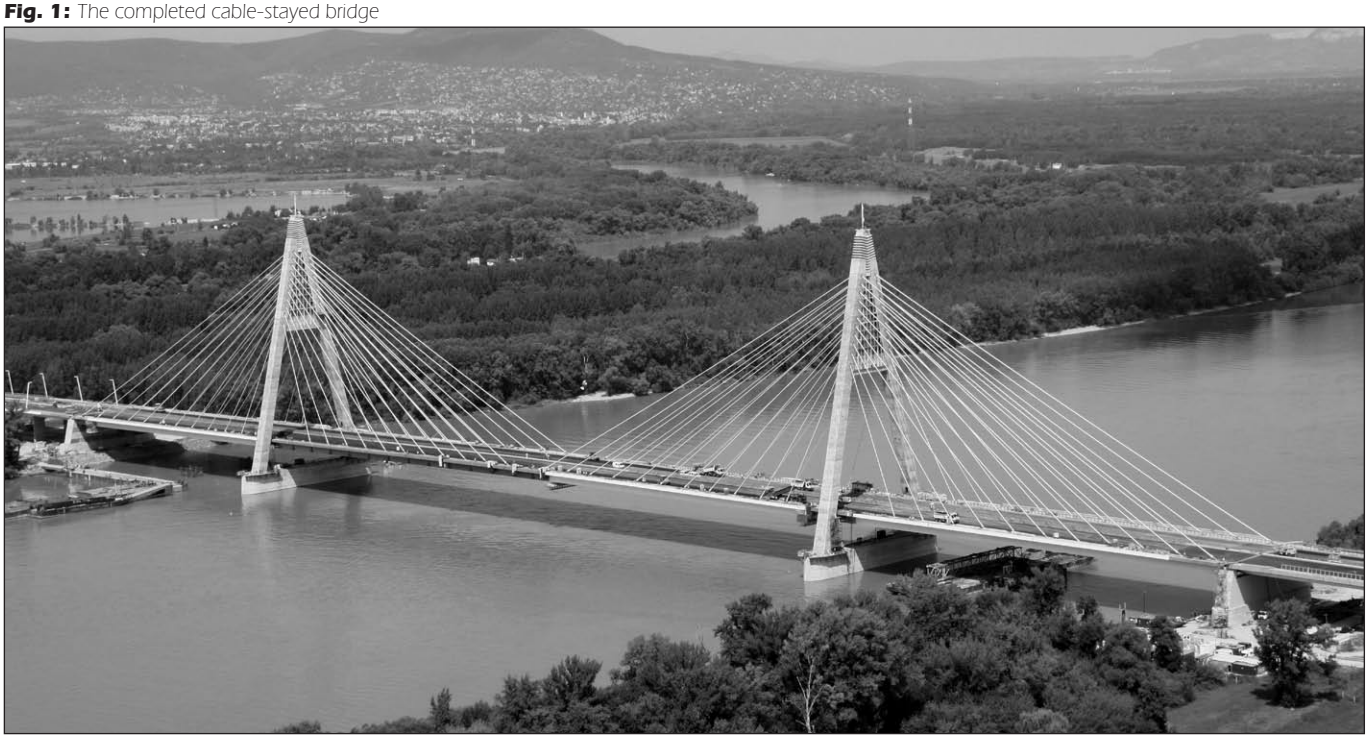

northern side of the bridge a cycle track, which is able also for disabled traffic, on the southern side a footway is arranged. An asphalt-based surface pavement is laid on the carriageway while the footway and the cycle track are covered by a multilayer, abrasion-resistant, roughened, chloride resisting system. The bridge is equipped by public lighting as well as by ship- and air-traffic navigational signals.

2. FOUNDATION

For the internal bed piers, hydrodynamic flow tests and scouring analyses have been carried out. These simulation tests did not show significant modification in the river flow due to the hydraulically designed piers so their favourable shape could be justified. The bed piers do not adversely affect the safety of the river navigation as well as the stability of the bed and the bank of the river.

The foundation of both the bed and the side piers has been made of large diameter, reinforced concrete bored piles. The piles of all the four piers are bored into the excellent load bearing capacity subsoil, the Oligocene aged, grey marl containing lean and fair clay. The strength class of concrete was C20/25 for the piles and their pile caps, C30/37 for the solid pier shafts and C35/45 for the load-distributing structural crossbeams at the top of the piers.

2.1 Side joint piers

The side joint piers, which also support the adjacent bridges, are supported by 16-16 piles. The diameter of the 19.0 m long piles is 1.5 m. The horizontal sizes of the reinforced concrete pile caps are 7.5 m in the longitudinal direction of the bridge and 49.4 m perpendicular to this direction while their depth is 2.0 m.

The side face of the pier shafts along the full perimeter has an inclination of 1:20 to the vertical plane. The cross section of the pier shafts has been designed with ogival ends protected by granite nose blocks. The lower 5.5 m high parts of the pier shafts have a thickness of 6.76-6.21 m and a width of 48.36-47.40 m. The upper 7.0 m high parts have a constant thickness of 4.60 m with a variable width between 40.20 m and 36.90 m.

The vertical support and the anchorage of the superstructure are realized at the top of the pier shafts, on the load-distributing structural crossbeams. The vertical downward reaction forces are received by two reinforced concrete bearing pads arranged with 28.83 m centre distance on each pier while the anchorage of the superstructure is ensured by other two anchorage points installed with 24.03 m centre distance between the supporting points. The lateral supports of the superstructure are positioned to the longitudinal axis of the bridge.

2.2 Bed piers

The substructures of the bed piers have been built by the reinforced concrete crib-wall technique, which was successfully applied for river bridge foundations many times in the past. Due to the big geometrical sizes of the substructures 3-3 crib-wall elements were placed and fixed onto each other to enclose the necessary working space.

The crib-wall elements together with their inside strutting system were filled with concrete using the outer wall as a formwork. Onto the top of the upper crib-walls, 5.0 m high, removable steel cut off walls were fixed whose top level

Fig. 2: Positioning of the crib-wall elements

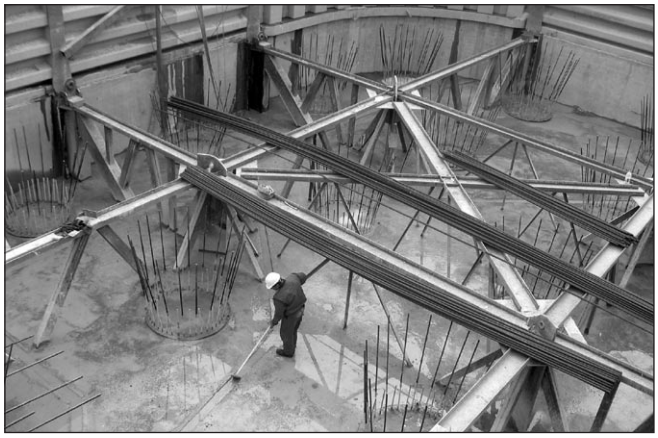

Fig. 3: Pile cap reinforcement above the lower shaft part cast under water

reached the 101.5 m above the Baltic sea level, by which, taking into account 0.5 m high waves, the dry working space could be ensured for water levels up to 101.0 m above the sea level.

The bed piers are supported by 46-46 reinforced concrete bored piles. The diameter of the 19.5-20.5 m long piles is 1.5 m. The horizontal sizes of the reinforced concrete pile caps are 16.5 m in the longitudinal direction of the bridge and 70.0 m perpendicular to this direction while their depth is 4.5 m including the lower shaft part cast under water. The top level of pile caps coincides with that of the upper crib-wall elements at 96.5 m above the see level (*Fig. 2*).

The side face of the pier shafts along the full perimeter has an inclination of 1:20 to the vertical plane (*Fig. 3*). The cross section of the pier shafts has been designed similarly to the side piers, applying ogival ends protected by granite nose blocks against abrasion effects due to floating debris and ice drift. The thickness and the width of the pier shafts vary between 8.0-7.0 m and 64.90-63.16 m, respectively, while their height is equal to 10.2 m. The pylon legs are fixed into the upper pier shaft parts designed and arranged as load distributing cross beams. The top surface of these cross beams has been designed with symmetric, 5% transversal slope for water draining reasons.

3. PYLON

The pylon structure of the Rheinbrücke Düsseldorf-Flehe cable-stayed river bridge (*Schambeck et al., 1979*) in Germany has been built with inclined pylon legs. The experiences gained from its construction were helpful during the execution of the Megyer Bridge.

The two pylons of the Megyer Bridge are "A"-shaped frame structures consisting of partially prestressed, reinforced concrete pylon legs having rectangular, box-shaped cross sections. Their height is 100 m above the substructures while the outer horizontal distance between the pylon legs at the bottom is 51.0 m. The outer cross sectional sizes of the pylon legs parabolically decrease from 5.0×4.0 m to 3.5×4.0 m parallel to the wall thickness decrease from 1.0 m to 0.5 m. The corner edges of the pylon legs are circularly curved along a 300 mm radius in order to reduce the wind turbulence effects. The applied concrete strength class was C40/50.

The bending moments arising in the plane of the pylon frame due to the self-weight of the whole bridge and the internal stay cable force system are eliminated by bonded internal prestressing. For this purpose, prestressing tendon bars having a diameter of 40 mm and a characteristic tensile strength of 1030 N/mm^2 run in the outer walls of the pylon legs (*Figs. 4 and 5*).

A reinforced concrete, box-shaped beam ties the pylon legs at 55.0 m above the substructure for each pylon. The steel units as the upper anchorages for the stay cables are arranged in pylon leg sections above these tie beams.

These anchorage units were positioned and fixed simultaneously with the concreting of the anchorage chamber floors. The vertical components of the anchorage forces are transmitted directly to the 0.6 m thick walls of the pylon legs while the horizontal components in the longitudinal direction coming from the two sides are mostly balanced in these steel anchorage units. The anchorage units contain steel shear bolts

Fig. 4: Anchorage of Ø 40 prestressing bars in the substructures

Fig. 5: Anchorage of Ø 40 prestressing bars in a construction joint

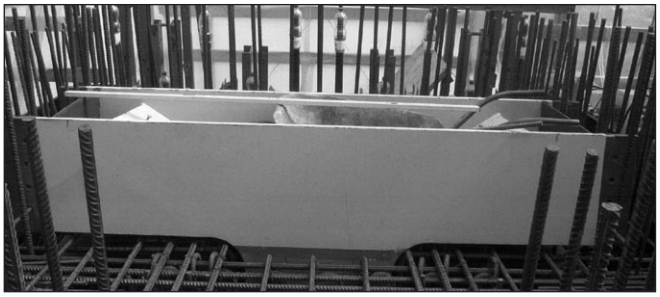

Fig. 6: Steel anchorage device for stay cables

at their bottom face that are fully embedded in the concrete chamber floors and intended to transmit the unbalanced horizontal components of cable forces during the construction stages and the cable replacement phases in the final stage of the bridge (*Fig. 6*).

The steel deck is supported between the pylon legs. The supporting structural elements are the 1.35 m high reinforced concrete corbels projecting out from the pylon legs at 9.0 m above the substructure, to which the reaction forces of the steel deck are transmitted by steel cantilevers as part of the deck itself.

The horizontal supports of the deck are arranged also on these corbels using hydraulic devices.

4. DETAILS OF THE PYLON CONSTRUCTION

The pylon legs have been erected by the climbing formwork technique generally using 4.07 m high units. At the connecting structural elements (supporting corbels, tie beam, stay cable anchorages, pylon head, etc.) additional construction joints had to be applied.

In order to decrease the bending moments in the plane of the pylons due to the long and inclined pylon leg cantilevers during construction, steel auxiliary beams as temporary struts were installed at 32.0 m and 52.0 m above the substructure. The upper auxiliary beams also supported the formwork of the tie beam. By the proper use of these auxiliary beams the internal forces under construction could be limited in such a way that they always remained below the corresponding values in the final stage of the pylon.

Two tower cranes were used for the pylon construction. One of them was installed and fixed into the northern end of the substructure as a 68 m high cantilever and then removed after the completion of the reinforced concrete tie beam. The other one was similarly installed at the southern end of the substructure and tied to the existing pylon leg at 38 m, 58 m and 80 m levels above its fixing. Its height simultaneously increased with the pylon up to 116 m (*Fig. 7*). Only two ties were active in the same time that allowed the optimization of crane forces on the pylon leg in such way that made necessary no additional, temporary strengthening of the pylon leg to carry these additional crane forces.

The site assembly of the deck according to the free cantilever method started before the completion of the pylons. For that reason the casting of the concrete floor that rigidly ties the pylon legs at 87 m above the substructure was controlled by exceptional measures (*Fig. 8*). The already anchored stay cable forces and the dynamic crane forces on the southern pylon leg might cause relative displacement between the still cantilevered pylon legs resulting in significant shear forces in the tying floor. Therefore the concreting of this had taken place as the last work phase in the afternoon then the southern crane was halted for

Fig. 7: *Pylon legs under construction*

the full subsequent day in order to avoid harmful movements of the fresh concrete. The hardening of concrete was influenced by accelerating admixtures and external heating. The construction process was resumed 36 hours after concreting.

In accordance with the sequence of the deck assembly, the floors, the vertical elevator shafts and the glass wall covers of the upper triangular parts of the pylons were built after the vertical and transversal fixing of the deck to its temporary supports in the side spans. This was necessary in order to reduce the wind effects on the pylon during these construction phases.

5. GEODETIC SYSTEM CONTROLLING THE PYLON CONSTRUCTION

The formwork of each construction unit along the pylon legs was very carefully adjusted. Geometrical deviances regarding the outer surface of the pylon leg, the diagonals and the side lengths of the cross section and the rotation of the pylon leg around its longitudinal axis were previously determined.

The geometrical reference points necessary for adjustment and control purposes were determined in a local coordinate system for each pylon. The sequence of the geometrical setting was parallel to the belonging construction process. First the inner formwork panels had been placed. After positioning the prestressing bars, the reinforcement and the occasional structural steel accessories the assembly of the outer formwork panels followed. The measurement point used for the adjustment and the control of the geometry were set at the top edge of the formwork panels.

The basic value of measurement points corresponded to the final state geometry of the structure. This basic value has been modified by a correction factor for each construction stage. These correction factors included the long term effects (creep, shrinkage), the current "camber" values for each unit as a consequence of the applied construction stages as well as the temperature effects, the elastic deformations due to construction loads and the possible additional correction values.

These "corrected" measurement points has been determined step by step for each unit with the full knowledge of the previous construction process and the current influencing factors. The temperature correction factor related to the temperature in time of the current construction stage was also determined, by which the effect of uniform temperature change was fully considered. These correction factors were transformed into a table of "vertical geometrical corrections" with a range between +/- 60 mm what contained modified top level of each formwork unit compared to the design level. This was the basis of the geodetic measurements during the full pylon construction process.

The geodetic measurements were conducted in the early mornings. Thus the effects of structural deformations due to the uneven temperature change on the structure could be considerably reduced.

6. SPECIAL DEVICES IN THE SUBSTRUCTURES

The deck is supported longitudinally at the pylons and transversally at both the side joint piers and the pylons.

Hydraulic devices placed on the pylon corbels are used to horizontally support the deck. These devices behave as rigid supports against short-term effects such as braking and traction forces, wind and earthquake effects but mobilize negligible horizontal reaction forces against long-term effects such as thermal, creep and shrinkage effects and settlements. The hydraulic devices are able to transmit both tensile and compression forces.

The capacity of these hydraulic supports is 2400 kN (*Fig. 9*). For reaction forces exceeding this value (for earthquakes higher than grade 5,5 according to the Richter scale) the hydraulic supports are released and the cable supported deck becomes a sway structure in the longitudinal direction. At that moment the structural system changes and the related internal forces significantly decrease. Parallel to this a longitudinal swing occurs but its maximum amplitude does not exceed 300 mm. This longitudinal movement is covered by the allowable movement range of the built-in expansion joints.

Fig. 8: *Tying of a tower crane to the pylon leg*

Fig. 9: *Longitudinally positioned horizontal hydraulic support*

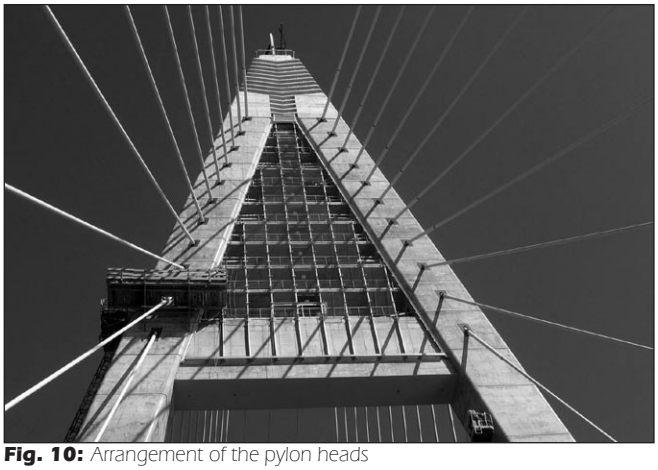

Fig. 10: *Arrangement of the pylon heads*

Fig. 11: *Point fixing of a glass-wall panel*

The transversal support for the deck is ensured by special wind supports placed at the longitudinal axis of the deck on the side joint piers. These devices are filled with high pressure gas and are able to carry compression forces only. They provide direct reaction force transmission between the structural cross beam of the deck and the pylon leg above the corbels. The wind supports behave as rigid supports against short-term effects such as wind, and earthquake effects but mobilize negligible horizontal reaction forces against long-term effects such as thermal, creep and shrinkage effects and settlements.

The vertical reaction forces of the deck transmitted by the bearings are not significant because the vertical support of the deck is mostly ensured by the stay cables. The vertical supports on both the side joint piers and the pylon corbels are made of widely used pot bearings. The vertical uplift of the cable-stayed deck ends at the side joint piers is prevented by special pendulum structures made of 19 strand prestressing cables.

7. ARCHITECTURAL AND MAINTENANCE ASPECTS FOR THE PYLONS

Due to their sizes and appearance the “A”-shaped pylons are the main structural elements of the cable-stayed bridge. The upper triangular space bordered by the pylon legs and the tie beam is covered by glass walls assembled to steel wall columns (*Figs. 10 and 11*).

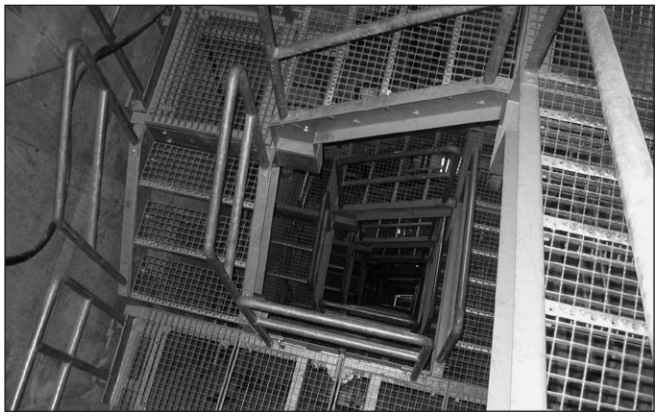

Fig. 12: Inside stairs in the pylon leg

The application of glass walls for bridges for aesthetical reasons is a new trend. Depending on the time in a day and the view-point of the spectator the appearance of a glass wall is continuously changing. The sunbursts pass through the wall and appear as shining thin membranes between the pylon legs, the framing reinforced concrete pylon legs are reflected on the glass surface. The wall panels are made of two 10 mm thick, semi-tempered, heat- and light-reflecting glass layers glued together without any framing. The stress-free glass panels are point-fixed by hinge-joints, which are widely used for high-rise buildings. The assembly and the cleaning of the glass-wall are carried out by alpinist techniques.

The lamellar form of the pylon heads is emphasized by its shade effects in daytime and by the artificial, strip-like lighting at nights.

The interior of the pylon legs has been arranged according to the requests of the investor.

The northern legs contain inner stairs from the bottom up to the lowest stay cable anchorage level while the southern legs are equipped by inner industrial lifts (*Fig. 12*). Vertical panorama lifts starting from the tie beams ensure the accessibility of all structural elements up to the pylon heads. The pylon leg sections, which are equipped by lifts, may alternatively be accessed by inner ladders.

8. GENERAL DATA FOR THE PYLONS

Materials used for the construction of one pylon:

Concrete:	C40/50	1700 m^3
Reinforcing steel	B500B	370 t
Prestressing bar	grade 1030	19 t
Anchorage device for stay cables		80 t

9. CONSTRUCTION AND CONCLUSIONS

The realization of the project has been carried out by The M0 Consortium for The Northern Danube Bridge established by the Hídépítő Co. and the Strabag Co.. The general designer has been the Céh Co.; the construction design has been carried out by the Unitef-Céh Engineering UP. as a contractor of the Consortium (*Fig. 13*).

The execution of the substructures and the whole piers has been made by the Hídépítő Co. The climbing formworks of the pylons and the associated technological work have been carried out by the Peri Ltd. The construction period of one bed pier was six months and that for the associated pylon lasted 11 months. The total height of the pylons, measured from the bottom end of piles up to the top of the pylon heads, is 132 m, out of which the height of the "A"-shaped part is 100 m.

The pylons are the main structural elements and the most exciting spectacle of the cable-stayed bridge across the wide Danube branch. Due to its harmonic aesthetical appearance, the whole bridge appropriately fits into the variety of bridges of Budapest improving the aesthetical value and increasing the number of the symbols and spectacles of the capital.

10. REFERENCES

Hunyadi, M. (2008): "The Northern Danube Bridge on the M0 ring. Preliminary design, authorization plan, tendering", *VASBETONÉPÍTÉS*, 2008/3, pp. 70-72. (in Hungarian)

Kisbán, S. (2008): „The M0 Northern Danube Bridge. Cable-stayed Bridge in Budapest", *Magyar Tudomány* 2008/4. (in Hungarian)

Pusztai, P,. Skultéty, A. (2008): "The Northern Danube Bridge on the M0 ring, Prestressed concrete flood area bridges", *VASBETONÉPÍTÉS*, 2009/1, pp. 11-14 (in Hungarian)

Schambeck, H., Foerst, H., Honnefelder, N. (1979): „Rheinbrücke Düsseldorf-Flehe/Neuss-Nedesheim. Der Betonpylon", *Bauingenieur* 54, pp. 111-117.

Dr. Sándor Kisbán (1949) civil engineer (BME, 1973) leading engineer at the Céh Co., managing director of the Céh-Híd Ltd. His bridge designer carrier started at the Uvaterv in 1975 where he was involved in designing long-span steel bridges (Northern Tisza Bridge at Szeged, highway bridge at Tiszapalkonya, cable-stayed bridge over the Danube in Novi Sad). He received his Dr.techn degree in the field of cable-stayed bridges in 1986 (Department of Steel Structures, BME). From 2002 he has been carrying his activity as a leading bridge designer in the Céh Co. where he has completed and managed the design of many domestic river and motorway bridges (M0, M31, M6 motorway bridges and viaducts, M0 Northern Danube Bridge). Member of the Hungarian group of ***fib***.

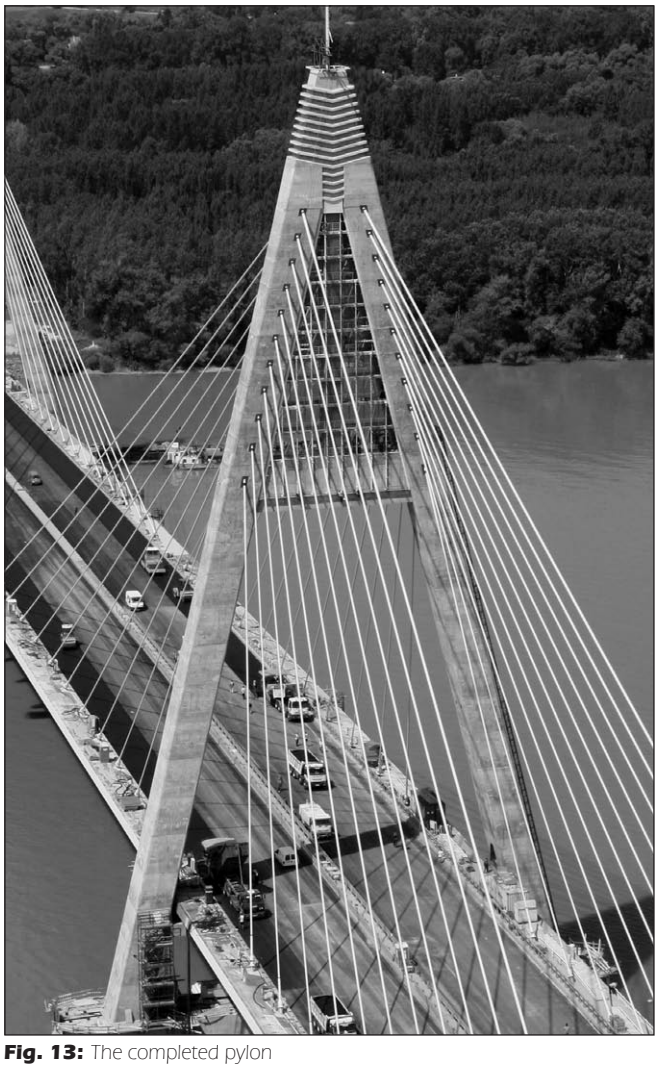

Fig. 13: The completed pylon

NEW METRO LINE IN BUDAPEST – OVERVIEW, CHALLENGES, CONSERVATION OF URBAN HERITAGE



István Bódi – Kálmán Koris – András Molnár

Budapest has a long tradition in building underground lines: the Millennium Underground Railway is the second-oldest underground line in the world. The construction works of the fourth metro line in Budapest started in 2004. This paper gives basic facts about the new metro line, and reports on the damage prediction project concerning urban buildings which was done at the Budapest University of Technology and Economics, Department of Structural Engineering.

Keywords: Metro 4, diaphragm wall, settlement, damage prediction, urban heritage

1. INTRODUCTION

On the 2nd May 1896, after two years of construction the worldwide second underground railway was inaugurated in Budapest. It is still in operation under one of the most elegant roads of Budapest, the Andrássy út, and in 2002 it has been listed as a UNESCO World Heritage Site. The second metro line crosses the city in east-west direction since 1972, and the third line in north-south direction on the Pest side since 1976.

The conception of the 4th metro line goes back in the early 1970s, and the Kálvin tér station of the 3rd metro line was already built with a connection tunnel towards the 4th line. After many years of preparation, the location of the stations and the track was finalized in 1996. After several years of delay, the construction works started in 2004 (Schulek, 2008), and the first section with 10 stations is expected to be opened in 2013.

The new metro line will connect the Kelenföldi and Eastern railway stations, and a later extension is planned to Bosnyák tér (*Fig. 1*). The tunnelling has to be made in an urban area, thus a careful analysis, and in some cases strengthening of the affected buildings and monuments was needed (Lichter, 2009).

The station and reversing facility at Eastern railway station are mainly constructed from the surface by cut-and-cover method using diaphragm walls. The station and the reversing facility are located very close to 2-6 storey high, 100 year old brick buildings and to the central building of the railway station itself. Our tasks were on one hand to determine the expected ground motions due to underground constructions and on the other hand to predict the expected damages of the buildings caused by ground settlements, as well as to determine the appropriate warning levels for the monitoring system to be able to provide immediate feedback in case of unwanted settlements. Based on the results of comprehensive analysis, the appropriate warning levels were specified for each building separately and the method for strengthening and renovation was also proposed in necessary cases.

2. BASIC FACTS ABOUT METRO 4

The Metro 4 in Budapest is constructed to provide an attractive and safe transport means for the travelling public with a transport capacity of 20100 persons/hour/direction in the peak hours. The 7.4 km long section spreading between Kelenföldi and Eastern (Keleti) railway stations (*Fig. 1*) will be a deep section. The deep alignment of the track is justified by several factors, such as crossing under the river Danube, high building density in urban areas, crossing the railway station at Kelenföld, as well as the ability of direct connections to existing metro lines. Two independent tunnels with circular cross-section are constructed for both directions. 10 stations will be constructed along the line of Metro 4, mostly by diaphragm wall technology and box station design (*Fig. 2*). Underground tunnel sections are constructed using boring shields. Tunnel walls were constructed of cast iron or reinforced concrete segments. Vertical alignment of the tunnels consists of various gradients, the highest gradient is 36.3‰. The deepest point of the line is next to the Danube at Szent Gellért tér running in a depth of 31 m under the surface. The terminal point of Metro 4 at Eastern railway station is a significant traffic junction of Budapest. The 83 m

Fig. 1: Trace of the new Metro 4 line

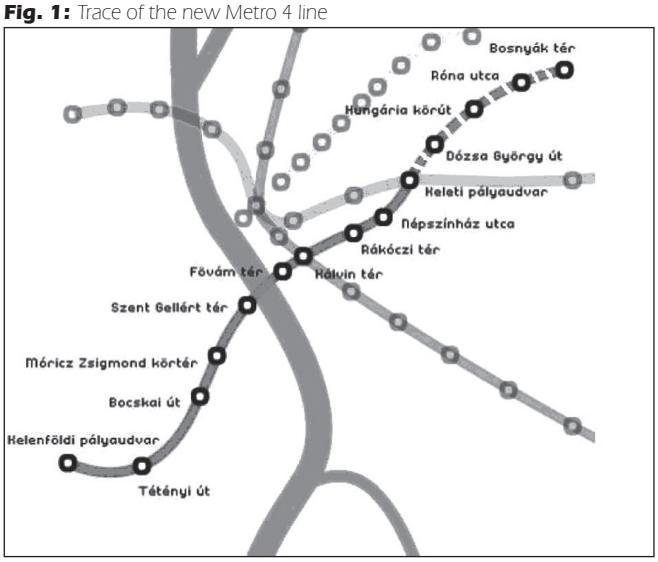

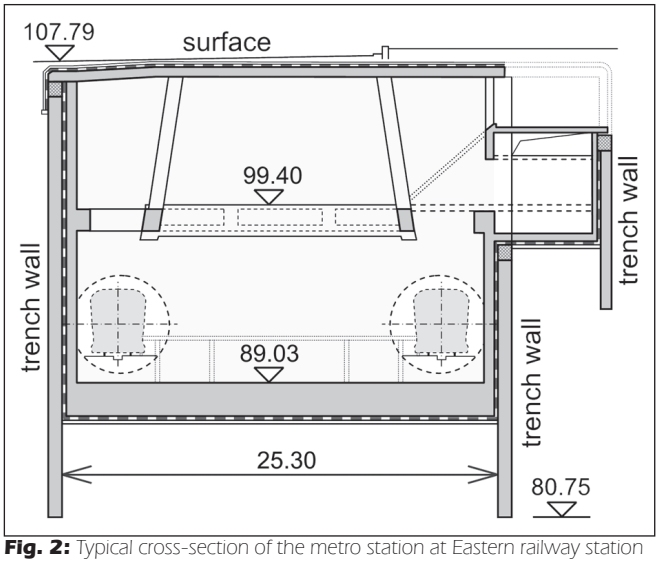

Fig. 2: Typical cross-section of the metro station at Eastern railway station

long middle-platform station and the reversing facility will be located 18 m deep mainly under Thököly road, providing direct connection to the existing Metro 2 line. Underground facilities are constructed by mixed method including cut-and-cover method and also mining method for parts lying under the building of Eastern railway station.

The new metro line has an overall architectural conception, which was selected on an open competition. The winner tender operates with uniform materials (architectural concrete, granite flooring), uniform structural system (multi-storey spaces between diaphragm walls without piles, complemented with trusses at various levels and alignment) and the uniform idea of having the human in the heart of the functional and aesthetical conception. The designers however found the way of creating own spirit and façade of each station (*Fig.3*) , and using these 21st century constructions was ment to be a real experience.

3. CHALLENGES IN DESIGN AND CONSTRUCTION

Building a new metro line in an urban area, and crossing two metro lines and a river is not a usual engineering task. The tunnelling through various layers and the construction of stations near heritage buildings and the Danube raised many difficulties, which were resolved by careful planning, front-rank technology and experienced professionals. This section highlights some interesting challenges of design and

Fig. 4: The station at Kelenföld – passageway under 28 tracks

construction. The longest station is the western terminal. The intermodal junction provides direct connection to the Kelenföldi railway station, which is the fourth biggest railway station in Budapest. The station (and the metro line) runs perpendicular to the railway, and includes a pedestrian passageway (*Fig. 4*) under the 28 tracks. This passageway runs just below the ground level thus the top slab functions as a row of railway bridges of 22 meter span. Together with the reversing facility the construction has an impressive length of 430 meters. (Pál, 2009) The design and the construction were highly influenced by the organisation of the construction site, since the railway station was in operation: the metro station was built in 5 sections, and only those at both ends were accessible on road.

Gellért tér is the deepest station of the new metro line – it lies 31 meters below ground level. The location of the station had to be determined very carefully, since it lies between the Danube and the CH building of the Budapest University of Technology and Economics, which is a national monument, and the famous warm cavern water basis and springs had to be preserved as well (Bencze, 2009). The organization of the construction had to take into account that some construction phases blocked a very important junction of the city, and at the same time, the construction of the main canalization channel had been undertaken along the Danube. The first application of the hydro-fraise technology in Hungary took place at the construction of the 40 meter deep diaphragm walls of this station.

The tunnel is being constructed by a tunnelling shield, which is able to operate in open and earth pressure balance mode as well. The crossing under the Danube was a critical section:

Fig. 3: Architectural design of the 21st century at Metro 4

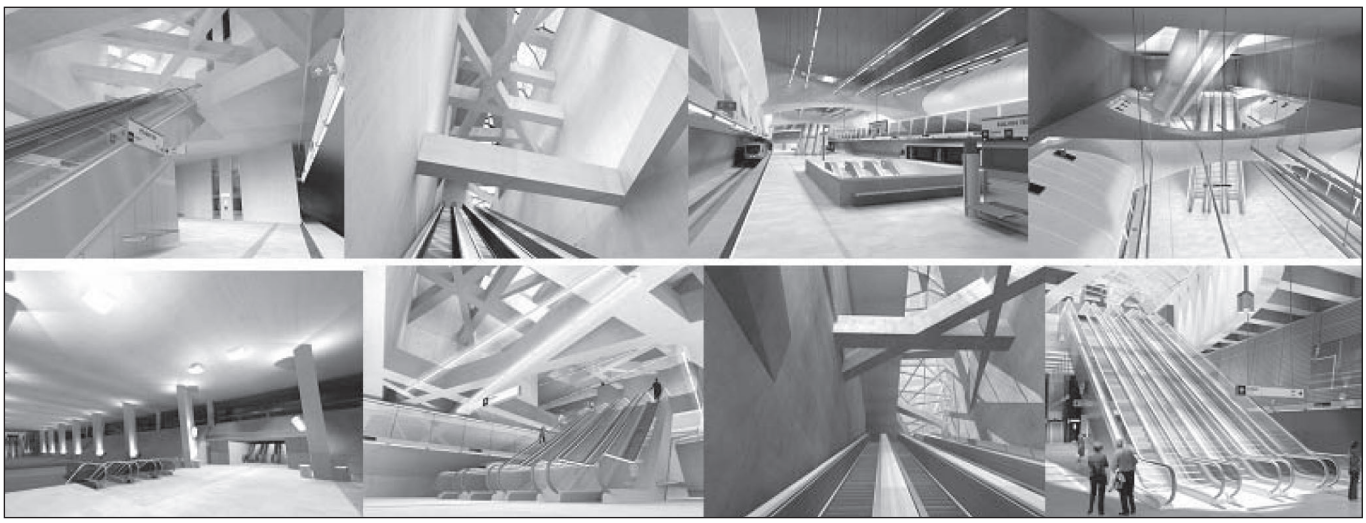

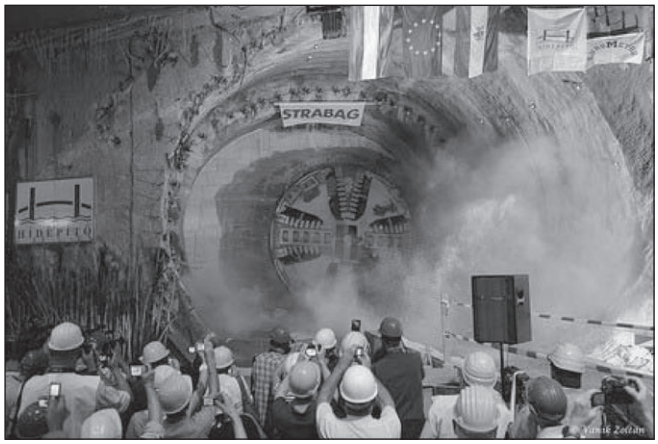

Fig. 5: *The tunnelling shield is arriving at the Fővám tér station*

Fig. 7: *Main building of the Eastern railway station*

the water-break-in had to be avoided, therefore the excavation pressure needed to be adjusted to the actual water level. The change of the Danube water level reached up to 5 meters in that period. The tunnelling started with the punching of a concrete plug, and it reached over two thirds of the distance under the river when the shield stopped. The hydraulic jacks were turned to maximal pressure, but the shield didn't move. Experts had to enter the cutting chamber which was under pressure to find out whether some hard rock blocks the shield or the cutting head is clogged by clay. The latter was the reason for stopping, and after cleaning the cutting head and altering the mixture in the chamber, the south-shield reached the Pest side (*Fig. 5.*), and with these experiences it was possible to prevent the northern shield from similar problems.

On the Pest side the first station is Fővám tér. The station has it entrance between the building of the Corvinus University of Budapest and the Danube. It was originally planned, that the platform tunnels run 45 meters under the Danube. The contractors have investigated various construction methods (e.g. building a temporary artificial island on the Danube to construct the station), but they were all too expensive and risky. Finally they agreed with the client, that the platforms will run only 20 meters under the Danube, which enables a thicker cover, and the other part will be built under the building of the University (Bencze, 2009). This required the redesigning of the elevators and service areas, but the tunnels were successfully constructed under the protection of a ground freezed vault, which was not only statically adequate, but also watertight.

4. DETERMINATION OF GROUND MOTIONS

The metro station and the reversing facility at Eastern railway station are located very close to 2-6 storey high, 100 year old

Fig. 6: *Buildings affected by ground motions*

residential buildings (*Fig. 6*) and to the central building of the railway station (*Fig. 7*) itself. These buildings are pretty sensitive to both vertical and horizontal ground motions because they are constructed of traditional brickwork without additional reinforcement. A close cooperation with the design engineers and constructor was necessary: the final decision on the construction phases, temporary supports and the structure itself had to be made together, since these had major influence on the resulting settlements.

To determine the expected ground motions caused by underground construction works, plain deformations of the surrounding soil were calculated by two-dimensional finite element analysis (using PLAXIS 8.6 software) at the typical cross-sections of the station and the reversing facility. Material properties of the surrounding Pleistocene sand and sandy gravel layers were derived from the report of preliminary geological works. The hardening soil model was used for the calculations. Different stages of the construction works were considered during analysis including initial state, excavation of soil till the working level, construction of the cut-off walls (Fig. 5), construction of upper reinforced concrete floor, excavation between cut-off walls, construction of intermediate reinforced concrete floor and upper lining walls and finally the excavation of the soil for the base slab (*Fig. 8*). Expected vertical and horizontal ground motions and deformations of the cutoff walls were determined (*Fig. 9*) for each step of construction described above.

Due to the more complex geometrical layout, soil settlements around the end of the station and the reversing facility were also calculated by three dimensional finite element analysis using Plaxis 3D Foundation 1.6 software. Vertical and horizontal ground motions around the end of station and reversing facility were evaluated considering the same construction stages as described in case of two dimensional analysis. The final distribution of settlements around the whole station and reversing facility was combined from the results of 2D and 3D analysis (*Fig. 10*).

5. ANALYSIS OF THE AFFECTED BUILDINGS

It has been determined in view of the results of the ground motion analysis that 13 residential buildings and the main building of Eastern railway station will be affected by considerable settlements during constructions. In-situ investigation of the affected buildings was carried out including geometrical surveying and non-destructive material tests. The investigated residential buildings are typically made

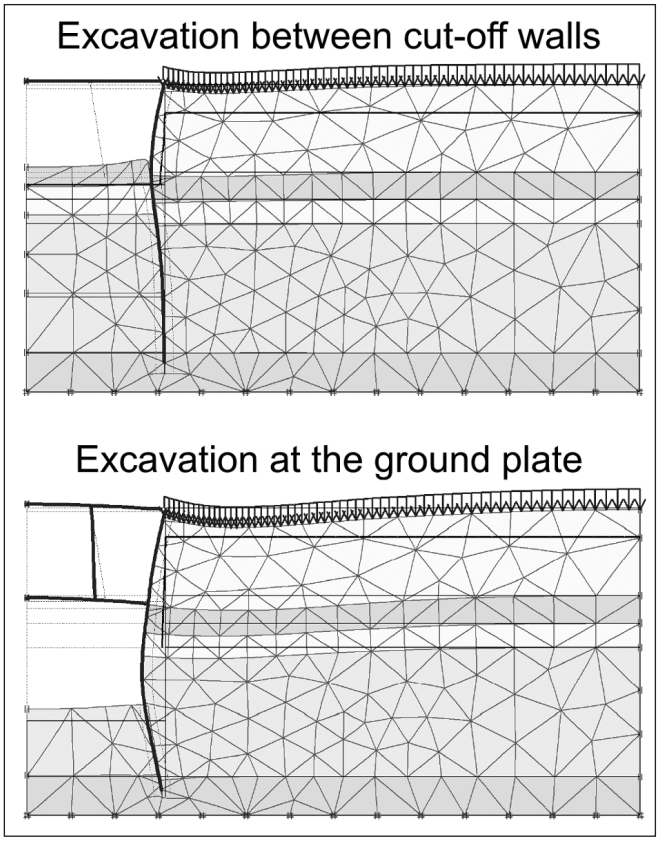

Fig. 8: *Deformed 2D FE mesh at different stages of construction*

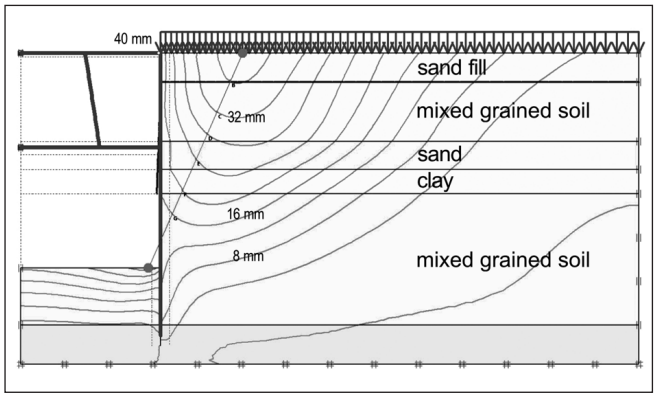

Fig. 9: *Vertical displacements of soil at final stage*

of traditional bricks with 40-80 cm thick walls. They have masonry strip foundations, there is usually barrel vault floor in the basement and there are Prussian vault floors between steel beams on higher levels. The roof of these houses is typically traditional couple roof made of timber.

The Eastern railway station was built between 1881 and 1884 in eclectic style. The roof of the main hall is supported by double-hinged steel arches with spans of 42.0 m, total length of the hall is 188 m. Load bearing walls of the station are 0.95-1.55 m thick masonry walls with timber pile foundations, while lateral wings of the building have masonry strip foundations. There are barrel vault roofs in the basement and Prussian vault floors on upper levels. Columns in the left wing of the station are made of cast iron.

The effect of expected ground motions to the buildings in question was analysed for each building separately. Aim of these analyses was to determine the formation of vertical and diagonal cracks (*Fig. 11*), rotation of the building and the overloading rate of load bearing walls and pillars caused by surface deformations. Slipping-down of abutments of barrel vaults, Prussian vaults and arches due to horizontal ground movements was also checked. Structural geometry was derived from the original architectural plans and results of in-situ measurements. Numerical analysis was performed using the measured material properties of bricks, mortar and cast iron. Strength of bricks was measured by Schmidt-hammer, mortar strength was estimated by visual inspection and scratch test while strength of cast iron was examined by Poldi-hammer.

Results of analyses were evaluated according to the Hungarian Standard (MSZ). Calculated values of crack width were compared to 1 mm (insignificant damage) and 10 mm (moderate or medium damage) limits provided by the standard. Width of cracks caused by surface settlements remain under the 10 mm limit for all buildings (typically 0-3 mm). In case of the highest examined building the crack width was significantly higher, reaching a value of 8.4 mm. Utilization of strength in vertical load bearing structures was checked for both ultimate and tolerable limit states. The criterion for ultimate limit state was satisfied for most buildings even after overloading of walls due to ground movements. However the utilization of strength in ultimate limit state exceeded 100% in several cases so these buildings could be classified as tolerable only. In case of these buildings the strengthening of specific structural parts

Fig. 10: *Vertical settlements around metro station and reversing facility (at +102,00 above sea level)*

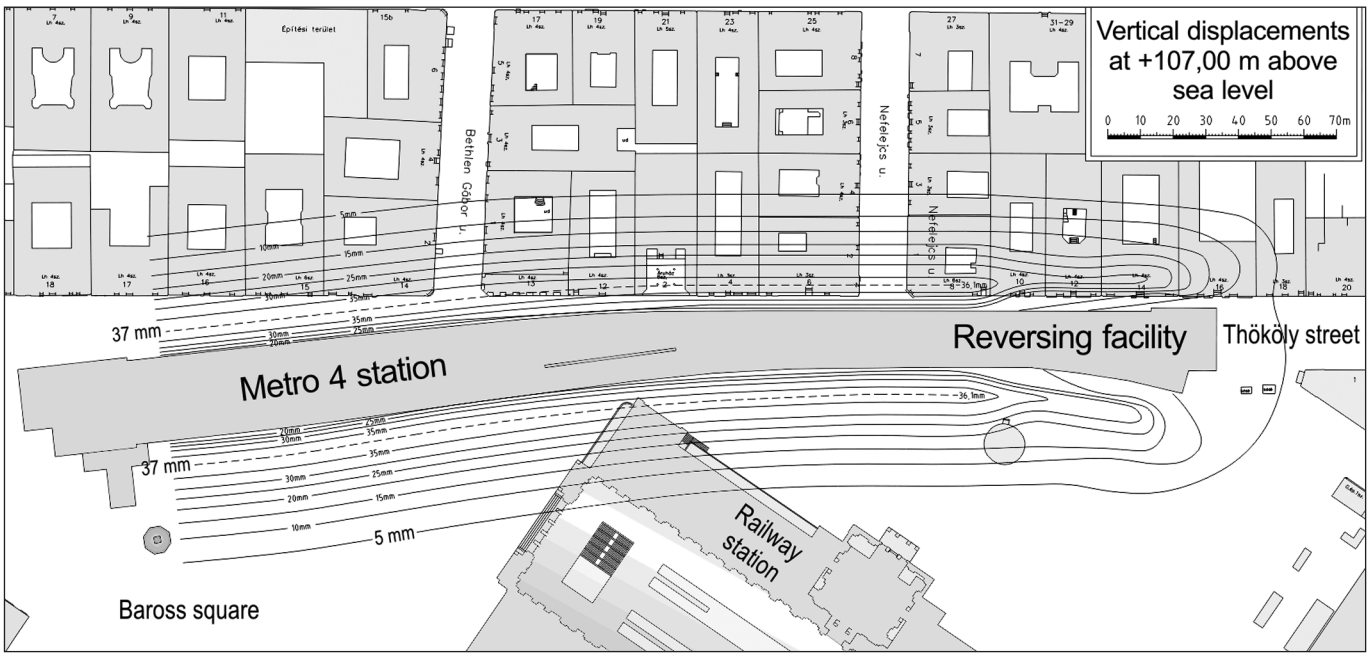

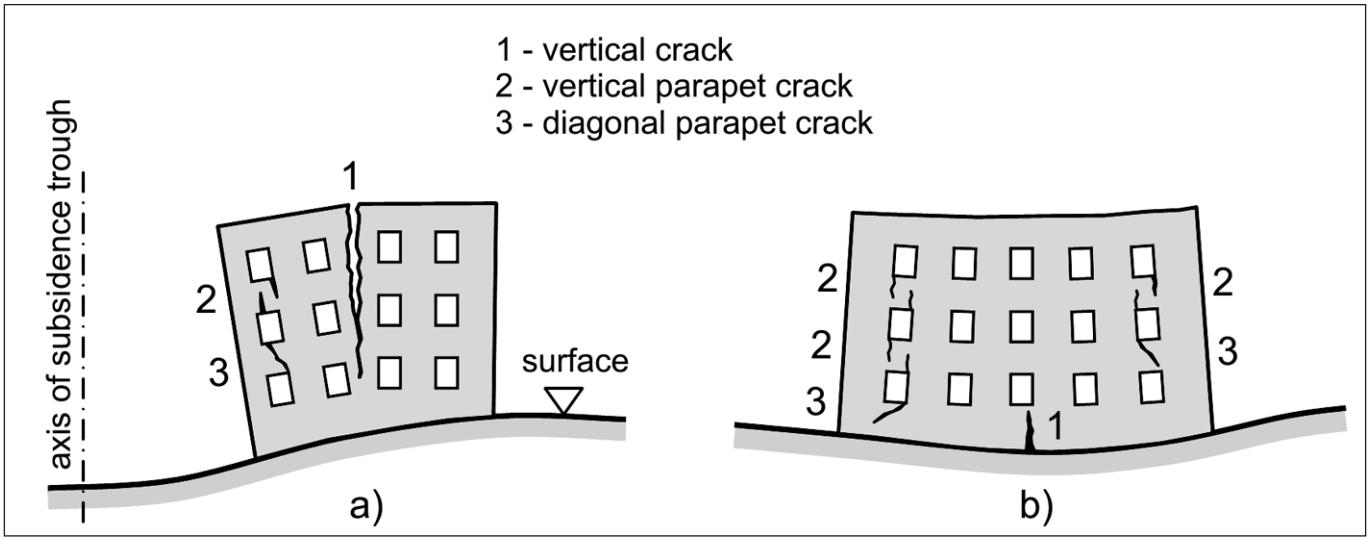

Fig. 11: *Crack development in case of different surface deformations a) building in saddle position b) building in synclinal position*

was recommended. The 1/500 [rad] limit for the rotation of the building was satisfied for all structures.

Due to its more complex architecture and importance as a public building and national monument, the main entrance region of the Eastern railway station was also examined by finite element analysis (using AxisVM 9.0 software). A typical section of the entrance arch together with joint structural parts was modelled. Geometry of the structure was derived from the original architectural plans and in-situ measurements. Considered material properties of the masonry wall were measured by Schmidt-hammer. Forces inside the wall were evaluated before and after the ground movements caused by underground constructions. The overloading rate of vertical load bearing members was determined (*Fig. 12*) and compared to the measured strength value. According to the previous examinations, the main building of Eastern railway station is subjected to insignificant damage (formation of moderate cracks) only.

Based on the results of numerical analysis described above, appropriate settlements limits were specified for each affected building separately. The specified limits were fed into the monitoring system that was previously installed to measure the vertical and horizontal movements of the building fronts. The automated system is able to provide immediate feedback if the specified settlement limits are approached, reached or passed.

6. CONCLUSIONS

In the introduction we gave a short overview of the Metro 4 project of Budapest, than we highlighted some great challenges: the longest and the deepest station, the tunnelling under the Danube and the construction works under the protection of a ground-freezed vault. Since underground works cause ground motions, the buildings over the tunnels and near the stations are affected. The task of the Budapest University of Technology and Economics, Department of Structural Engineering was the preliminary investigation of buildings at Eastern railway station. We predicted the damages, and set up settlements limits according to predefined hazard levels, which were fed into the continuous monitoring system. We believe that this work

Fig. 12: *Increase of vertical forces due to ground motions a) forces in initial state b) forces after movement of the supports*

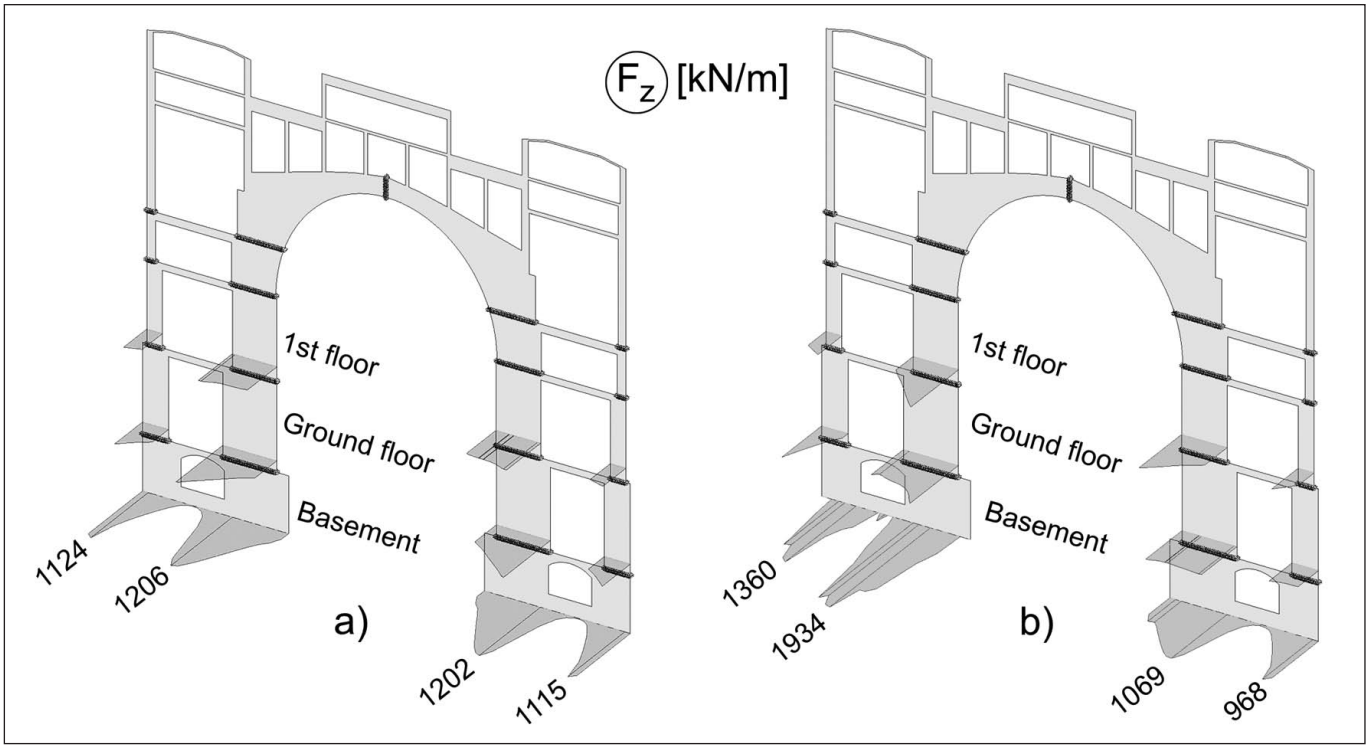

contributes to the quality of the Metro 4 project which is one of the most influencing projects of the past 20 years. The new metro line will induce alteration of the public transportation network, and it will highly influence the future development of the city. The established architectural quality, the gathered construction know-how will have a long-lasting impact to the building and construction industry of Hungary.

7. REFERENCES

Arató, Dulácska, Nemestóthy, Barabás (1975), "Protection of buildings from settlements caused by metro line constructions handbook" (in Hungarian), BUVÁTI. Budapest, 1975.

Arató, A., Burján, Z. (1977), "Damages to buildings and protection against them" (in Hunagrian), Magyar Építőipar 1977/9-10, pp. 513-528.

Bencze, Á. (2009), „Unique solutions at the construction of Metro 4" (in Hungarian), Mélyépítő Tükörkép Magazin 2009/2, pp. 14-15.

BME Építőmérnöki Kar, Sámson Kft. Construct Trade Kft. (2007), "Report on the expected ground motions at Metro 4 station at Eastern railway station" (in Hungarian), Budapest 2007.

Dulácska, E. (1976), "Crack formation on buildings due to ground settlements" (in Hungarian), Magyar Építőipar, 1976/10-11., pp. 630-634. 667-671.

Dulácska, E. (1982), "Protection of building against blasts of tunnelling" (in Hungarian), Műszaki Könyvkiadó - ÉTK Budapest 1982

Dulácska, Fekete, Varga. (1982), "Interaction of structure and soil (in Hungarian), Akadémiai Kiadó, Budapest 1982.

Dulácska, E. (1992), "Soil settlement on building", Elsevier. Amsterdam-London-New York-Tokyo, 1992

Lichter, T. (2009), "Strengthening of the monument church at Kálvin tér" (in Hungarian), Vasbetonépítés 2009/1, pp. 2-13.

Németh, M. T. (2009), „Metro 4 under the Danube" (in Hungarian), Mélyépítő Tükörkép Magazin, 2009/3, pp. 30-33.

Pál, G. (2009), „Design – the deepest and longest stations of Metro 4" (in Hungarian), Mélyépítő Tükörkép Magazin 2009/2, pp. 17.

Schulek, J. (2008), „Budapest Metro line 4 under construction", Concrete Structures 2008, pp. 10-14.

Dr. István Bódi (1954) civil engineer, post-graduate engineer in mathematics, PhD, Associate Professor at the Department of Structural Engineering, Budapest University of Technology and Economics. Research fields: Reconstruction and strengthening of reinforced concrete and conventional structures, modelling of timber structure joints. Member of the ACI (American Concrete Institute), the ACI Subcommitte#423 „Prestressed Concrete" and the Hungarian Chamber of Engineers. President of the standardization committee Eurocode 5 - MSZ NAD (Timber Structures). Member of the Hungarian Group of *fib*. Member of the „Schweizerische Arbeitsgemeinschaft für das Holz".

Dr. Kálmán Koris (1970) structural engineer, MSc, PhD, Senior Assistant Professor at the Department of Structural Engineering, Budapest University of Technology and Economics. Research fields: safety of reinforced concrete structures, analysis of prefabricated, prestressed concrete structures, strengthening of structures. Member of the standardization subcommittee "NAD MSZ ENV 1992 Eurocode 2, Design of concrete structures". Member of the Hungarian Group of *fib*.

András Molnár (1983) civil engineer, MSc, PhD student at the Department of Structural Engineering, Budapest University of Technology and Economics. His main field of interest is the structural application of fibre reinforced polymers at upgrading structures and structural members, and strengthening of existing reinforced concrete and timber structures with regard to prestressed application. Member of the Hungarian Group of *fib*.

CONSTRUCTION OF THE TISZA-BRIDGE SPANNING THE RIVER ON THE MOTOR ROAD M43

László Mátyássy

The motorroad M43 connecting Szeged with Makó, that can be later developed into a motorway is built as a road fork of the north-south motorway M5. The Tisza-bridge, that will be built as a part of the motorroad is not only a simple crossing point, but a landscape-forming engineering work. This in Europe matchless river-bridge is – regarding its construction system – an extradosed box girder with corrugated steel webs connecting the top and bottom concrete slabs.

Keywords: extradosed bridge, corrugated steel web, stay cables, balanced cantilever

1. INTRODUCTION

The plotting of the bridge was influenced by the crossing angle (~85°) with the river Tisza, the width of the flood area, but mostly by the limitations through the functioning oil-wells. The motor road crosses the river Tisza at the river km 182.970.

The horizontal tracing of the motor road in the whole segment of the bridge is totally straight. The bridge spanning the river will be built in dome-shaped rounding of R_d = 15000 m radius. The rated velocity on the Tisza-bridge is 110 km/h. Two traffic lanes of 3.75 m each and an emergency lane on both sides lead through the bridge. For the safe positioning of the extradosed stay cables the separation zone is wider. Therefore, the distance between the left and right track was slightly increased.

The used solution with extradosed stay cables has several advantageous features in comparison with ordinary box beam bridges. The girder height and the self-weight are namely substantially lower than in the case of the beam bridges. In addition to that, the necessary quantity of the concrete and of the span cables will be less than in the case of a beam bridge.

The tension unsteadiness from the live load is smaller on the extradosed stay cables than in the case of cable stayed bridges, because the pylon is lower. The allowed tensioning force can be received in a similar way as at the girder bridges. (In this way 30 percent saving can be reached.)

Through the application of the corrugated steel web the majority of the tensioning force affects the top and bottom slabs, because the corrugated web withstands the shear force without receiving significant normal force from the axial tensioning (*Fig. 1*). Thereby the self-weight of the main girder will be smaller too. This reduces the costs and also longer constructional units can be used. The reduction of the number of constructional units can shorten the time of erection too (*Fig. 2*).

Fig. 1: Landscape-matched image of the bridge

Fig. 2: Status in the course of construction

The bridge will be built as an investition of Nemzeti Infrastruktúra Fejlesztő Co. (National Infrastructure Development Co.), the building contractor is Hídépítő Co. The plans of the bridge spanning the river were made by Pont-TERV Co., the ones of the flood area bridges by Uvaterv Co. The stay cables and the upper disalignment saddle are supplied by VSL, the cable constructor (*Fig. 3*).

The fatigue test of the corrugated steel plate was made by the Department of Structural Engineering of the Budapest University of Technology and Economics, the wind tunnel tests were made by the Department of Fluid Mechanics.

2. CONSTRUCTION OF THE BRIDGE SPANNING THE RIVER

The Tisza-bridge of 661.20 m entire length consists of three bridge parts, the bridge spanning the river (river-bridge) and the two flood area bridges. The river-bridge consists of one, the flood area bridges of two (right and left) detached lane constructions.

Spans of the river-bridge are: 95.00+180.00+95.00 m (*Fig. 4*). The superstructure of 372.00 m entire length is built

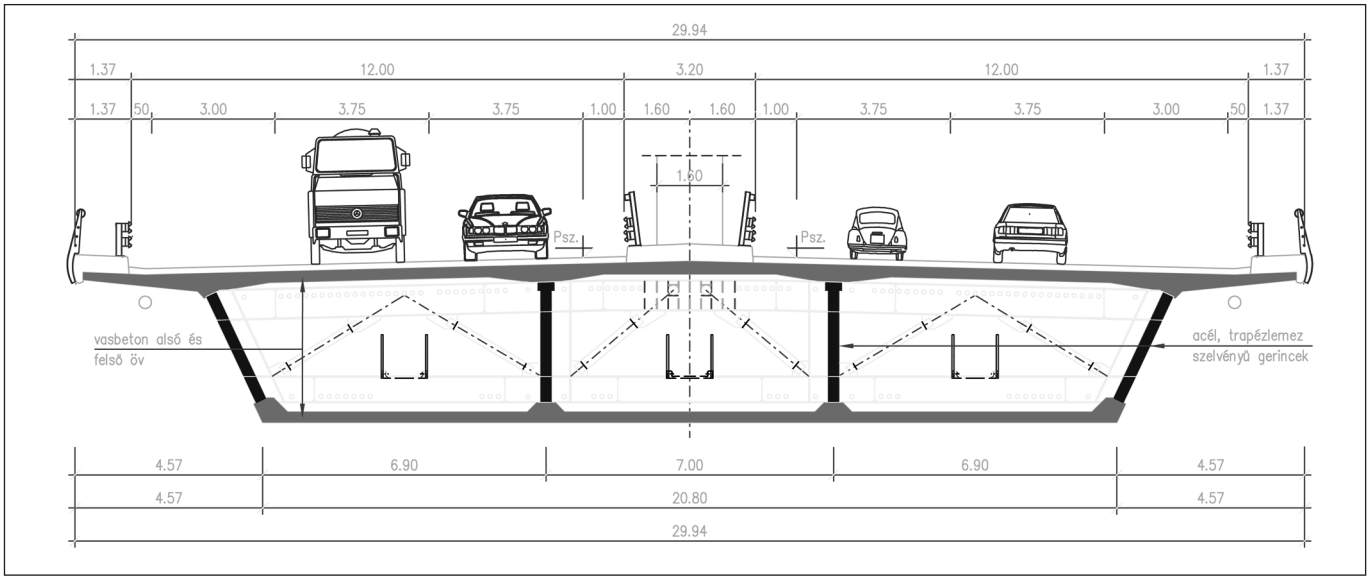

Fig. 3 Cross-sectional view

on massive reinforced concrete piers with pile foundation. Because of the extraordinarily disadvantageous soil conditions 39-42 m long piles were used with 1200 mm diameter for the foundation. The entire length of the piles only under the river-bridge adds up to 6000 m. The piers in the edge of the bank are parallel with the bank (included angle with the bridge axis 85°) and they will be built in a pointed form with granite frontal stones. The curvature at the joint piers is round-arch.

The superstructure consists of a box cross section beam with three cells. The lower and upper slabs are prestressed concrete plates. Cables are running parallelly to the bottom slab in the inner part of the box over the bottom slab. In the top slabs cables are also built in.

For enhancing the prestressing-effectivity (that means increasing the load carrying capacity) also extradosed tensioning cables outside of the bridge construction are used. These are anchored on the top of the 22.00 m high pylons positioned over the intermediate columns in the bridge axis. Four webs of the box girder are made of trapezoidal corrugated steel plates stiffened every 5.00 m with steel cross frames. The height of the cross-section is variable, the bridge is haunched at the intermediate columns. The construction height is 4.00 m at the middle of the span and 6.00 m over the piers. There are 18 blocks on each bridge cantilever, in their middle cross section stiffened with steel cross frames. Between the blocks 7 and 14 all the elements are suspended on the pylon with the extradosed stay cables.

The pylons are reinforced concrete constructions. The steel saddle is fixed into the massive pylon-head. The pylons widening upwards are inside hollow with a wall thickness of 0.50 m to 0.80 m.

3. FLOOD AREA BRIDGES

Spans of the bridge on the right bank are: 52.00+2·64.00+52.00 m and on the left bank 52.00 m. The piers of the 234.00 m and 54.00 m long superstructures are massive reinforced piers with pile bases and passable reinforced concrete abutments. The bridges in the flood area are composite box beam bridges with parallel webs. The boxes are unicellular, because the two traffic directions are led on separate beams. Their structural height is 4.00 m.

4. CONSTRUCTION TECHNOLOGY

The river-bridge is made by the in-situ balanced cantilever method (*Fig. 5*). The two cantilevered fitted bridge arms are made at the same time. The building of the superstructure

Fig. 5: Building of the bridge with the traveller

Fig. 4: Side view of the superstructure

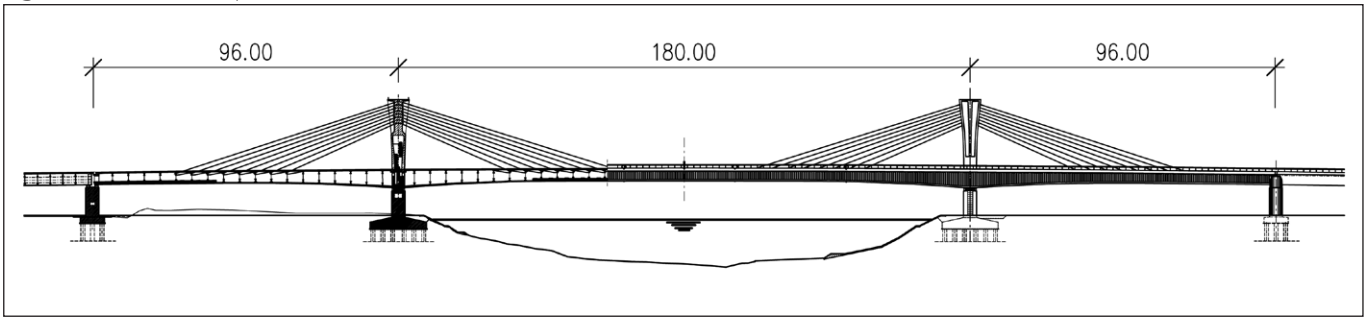

begins with making the starting blocks and the pylons, then the travellers and subsequently the 5.00 m long blocks are positioned. The two bridge arms are connected by a closing block. During the building of the cantilevers, auxiliary supports assure the stability.

The steel beams of the composite box beam construction of the flood area bridges are transported to the field on public roads and they will be assembled in their definite positions on provisional scaffoldings. The constructional units are connected by welded joints. The casting of floor slab happens on-site.

5. ARCHITECTURAL ASPECTS OF THE BRIDGE

The outside frames with bolted side surfaces are shaped uniformly in the entire length of the bridge. The car lane is bordered by leading barriers. Their safety was verified by shock tests. The operating platform on the outside part is enclosed by a 1.10 m high custom-built barrier.

The bridge bearings of the river-bridge are calotte shaped, the ones of the flood area bridges are pot shaped neoprene bearings. The fixed bearing on the river-bridge is positioned on the pier 6 in the bridge axis, on the flood-area bridges on the piers 3 and 8 under the inner (higher) girder.

The rainwater is led off the bridge through the gullies positioned at the inner side of the outer elevated edge. The flow-in to the gullies happens vertically. As the rainwater cannot run either directly into the river or to the flood area, it gets in glass fibre reinforced polyester collecting pipes which are tapped into the shafts behind the bridge abutments.

The inner part of the boxes and pylons is walkable, therefore also the inspection of the inner parts can be solved easily. The piers and the bearings can be monitored using vehicles with elevator cages from the operating road that will be built in the flood area. All piers can be reached from the operating road.

The floodligthing of the stayed girders and of the pylon enhance the characteristic elegant shape of the bridge.

6. CONCLUSION

The M43 motorway river-bridge over the Tisza river in Hungary (*Fig. 6*) is being erected with a special type of construction technology.

Part of the tensioning cables built in the superstructure run near the columns outside of the cross section on the upper part of the pylon. In this way their effectiveness is considerably improved.

Fig. 6 *Sight plan of the bridge*

The top and bottom slabs of the three-cell box cross-section beam is made of prestressed steel reinforced concrete and the web of the main beam of trapezoidal bent steel plate. The corrugated steel web reduces the self-weight of the bridge and increases the effectiveness of the post-tensioning.

Regarding the construction system the river-bridge is a three-span beam bridge with (concrete top and bottom slabs, extrados) extradosed trapezoidal corrugated steel web. Until now bridges were built with this constructional system only in Far-East (Japan). This will be the first such solution in Europe. Its advantage is the lower self-weight, the economical material-input and the slim appearance.

László Mátyássy (1949), qualified construction engineer (1972 Technical University of Budapest). General manager of Pont-Terv Co. 1972-84: bridge-planning engineer of Uvaterv Co., later leading planner. 1982: co-worker of Voest-Alpine in Linz (Austria). 1988-94: head of the department Híd-3. Since 1994 member of the management of Pont-terv Co. He took part in the planning of many bridges in Hungary and of exported bridges in his professional career. He acquired considerable skills both in the planning of big steel bridges and of prestressed concrete constructions. He took part in the planning of the Tisza-bridge Bertalan in Szeged, of the Árpád-bridge in Budapest, of the Saint-Stephen's bridge in Szolnok, of the Rába-bridge in Győr and of the Tisza-bridge in Újvidék (Novi Sad). Under the direction or the planning of him the Dulácska viaduct on the motorway M0, the Tisza-bridge in Cigánd, the Tisza-bridge in Tiszaug, the Mária-Valéria bridge in Esztergom, the river-bridge of the Saint Ladislaus bridge in Szekszárd, the flood area constructions of the Pentele-bridge in Dunaújváros and the viaduct Kőröshegy were built. Numerous publications of him appeared in learned journals. He was president of the Bridge Building Department of the Hungarian Engineer Chamber from 1998 till 2008 and presidium member of the Supporting Structure Division from 2004 till 2008. His work was appreciated by Feketeházy János Award (2007) and Gold Milestone Award (2008). He is member of the Hungarian Group of ***fib***.

STRUCTURE OF HYPERMARKETS AND SHOPPING CENTRES IN HUNGARY


József Almási – László Polgár

The article is intended to give an overview of the customary structural concepts of buildings designed for hypermarkest and shopping centres purposes[1] in Hungary.

Keywords: structures, prefabrication, structural nods, cast-in-situ concrete

1. INTRODUCTION

After the change of regime in 1990 the first bigger shopping centre was built in 1995 under the name of Duna Plaza in Budapest. The chosen grid system for the four-storey-building was 8.1 · 10.5 m. The framework of the building was made of a ribbed floor diaphragm system (main beams, secondary beams and slab) placed between the cast-in-situ reinforced concrete stiffening staircase and air engineering shafts. The columns and main beams were made in situ, the secondary beams and slab from prefabricated elements covered by in-situ slab.

Another characteristic building type was used in 1998 by the commercial chain AUCHAN. It had a grid of 12.0 · 18.0 m and a framework which was usually constructed of precast elements. The horizontal stiffness was ensured by the columns clamped into foundation sleeves, while the combined reinforced beams (main and secondary beams with a combination of prestressed and non-pre stressed reinforcements) created the roofing and the support of the HVAC units.

Countless versions of these building types have been executed and designed by the authors since then, respectively.

Some characteristic layouts, sections and nodes of different building types shall be presented in the followings.

Fig. 1: Layout - Sopron Spar

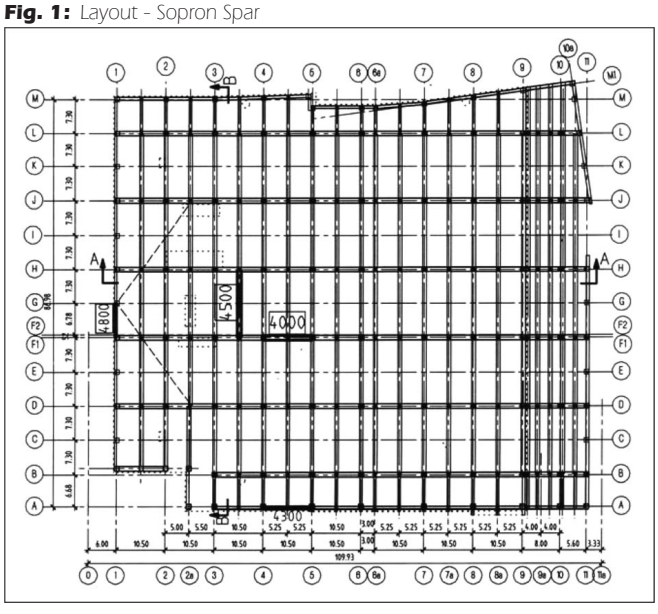

[1] The article regards as hypermarkets the usually single-storey (and single function) buildings, whereas shopping centres are multi-storey (and at the same time multipurpose) buildings.

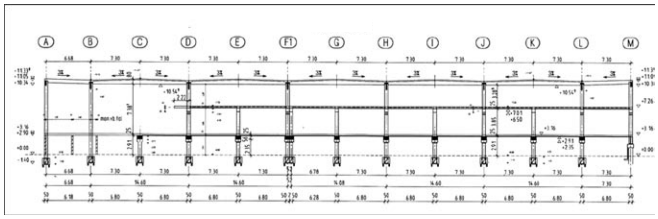

Fig. 2: Typical section - Sopron Spar

2. SOPRON-SPAR DEPARTMENT STORE

Layout dimensions are: 106.60 · 86.98 m (*Fig. 1*), with a 10.50 · 7.30 m grids (*Fig. 2*). Under the entire ground level of the building there is a parking for customers, so the store level is at +3.30 m. At level +7.30 m are the floors of the warehouse and engineering areas (*Fig. 3*).

3. ÁRKÁD SHOPPING CENTRES – ECE

The overall dimensions of the shopping centre are 302.0 · 115.5 m, the area being divided by column doubling into four expansion fields. The shopping centre is usually a ground floor plus one storey. On the slab above floor level 1 there is a parking and engine rooms with steel structure. The section between axes A 27-29/A-E is a ground floor plus three-storey building part.

Grid sizes and structural dimensions can already be regarded as standard with ECE. The basic grid is 10.00 · 8.25 m. The only deviation is the grid of the cross-mall which is sized

12.00 · 8.25 m. In case of the longitudinal mall the 10.00 · 16.50 m size is made up of the intertwining of two grids. Next to axis A, along the staircases and engine rooms the 8.25 m

Fig. 3: Floor nodes

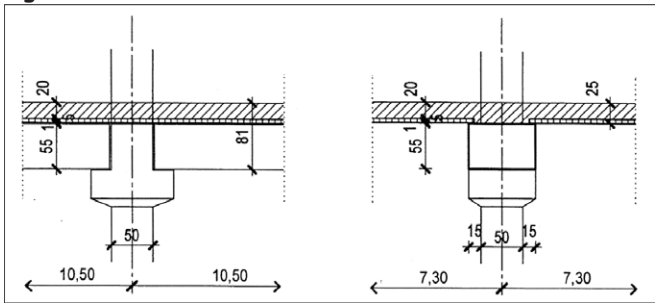

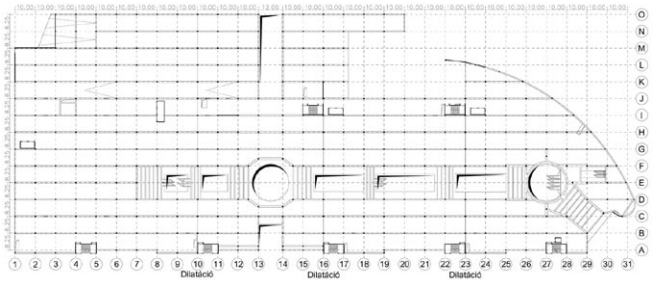

Fig. 4: Layout of the first level floor - Árkád Győr

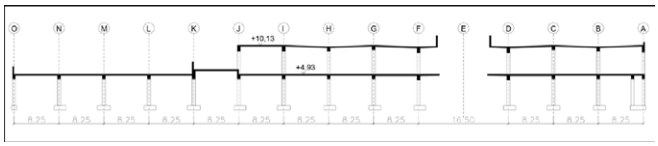

Fig. 5: Cross section

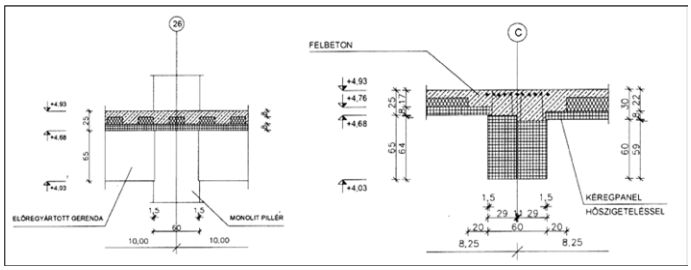

Fig. 6: Typical Sections

grid is extended to 9.75 m (*Fig. 4, Fig. 5, Fig. 6* and *Fig. 7*). According to the ECE standard the live load of the floors below the sales areas is 5.0 kN/m^2. The live load includes also the weight of the mounted partition walls. The weight of the 25 cm thick Ytong partition walls was considered as a separate load. The permanent load of the floor finishing (7 cm cover thickness) together with the suspended engineering cabling and the false ceiling make up 2.4 kN/m^2. The live load of the parking is 3.5 kN/m^2. In parking areas the dead load of the floor finishing is 4.3 kN/m^2 (if the slope is rendered by the framework), respectively 6.6 kN/m^2 (if the slope is formed by a finishing layer). The dimensioning of the reinforced concrete structures was done based on MSZ ENV Hungarian-European Code 1992-1-1:1999.

Fig. 7: Styropor Lightened Floor Planks with Truss

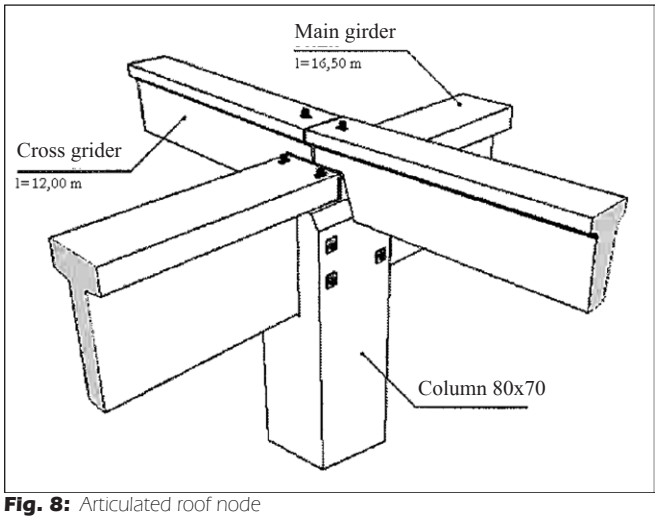

Fig. 8: Articulated roof node

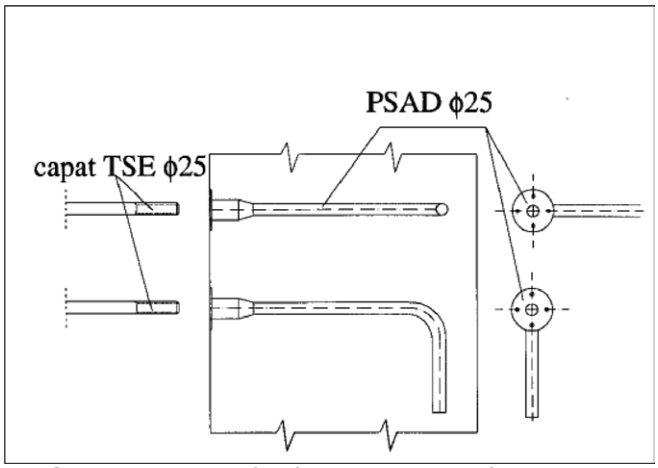

Fig. 9: Monolithic casting of reinforcement connecting fittings

4. CONSIDERATION OF THE SEISMIC EFFECT

The avoidance of seismic risks when using only precast elements requires special node solutions. Some of the solutions applied are listed below.

- For articulated roof nodes a preferred solution is to place main beams into the fork of column caps, respectively fastening them by horizontal screws (two at each beam end) and vertical dowels. These later are fastened by screws and bearing pads (*Fig. 8*).

- On the intermediate floor level at the clamped perimeter nodes special fittings were introduced to lead on the reinforcement (*Fig. 9*).

5. SOLUTION PATTERNS

The typical solution patterns of the frame and floor structures are summarised in *Fig. 10*.

In addition to the node solutions the importance of horizontal building stiffness has to be also emphasized. This is usually done in Hungary by the staircase shear walls and engineering shafts made of cast-in-situ reinforced concrete.

A major aspect is to assure the load distribution role of the floor slab by inserting the necessary quantity of tie reinforcement.

6. REFERENCES

Balogh, B. (2006), "Shopping Centre Structure Árkád Győr" (in Hungarian), *Magyar Építéstechnika,* 2006/12.

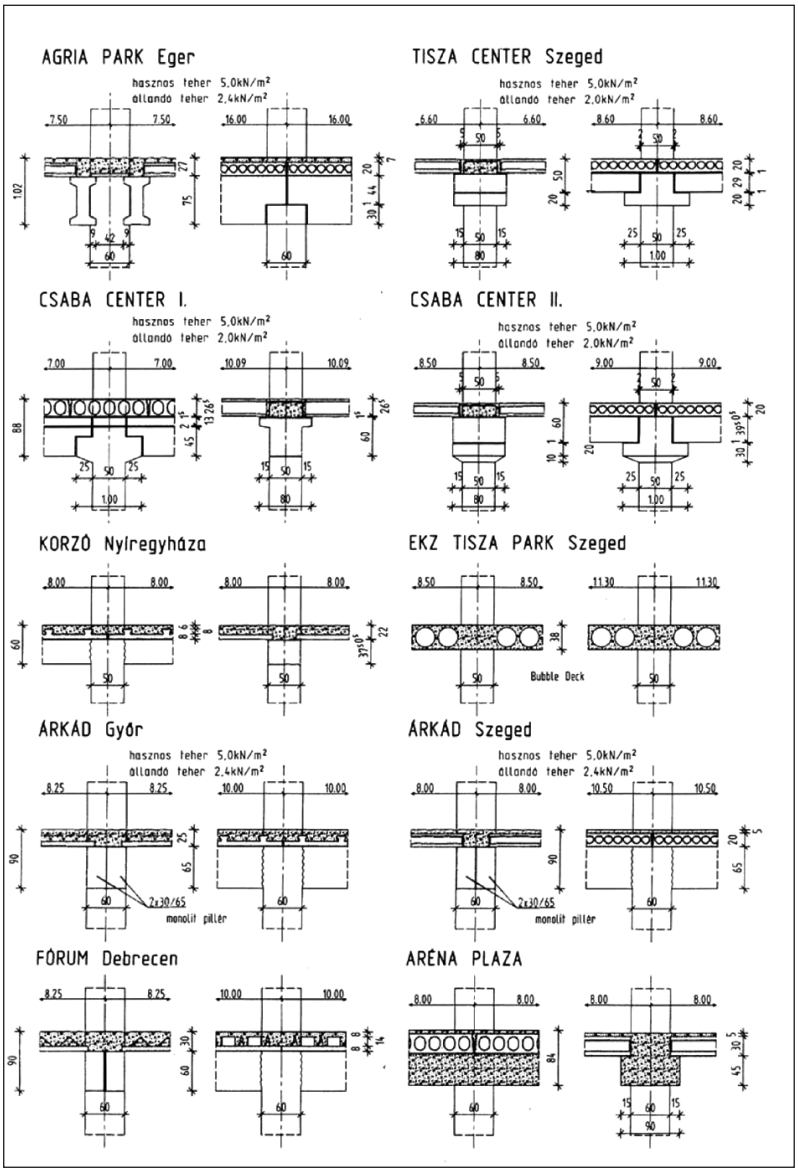

Fig. 10: *Typical structural nodes*

Kaposvári, Zs. (2006), " Hypermarket Structure Interspar Sopron" (in Hungarian), *Magyar Építéstechnika* 2006/12

Polgár, L. (2007) "Building Welt" (in Hungarian), *Magyar Építéstechnika* (Spec. issu) 2007

Kiss Z., Dragomir P. (2006), „Proiectul structurii complexului comercial Cora, Lujerului, (Structural design of the Cora commercial) Manuscript 2006.

Dr. József Almási (1940) civil engineer, MSc, graduated 1964, doctoral thesis 1972, earlier Associate professor at the Department of Structural Engineering, Budapest University of Technology. Now designer at CAEC Ltd, Budapest, member of the Hungarian Group of ***fib***.

László Polgár (1943) civil engineer, MSc, graduated 1967, now technical director at building company ASA, member of the Hungarian Group of ***fib***.

RENOVATION OF A NATIONAL MONUMENT IN HUNGARY: THE KEREPESI GRANDSTAND

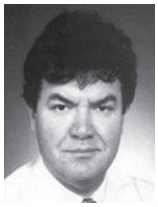

István Bódi – Kálmán Koris – András Molnár

The racecourse "Kerepesi Ügető" in Budapest was closed in year 2000 and all of its buildings were demolished except the Class II Grandstand which was earlier declared as a National Monument. Our task was on the one hand to perform the comprehensive statical investigation of this Grandstand and on the other hand the development of the methodology for structural strengthening. Investigations included in-situ measurements, laboratory material tests and finite element analysis of the structure. According to the results of statical calculations, the method of strengthening was proposed, which included the injection of cracks, integration of new structural elements, application of concrete jacketing and bonded CFRP sheets. The applied strengthening and renovation method extended the life-span of the Grandstand with 50 years.

Keywords: renovation; strengthening; urban heritage; grandstand; reinforced concrete; CFRP sheet; concrete jacketing

1. INTRODUCTION

The building-complex of the racecourse "Kerepesi Ügető" in Budapest included several reinforced concrete grandstands of different classes to be used by the audience. The racecourse was closed in the year 2000 and the land was sold to investors who utilized the ground for the construction of the second largest shopping centre and amusing complex in Europe. All of the buildings of the racecourse were demolished except the Class II Grandstand (*Fig. 1*) which had to be protected since it was declared as a national monument. Our tasks were to perform a complete statical investigation for this Class II Grandstand and to develop the strengthening and renovation method of the structure. An important objective of the work was to ensure the seamless integration of the old Grandstand and the surrounding urban environment including the complex of the new shopping centre (Bódi, Koris, Erdődi; 2002). The life-span of the Grandstand was extended by 50 years and the function of the structure was renewed by the applied renovation method.

2. HISTORICAL AND STRUCTURAL BACKGROUND

The building-complex of the racecourse including the Class II Grandstand was built between 1935 and 1941 according to the original plans (*Fig. 2*) of the architect Ferenc Paulheim Jr.

Fig. 1: The Class II Grandstand before renovation

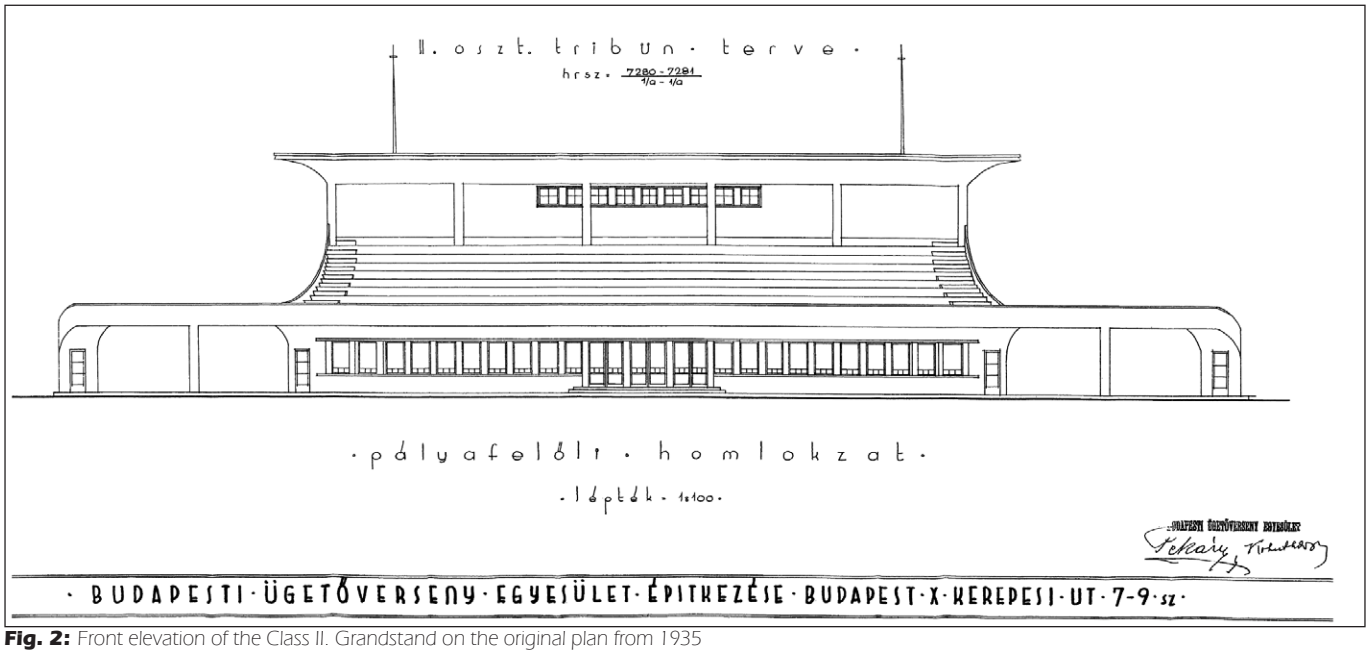

Fig. 2: Front elevation of the Class II. Grandstand on the original plan from 1935

(Paulheim, 1935). Statical calculations and structural drawings were produced by Vilmos Obrist civil engineer (Obrist, 1936) in 1936. The Class II Grandstand was built on the basis of the original plans with minor changes in the construction. The structure was not modified or strengthened during the next 66 years, it remained intact even during the World War II.

The superstructure of the Class II Grandstand consists of monolithic reinforced concrete frames connected with crossway beams supporting the concrete slabs (Obrist, 1936). The roof is a ribbed concrete slab structure supported by cantilever beams of the frame. Equilibrium of the cantilever roof beams are ensured by concrete columns under tension. The reinforced concrete columns have pillar foundations. The two-storey Grandstand has curved concrete stairs leading to the second floor.

3. PERFORMED INVESTIGATIONS

3.1 Investigations on site

The Grandstand was investigated altogether six times in 2002. Physical conditions of the building were recorded by visual inspection and the amount and types of structural damages were also registered. Concrete core samples were bored at seven different locations and these samples were tested later in the laboratory. Structural uncovering was performed at several locations to identify the reinforcement. A Proceq Scanlog profometer was also used for the same purpose at different locations of the building. The strength of reinforcing steel was examined by Poldi hardness tester. Some results of the investigations by Poldi hardness tester are presented in Table 1. Non-destructive concrete strength tests were also performed by N-type Schmidt hammer in 49 different points of the structure. Results of non-destructive concrete strength tests were corrected by the laboratory test results.

During the in-situ investigations, no visible sign of major damage or overloading of the load carrying structural members was detected (Bódi, Koris, Erdődi; 2002). However, cracks were spotted at the connections of the outside columns and cantilever beams. These cracks were mainly caused by tensile forces in the columns and the cantilever beams. Some cracks caused by shrinkage of the concrete were also detected in the secondary structures such as concrete barriers and banisters. Significant corrosion of reinforcing steel bars and the lack of concrete cover were observed on the outdoor structural members including columns, beams and slabs (*Fig. 3*). These problems were mainly caused by inappropriate waterproofing. No sign of surface corrosion or decrease of bond between steel

Table 1: Results of in-situ investigations by Poldi hardness tester

Number	Place of investigation	Impression [mm]		Strength [Mp/in²]		Design value of strength [N/mm²]	Remarks
		Rebar	Comparison metal	Measured values	Mean value		
1	*Column*	3.70	3.00	22.2	21.8	225	Ø = 24 mm (plain)
2		4.00	3.20	21.5			
3		4.05	3.25	21.6			
4	*Beam*	2.95	2.50	25.7	22.3	230	Ø = 16 mm (plain)
5		3.25	2.60	21.1			
6		3.25	2.55	20.05			

Fig. 3: *Spalling of concrete cover and corrosion of steel bars at different structural elements*

bars and concrete was detected during the uncovering in case of undamaged beams and columns.

3.2 Laboratory tests

Cylinder shaped concrete specimens were prepared from the core samples bored on site for the purposes of destructive testing. The diameter of the specimens was 63 or 73 mm (according to the inner diameter of the drill head used on site) and the height of the cylinders varied between 98 and 141 mm. Uniaxial compression tests were carried out on the concrete specimens in the Structural Laboratory of Budapest University of Technology and Economics (*Fig. 4*). Test results were evaluated according to the Hungarian Standard MSZ 4720 for different structural parts (beams, columns, slabs, balustrades) so we achieved the characteristic values of concrete strength for different structural members separately (Bódi – Koris – Erdődi, 2002). Deviation of the concrete strength in case of some columns was significantly higher than expected. It turned out that there were originally chimneys inside these columns. The impact of the high temperature gases streaming inside these chimneys resulted in significant decrease of the local concrete strength. Concrete strength was also evaluated by in-situ non-destructive tests based on the hardness of the concrete surface. Results of the compression tests were used for the calibration of the non-destructive in-situ test results. Strength of the smooth steel bars was determined by in-situ investigation using Poldi hardness tester (Bódi, Koris, Erdődi; 2002). The value of steel strength was around 210 N/mm^2. Tensile test was performed in the laboratory on some steel bars taken from the Grandstand during the investigation on site. Results of the tensile tests were used for the refinement of the in-situ test results.

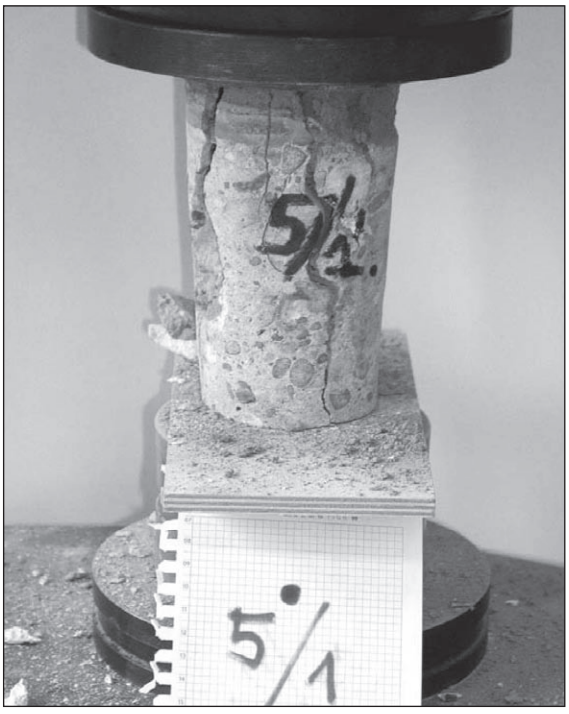

Fig. 4: *Uniaxial compression test of a concrete cylinder specimen*

3.3 Statical calculations

The design values of internal forces were derived by finite element analysis (Bódi, Koris, Erdődi; 2002). The Axis VM 6.0 software package was used to prepare the finite element model (*Fig. 5*) of the Grandstand's characteristic segment. Geometrical sizes measured on site and material properties derived from in-situ and laboratory tests were used during the calculations. The actions were calculated according to the European Standard "MSZ ENV 1991 Eurocode 1: Basis of design and Actions on Structures". The possible action groups as well as local effects – such as snow trap load or concentrated

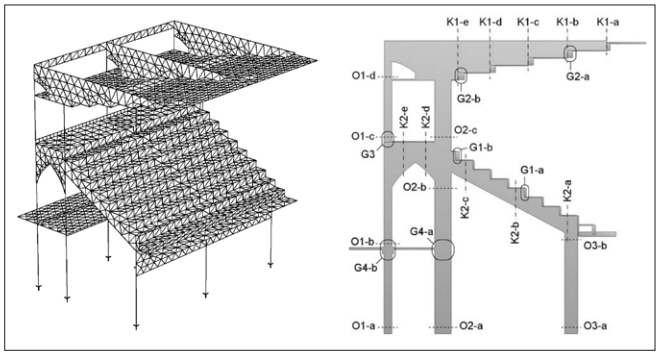

Fig. 5: Finite element model of the Grandstand and the locations of the controlled cross-sections

service load – were considered during the analysis. A simplified calculation method was also used to verify the results of the finite element simulation.

The typical cross sections were controlled by using the Standard MSZ ENV 1992-1-1 Eurocode 2: "Design of Concrete Structures. General rules and rules for buildings". Investigations were performed in 26 different cross sections. Beam sections were examined for bending and shear with or without simultaneous axial force (depending on the location of the beam). Column sections were examined for eccentric compression or tension. Deflection of the structure was also evaluated and controlled. Local values of concrete and reinforcing steel strengths derived from in-situ and laboratory tests were used for the calculation. The geometrical data (including the amount of reinforcing steel) of different cross sections were taken from structural investigations on site and original plans as well. Most of the controlled cross sections fulfilled the requirements of the Eurocode Standard; however, the load carrying capacity was insufficient in some places. The tensioned columns outside the roof that provide anchorage to the cantilever beams were practically in ultimate limit state. The load carrying capacity of the 6 cm thick stepped concrete slab was satisfactory in case of distributed loads but it was insufficient in case of concentrated live load (Q = 1.5 kN as demanded by Eurocode 1). Load carrying capacity of the

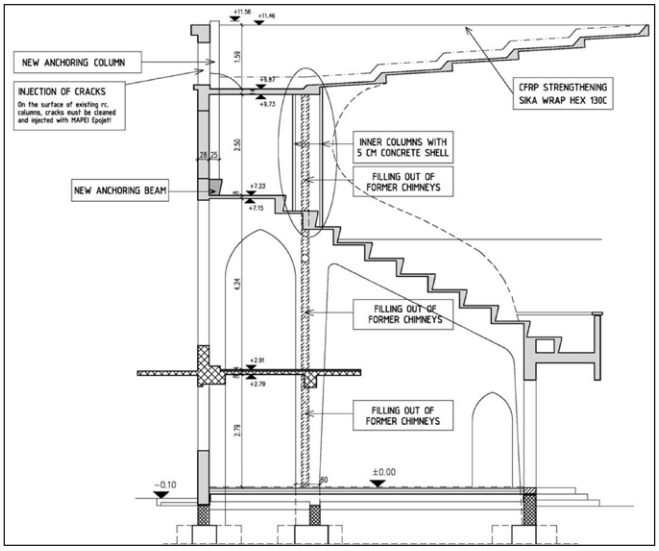

Fig. 6: Strengthening plan of cantilever structure (CAEC Kft, 2003)

longitudinal beams on the first floor, as well as the resistance of the front column under the first floor, was insufficient. Due to these problems the strengthening of the Grandstand had to be performed.

4. STRENGTHENING OF THE GRANDSTAND

Results of the complete statical investigation were used to plan the methodology for the necessary strengthening that could extend the life-span of the Grandstand with additional 50 years (Bódi, Koris, Almási; 2008). No major damage of the reinforced concrete structure was found; however, the resistance of some cross-sections did not fulfil the requirements of the Eurocode Standard; therefore, the following actions were implemented (Almási, Varvasovszky, Juhász; 2003).

To provide the necessary anchorage for the cantilever roof beams, new anchoring columns were manufactured (*Fig. 6*). A new anchorage beam was also applied above the second

Fig. 7: Strengthening of the cantilever structure: a) New suspension column; b) Injection of cracks; c) CFRP sheets

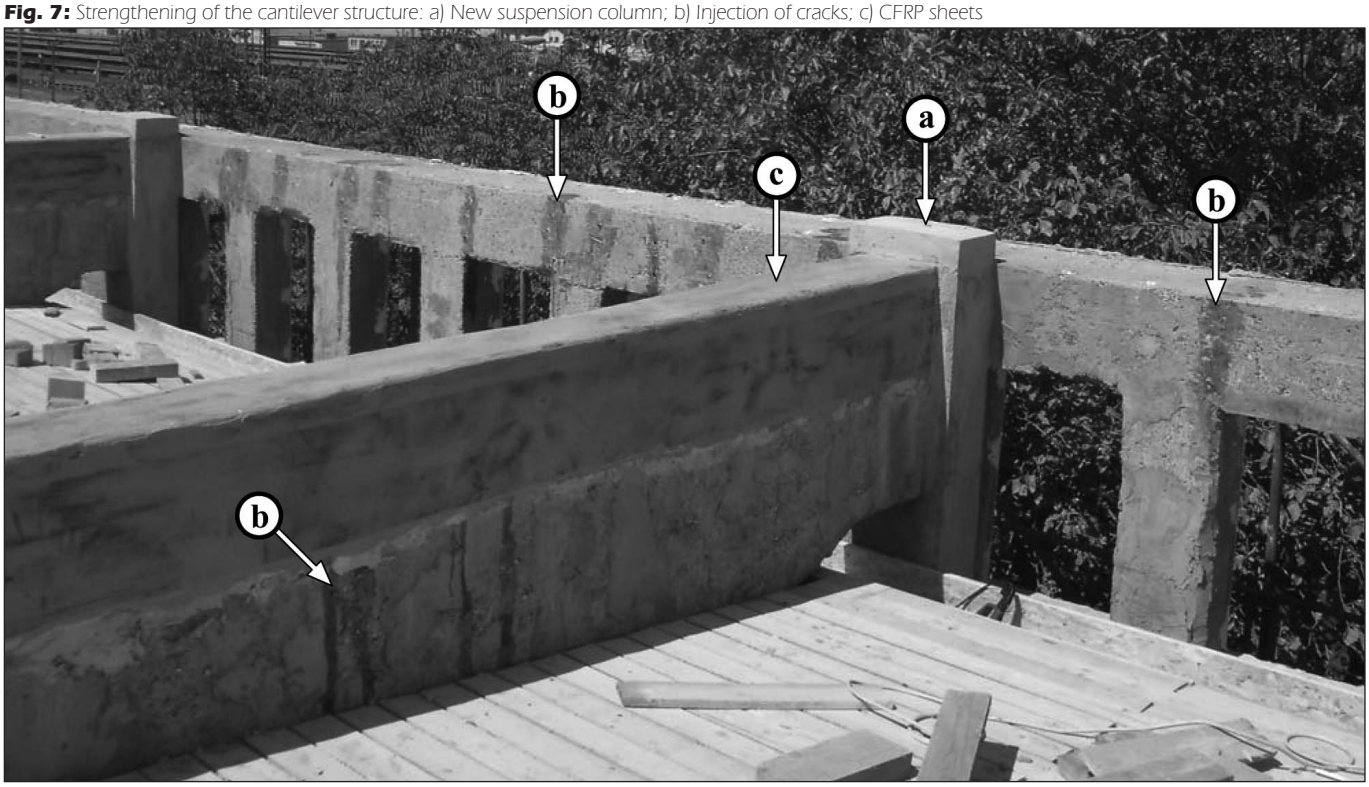

Fig. 8: *The Class II Grandstand after complete renovation*

level to withstand the additional tensile forces. Cantilever beams on the roof were strengthened by bonded CFRP sheets (*Fig. 7*) to provide the necessary load bearing capacity (Sika Hungária, 1999). Cracks in the concrete structure were cleaned and injected with MAPEI Epojet resin before strengthening (*Fig. 7*). The concrete strength in the upper section of middle columns was insufficient therefore these columns were also strengthened by 50 mm concrete jacketing (*Fig. 6*). Former chimneys were cleaned with water jet and the holes were filled with concrete of C20-8/K quality. The stepped concrete slab was originally built with a thickness of 60 mm and the applied reinforcing steel inside the slab was only Ø5/120 mm. Due to these reasons the resistance of the slab is insufficient against concentrated live load. A force distribution layer was applied on this slab to provide the necessary resistance against concentrated loads. Shrinkage cracks were observed in the secondary concrete structures, such as curved stairs, concrete barriers and banisters. These cracks were again cleaned and injected with MAPEI Epojet resin to avoid further corrosion problems.

Strengthening of the reinforced concrete structural parts was followed by complete restoration of the Grandstand including isolation of the roof, facing of walls and columns and tiling of floors and stairs, decorative lighting, etc. (*Fig. 8*).

5. CONCLUSIONS

Most of the buildings of the former racecourse in Budapest were demolished to enable the construction of a new shopping centre. The building of the Class II Grandstand was declared as a national monument so it was preserved and integrated into the new building complex. A complete statical investigation of the Grandstand was carried out including measurements on site, laboratory tests and computer analysis. The strengthening of the building was designed and performed in view of the results of the previous investigations. The complex strengthening and careful renovation (*Fig. 8*) restored the original structural conditions, extended the life-span of the building with 50 years and ensured the integration of the 70-year-old Grandstand and the surrounding urban environment.

6. REFERENCES

Bódi, I. – Koris, K. – Erdődi, L. (2002), "Statical condition of load bearing structures of Class II and III Kerepesi Grandstands, Budapest" (in Hungarian) *Final Report (№ 34201/2007)*, BUTE Department of Structural Engineering, Budapest.

Bódi, I. – Koris, K. – Almási, J. (2008), "Upgrading of a 70 year old Grandstand", *Proceedings of the 17th IABSE Congress "Creating and Renewing Urban Structures, Tall Buildings, Bridges and Infrastructure"*, p.1-6, Chicago, USA.

Paulheim, F. jr. (1935) "Plans of the Class II Kerepesi Grandstand" (in Hungarian) Budapest.

Obrist, V. (1936) "Statical calculations of the reinforced concrete structures and the foundations of Class II Kerepesi Grandstand" (in Hungarian) *Manuscript*, Budapest.

Almási, J. – Varvasovszky, P. – Juhász, S. (2003) "Strengthening plan of cantilever structure of Class II Kerepesi Grandstand" (in Hungarian) *Manuscript*, CAEC Kft, Budapest.

Sika Hungária Kft (1999) "Technical Guide for the Sika CarboDur Composite Strengthening Systems" (in Hungarian) Budapest.

Dr. István Bódi (1954) civil engineer, post-graduate engineer in mathematics, PhD, Associate professor at the Department of Structural Engineering, Budapest University of Technology and Economics. Research fields: Reconstruction and strengthening of reinforced concrete and conventional structures, modelling of timber structure joints. Member of the ACI (American Concrete Institute), the ACI Subcommitte#423 „Prestressed Concrete" and the Hungarian Chamber of Engineers. President of the standardization committee Eurocode 5 - MSZ NAD (Timber Structures). Member of the Hungarian Group of ***fib***. Member of the „Schweizerische Arbeitgemeinschaft für das Holz".

Dr. Kálmán Koris (1970) structural engineer, MSc, PhD, Senior assistant professor at the Department of Structural Engineering, Budapest University of Technology and Economics. Research fields: safety of reinforced concrete structures, analysis of prefabricated, prestressed concrete structures, strengthening of structures. Member of the standardization subcommittee "NAD MSZ ENV 1992 Eurocode 2, Design of concrete structures". Member of the Hungarian Group of ***fib***.

András Molnár (1983) civil engineer, MSc, PhD student at the Department of Structural Engineering, Budapest University of Technology and Economics. His main field of interest is the structural application of fibre reinforced polymers at upgrading structures and structural members, and strengthening of existing reinforced concrete and timber structures with regard to prestressed application. Member of the Hungarian Group of ***fib***.

INTRODUCTION OF A CONSTITUTIVE MODEL FOR THE REBOUND SURFACE HARDNESS OF CONCRETE



Katalin Szilágyi – Adorján Borosnyói – István Zsigovics

Surface hardness testing of concrete is a long established NDT method for in-situ strength estimation. Nowadays, the so-called Schmidt rebound hammer is the surface hardness testing device for concrete of the most widespread use. The device has been in use from the 1950's and considerable practical experience is collected and published in the technical literature. However, based on a comprehensive literature review it is realized that no general theory has been developed in the last more than 50 years that could describe the relationship between the measured surface hardness values and the compressive strength of concrete. Present paper introduces a phenomenological constitutive model (SBZ-model) that can be formulated for the surface hardness of concrete being a time dependent material property. The generating functions of the model are founded on the time dependent development of the capillary pore system of the hardened cement paste in concretes that is characterised by the water-cement ratio as a practical simplification. Parametric simulation and an extensive experimental verification of the model clearly demonstrated the reasonable application possibilities.

Keywords: Schmidt rebound hammer, surface hardness, rebound index, strength estimation

1. INTRODUCTION

In-situ surface hardness testing of materials is an accepted method for strength estimation. Development of surface hardness testing devices goes back more than 100 years. Hardness research was initialized by the pioneering work of *Hertz* in the 1880's (Hertz, 1881). Nevertheless, hardness testing was also the first material testing effort from the 1600's in engineering as scratching hardness testing (1614 – *Barba*; 1722 – *Réaumur*; 1768 – *Kvist*; 1801 – *Haüy*; 1812 – *Mohs*). In-situ testing of concrete structures was started in the 1930's. The testing methods at that time covered chisel blow tests, drilling tests, revolver or special design gun shooting tests, splitting tests, pull-out tests, strain measurements from loading tests and the adaptation of the *Brinell hardness* testing method (Skramtajew, 1938). This latter technique was found to be the most popular in the European testing practice for decades according to its relatively simple and fast operation (Gaede, 1934; Williams, 1936). Nowadays the most widespread method for the surface hardness testing of concrete is the rebound hammer method that is appeared in the 1950's by the *Schmidt* rebound *hammer* (also known as *Swiss hammer*) (Schmidt, 1950).

2. SCLEROSCOPE HARDNESS TESTING OF CONCRETE

The concrete rebound hammers use the scleroscope method introduced by *Shore* in 1911 (Shore, 1911). Scleroscope devices are impact testers in which spring accelerated or gravity accelerated hammer masses impinge against the tested surface and the hardness index is defined as a measure of the impact rebound. Two types of hardness index are defined usually: 1) the ratio of the paths driven by the hammer mass before and after impact (R-value), and 2) the ratio of the velocities of the hammer mass before and after impact (Q-value). Both types of hardness index are used for metal as well as for concrete hardness testing (see *Table 1*.)

Concrete rebound hammers can be spring hammers or pendulum hammers. Present paper focuses exclusively on spring hammers that are indicated as N-type rebound hammers by the original design of *Schmidt*. In the N-type rebound hammers a mass accelerated by a spring is sliding along a guide bar and impacts one end of a steel plunger the far end of which is compressed against the concrete surface (Proceq, 2003). The impact energy is constant (2.207 Nm) and independent from the operator, since the tensioning of the spring during operation is automatically released at a maximum position causing the hammer mass to impinge with the stored elastic energy of the tensioned spring. The hammer mass rebounds from the plunger and its movement is recorded. Based on the recordings either the rebound index (R) or the square of the coefficient of restitution (i.e. the Q-value) can be resulted, given by different hardness testers. The details of the operation of the devices are given elsewhere (Szilágyi, Borosnyói, 2009).

Table 1. Scleroscope hardness testing methods.

Hardness index based on hammer mass rebound: R-value	Hardness index based on hammer mass velocity: Q-value or C_R-value
for concretes	
The original design of Schmidt rebound hammer	The 2008 design of Silver Schmidt rebound hammer
for metals	
SKL scleroscope Duroskop tester	Leeb tester

3. EXPERIENCES OF THE SURFACE HARDNESS OF CONCRETE

Rebound surface hardness measurements were found to be very popular in the in-situ material testing due to the inexpensive testing devices and their relatively simple use. Numerous publications are available in the technical literature concerning experimental results and analyses. Based on a comprehensive literature review it is realized that no general theory has been developed in the last more than 50 years that could describe the relationship between the measured surface hardness values and the compressive strength of concrete (Szilágyi, Borosnyói, 2009). Only one semi-empirical derivation for such a relationship was attempted by the designer of the concrete rebound hammers and the model covered also the Brinell hardness of concrete (Gaede, Schmidt 1964). As a consequence, the model can not be generally used since very limited data have been published for the Brinell hardness of cementitious materials. Neither accurate theory for the hardness of porous solids nor acceptable compressive strength vs. hardness relationships is available in the technical literature. Future research should provide better understanding and modelling of the surface hardness behaviour of porous solids, especially that of cementitious materials.

On the other hand, numerous empirical relationships were proposed by several researchers concerning the surface hardness vs. compressive strength of concrete in the last more than 50 years. Based on a comprehensive literature review the following fundamental observations can be emphasized (Szilágyi, Borosnyói, 2009):

- The empirical rebound surface hardness vs. compressive strength relationships are generally non-linear. Most accepted form is the power function.
- Several linear relationships were also published based on experiments of narrow strength ranges.
- Concrete strength estimation for a given rebound index is found to be published in a ±40 to 60 N/mm^2 wide range (it is possible to find estimated strengths for different concretes with 40 to 60 N/mm^2 strength differences corresponding to the same rebound surface hardness).
- Statistical analysis of the surface hardness vs. compressive strength relationships is usually indicates heteroscedastic behaviour (i.e. increasing standard deviation in strength (Y variable) for increasing rebound index (X variable)). Even the manufacturer of the original design concrete rebound hammers suggests increasing standard deviations to be taken into account for increasing rebound surface hardness. Heteroscedastic behaviour is indicated in *Fig. 1.* (Schmidt, 1950) and *Fig. 2.* (Zoldners, 1957).
- Strength estimation (based on tests carried out under ideal laboratory conditions) can provide an accuracy of ±15 to 20%; however, in a practical situation it is unlikely that a strength prediction can be made with an accuracy better than ±30 to 40%.
- Current European Standard testing practice (EN 13791:2007) excludes the use of the rebound surface hardness test for strength estimation on its own due to the limited accuracy provided. Testing of drilled cores together with the rebound surface hardness tests is suggested for an acceptable reliability.

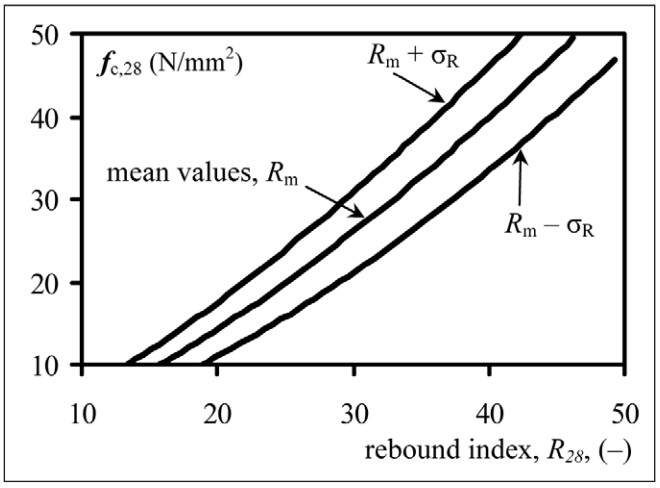

Fig. 1. Heteroscedastic behaviour of the rebound surface hardness vs. compressive strength relationship (based on Schmidt, 1950).

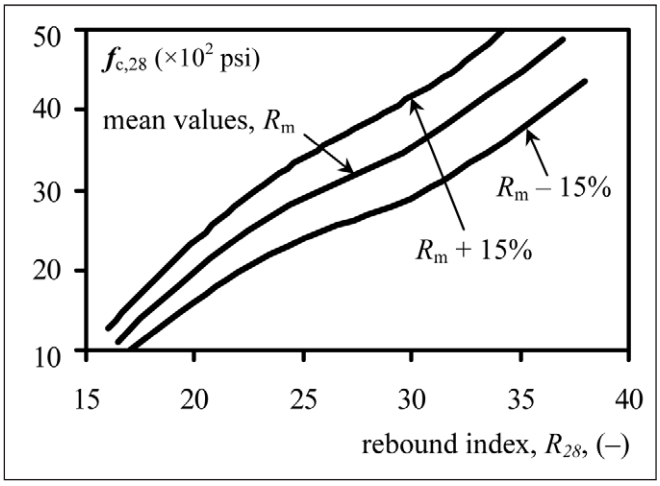

Fig. 2. Heteroscedastic behaviour of the rebound surface hardness vs. compressive strength relationship (based on Zoldners, 1957). Note: 1 psi = 6,894×10^{-3} N/mm^2.

4. GENERATING A PHENOMENOLOGICAL CONSTITUTIVE MODEL

The primary factor that governs the characteristics of cementitious materials is porosity. It was found experimentally that the evolution of porosity in concrete can be described reasonably well by the gel-to-space ratio (Powers, Brownyard, 1947). Working with gel-to-space ratio it is necessary to know the degree of hydration in the hardened cement paste, therefore, the water-cement ratio (w/c) is a much more practical measure for the porosity of concrete (Neville, 1995). For practical purposes it can be accepted that the water-cement ratio (w/c) determines the capillary porosity of a properly compacted concrete at any degree of hydration (Mindess, Young, 1981). As a consequence, strength and related properties of concrete can be accepted to depend primarily on the w/c ratio as it was realized more than 100 years ago (Feret, 1892; Abrams, 1918). Surface hardness of concrete is also considerably influenced by the w/c ratio in addition to the modulus of elasticity of the aggregate particles (which is usually considered to be constant in time). Hydration of clinker minerals in the hardened cement paste makes the per se heterogeneous concrete to be a material with time dependent properties. Based on this general behavioural scheme, a phenomenological constitutive model (*SBZ-model;* the abbreviation was put together from the names of the authors) can be formulated for the surface hardness of concrete being a time dependent material property.

The generation scheme of the SBZ-model as well as the symbolic shapes of the individual functions given by Eq. (1) to Eq. (5) can be studied in *Fig. 3*. The formulation of the model

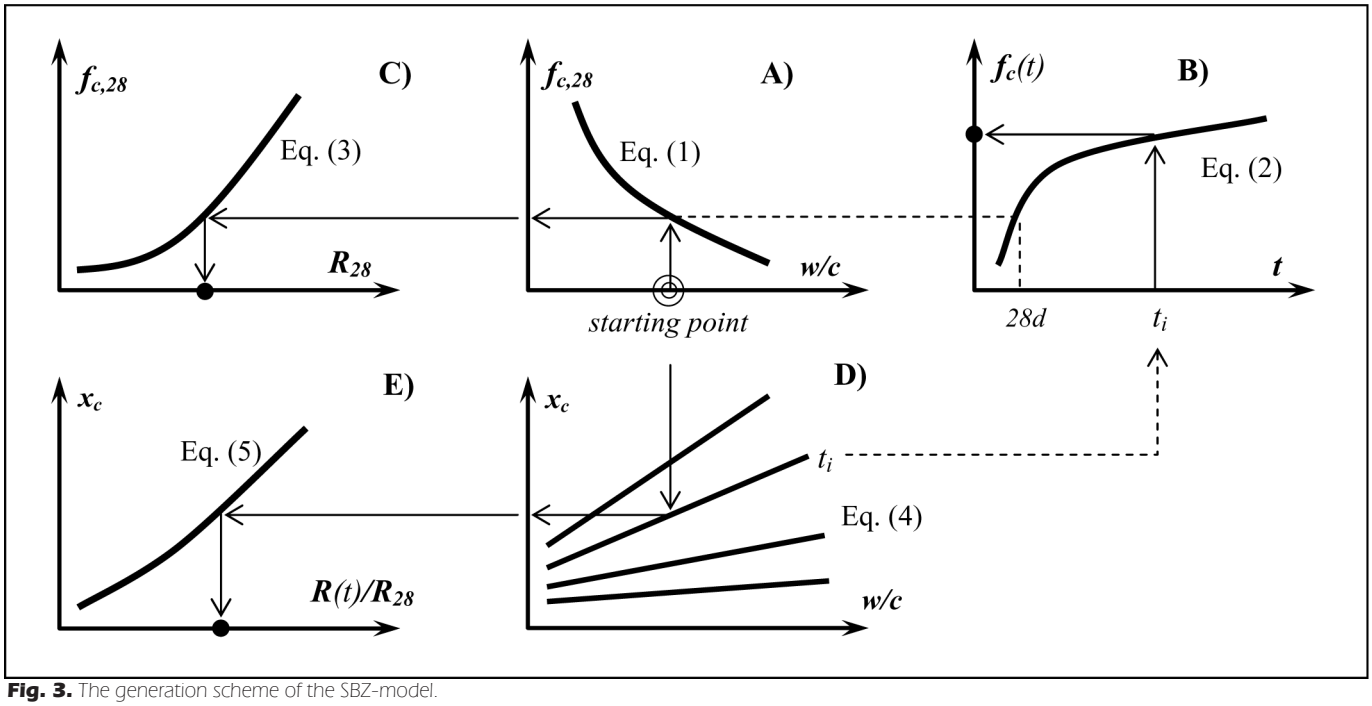

Fig. 3. *The generation scheme of the SBZ-model.*

includes the following experimental findings:

A) The compressive strength of concrete at the age of 28 days can be described by an exponential function of the w/c ratio (Eq. 1).

$$f_{c,28} = a_1 \cdot exp\left\langle a_2 \cdot (w/c)^{a_3} \right\rangle \qquad \text{Eq. (1)}$$

with
$a_1 > 1$
$a_2 < 0$
$0 < a_3 < 1$

B) The development of the compressive strength of concrete with time can be followed by an exponential function of time (Eq. 2).

$$f_c(t)/f_{c,28} = exp\left\langle a_4 \cdot (1-(28/t)^{a_5} \right\rangle \qquad \text{Eq. (2)}$$

with
$0 < a_4 < 1$
$0 < a_5 < 1$
and both parameter a_4 and a_5 is a function of ***w/c***

C) An empirical relationship of a power function can be assumed between the strength of concrete and the rebound index at the age of 28 days (Eq. 3).

$$f_{c,28} = a_6 \cdot R_{28}^{\ a} \qquad \text{Eq. (3)}$$

with
$a_6 > 0$
$a_7 \geq 1$

D) The development of the carbonation depth in concrete with time can be described by models based on *Fick*'s law of diffusion (Eq. 4).

$$x_c = \left(a_8 \cdot (w/c) - a_9\right) \cdot t^{a_{10}} \qquad \text{Eq. (4)}$$

with
$0 < a_8 < 1$
$0 < a_9 < 1$
$0 < a_{10} < 1$

E) Carbonation of concrete results an increase in the surface hardness that can be assumed to be modelled by a power function of the carbonation depth (Eq. 5).

$$R(t)/R_{28} = \frac{1}{1 + a_{11} \cdot x_c^{\ a_{12}}} \qquad \text{Eq. (5)}$$

with
$a_{11} < 0$
$a_{12} > 0$

The SBZ-model can provide corresponding compressive strength, f_c(t) and rebound index, R(t) values for any w/c ratio at any age of concrete (t).

A typical f_c(t) vs. R(t) relationship is represented in *Fig. 4*: the output of the model is a set of curves corresponding to different w/c ratios at different ages of the concrete. It should be noted that the shape and curvature of the individual curves are depending on the actual values of the twelve empirical constants a_1 to a_{12} covered in Eqs. (1) to (5) and *Fig. 4* indicates a possible general case.

It can be realized that the SBZ-model provides a reasonable depiction of the surface hardness of concrete as a time dependent material property, as a function of known concrete technological data. It should be also noted that the SBZ-model gives a clear explanation for the experimental findings about the *apparent heteroscedastic behaviour* of the rebound index vs. compressive strength data pairs. The SBZ-model calls the attention that the graphical representation of these results should not be carried out by the simplifying assumption that concretes of different w/c ratios and different ages provide data being in the same population. It can be clearly seen that the simplification could result misleading representation and the influencing parameters should be separated in the graphical visualization as it is suggested by the SBZ-model.

5. PARAMETRIC SIMULATION FOR THE SBZ-MODEL

The present chapter gives a parametric simulation for the SBZ-model. Empirical formulations are selected from the technical literature for the generating functions of the model as follows.

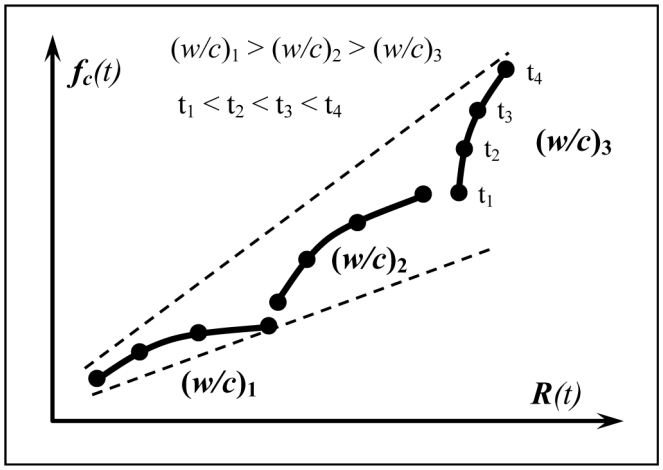

Fig. 4. Typical fc(t) vs. R(t) response as an output of the SBZ-model: a set of curves corresponding to different w/c ratios at different ages of the concrete.

Most simple exponential formulation of the compressive strength of concrete as a function of the w/c ratio was suggested by *Abrams* in the form of:

$$f_{c,28} = A \cdot exp\langle B \cdot (w/c)\rangle \qquad \text{Eq. (6)}$$

It can be demonstrated that the formula given by Eq. (6) can not be fitted to the experimental data available for different cement types, therefore an improvement of the formulation was suggested; see Eq. (1) (Ujhelyi, Popovics, 2006). For present parametric simulation the empirical formula of *Ujhelyi* (2005) is applied to the exponential function between the compressive strength of concrete at the age of 28 days vs. the w/c ratio for CEM I 42.5 N and Eq. (1) is rewritten as:

$$f_{c,28} = 406 \cdot exp\langle -3.30 \cdot (w/c)^{0.63}\rangle \qquad \text{Eq. (1*)}$$

Development of the compressive strength of concrete is depending on the type of cement and the w/c ratio (Wood, 1991). However, models available usually neglect the influence of the w/c ratio. For present parametric simulation the proposal of the CEB-FIP Model Code 1990 (CEB, 1993) is applied to the exponential function of the development of the compressive strength of concrete with time, neglecting the influence of the w/c ratio and Eq. (2) is rewritten as:

$$f_c(t)/f_{c,28} = exp\langle 0.25 \cdot (1-(28/t)^{0.50}\rangle \qquad \text{Eq. (2*)}$$

Rebound surface hardness vs. compressive strength relationships are generally non-linear, and several different types of functions (power functions, polynomial functions, exponential functions, logarithm functions, even linear functions) have been published so far and collected by the Authors of present paper (Szilágyi, Borosnyói, 2009). For the parametric simulation demonstrated herein the proposal of Proceq SA (manufacturer of the *Schmidt* rebound hammers) (Proceq, 2003) is applied to the empirical relationship of a power function that is assumed between the strength of concrete and the rebound index at the age of 28 days, so Eq. (3) is rewritten as:

$$f_{c,28} = 3.07 \times 10^{-2} \cdot R_{28}^{1.952} \qquad \text{Eq. (3*)}$$

The hardened cement paste in concrete reacts chemically with carbon dioxide (CO_2). The amount of CO_2 present in the atmosphere is sufficient to cause considerable reaction with the hardened cement paste over a long period of time. The chemical

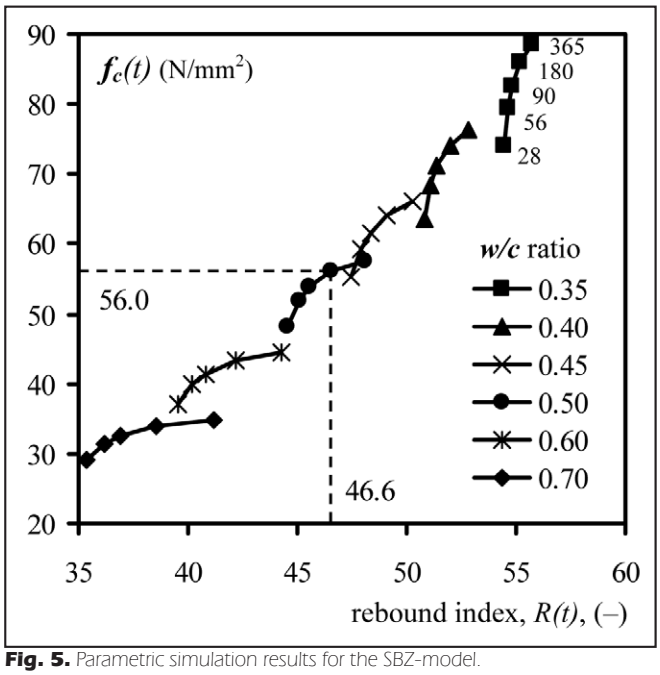

Fig. 5. Parametric simulation results for the SBZ-model.

reaction is referred as *carbonation*, whenever the hydrated lime content of the hardened cement paste turns to limestone by the chemical reaction with CO_2. Rate of carbonation depends on the relative humidity and was found to be greatest around 50% RH (Neville, 1995). Development of the depth of carbonation in concrete with time can be described reasonably well by models based on *Fick*'s law of diffusion. For present parametric simulation the model of *Papadakis et al* (1992) is applied to the carbonation depth of concrete. Its generalized form for the development of the carbonation depth with time is:

$$x_c = \psi 0.35 \rho_c \frac{w/c - 0.30}{1 + \frac{\rho_c}{1000} w/c} f(\mathrm{RH}) \cdot \cdot \left(\left(1 + \frac{\rho_c}{1000} w/c + \frac{\rho_c}{\rho_a} a/c \right) C_{CO_2} \frac{23.8}{44} 10^{-6} t \right)^{0.50}$$

Eq. (7)

In Eq. (7) the parameter f(RH) can be taken according to the results of *Matoušek* (1977). If one accepts f(65% RH) = 0.45, C_{CO2} = 800 mg/m^3, ρ_c = 3150 kg/m^3 and ρ_a = 2650 kg/m^3 the generalized form of Eq. (7) can be simplified and rearranged and Eq. (4) can be rewritten as:

$$x_c = (0.50 \cdot (w/c) - 0.14) \cdot \sqrt{t} \qquad \text{Eq. (4*)}$$

Limits of use of application for Eq. (4*) are $0.35 < w/c < 0.65$ and $4.50 < a/c < 6.50$. It means c = 290 kg/m^3 to 420 kg/m^3 cement content to be assumed. For different relative humidity (RH ≠ 65%) and CO_2 concentration values Eq. (7) applies.

Surface hardness of concrete can be considerably changed by carbonation (Wesche, 1967). Therefore, in the evaluation of rebound surface hardness tests the influence of carbonation should be taken into account. For present parametric simulation the proposal of the Chinese Standard JGJ/T23-2001 (Proceq, 2003; Szilágyi, Borosnyói, 2009) is applied to describe the influence of carbonation depth on the surface hardness of concrete, so Eq. (5) can be rewritten as:

$$R(t)/R_{28} = \frac{1}{1 - 0.047 \cdot x_c^{1.0}} \qquad \text{Eq. (5*)}$$

The limit of use to apply Eq. (5*) is $x_c < 6.0$ mm.

A result of the present parametric simulation can be studied in *Fig. 5*. For one point on the series of curves (indicated with dashed lines in *Fig. 5.*) as an example the following details are given. Starting value for water-cement ratio is $w/c = 0.50$ and age of concrete is $t = 180$ days. Based on formulae covered by Eq. (1*) to (5*) the numerical results can be calculated as follows.

By Eq. (1*): $f_{c,28} = 406 \cdot exp\langle -3.30 \cdot 0.50^{0.63} \rangle = 48.13$ N/mm^2

By Eq. (2*): $f_c(180) = 48.13 \cdot exp\langle 0.25 \cdot (1 - (28/180)^{0.50} \rangle = 56.0$ N/mm^2

By Eq. (3*): $R_{28} = 5.96 \cdot 48.13^{0.512} = 43.35$

By Eq. (4*): $x_c(180) = (0.50 \cdot 0.50 - 0.14) \cdot \sqrt{180} = 1.48$ mm

By Eq. (5*): $R(180) = 43.35/(1 - 0.047 \cdot 1.48) = 46.6$

It can be realized that the SBZ-model gives a realistic formulation for the time dependent behaviour of the rebound surface hardness of concrete.

6. EXPERIMENTAL VERIFICATION OF THE SBZ-MODEL

An extensive experimental study was carried out at the Budapest University of Technology and Economics (BME), Department of Construction Materials and Engineering Geology for the verification of the developed SBZ-model. The tested concrete mixes were prepared in accordance with present concrete construction needs during the experiments, i.e. slightly over-saturated mixes with different admixtures were designed. Consistence of the tested concrete mixes was constant: 500±20 mm flow. Design air content of the compacted fresh concrete for the tested concrete mixes was 1.0V%. As curing the specimens were stored in water tank for 7 days. After 7 days the specimens were stored at laboratory condition (i.e. 20±3°C temperature and 65±5% relative humidity). Test parameters were:

Water-cement ratio:
0.38 – 0.41 – 0.43 – 0.45 – 0.47 – 0.50 – 0.51 – 0.55 – 0.60

Cement type:
CEM I 42.5 N – CEM II/A-V 42.5 N – CEM III/B 32.5 N

Cement content (kg/m³):
300 – 350 – 400

Mixing water content (kg/m³):
150 – 165 – 180

Cement paste content (litres/m³):
247 – 263 – 278 – 293 – 309

Aggregate-cement ratio:
4.5 – 4.6 – 4.7 – 5.3 – 5.4 – 5.5 – 6.3 – 6.5 – 6.6

Admixture type:
accelerator admixtures (3 types)

Age of concrete at testing (days):
7 – 14 – 28 – 56 – 90 – 180

The experimental programme made possible a detailed verification study to be carried out on a wide range of compressive strengths and ages of concrete at testing. Total number of 864 specimens (150 mm cubes) were tested at six different ages for present verification study. Typical results are indicated in *Fig. 6.* corresponding to concrete specimens prepared with CEM I 42.5 N cement. *Fig. 6.* represents test results for 104 specimens. The following observations can be emphasized:

1) An apparently coherent population of data is resulted if one does not differentiate water-cement ratios and ages of concrete in the graphical representation of test data (*Fig. 6a.*). A completely misleading trend of results is realized and an apparent power function or exponential function relationship can be the output of a regression analysis (usually with considerably good correlation coefficient which further ratifies the misleading direction of this analysis). In *Fig. 6a.* 52 data points are indicated as the pair-averages of the 104 specimens (covering 9 different water-cement ratios and 6 different ages of concrete at testing). Regression curve of an exponential

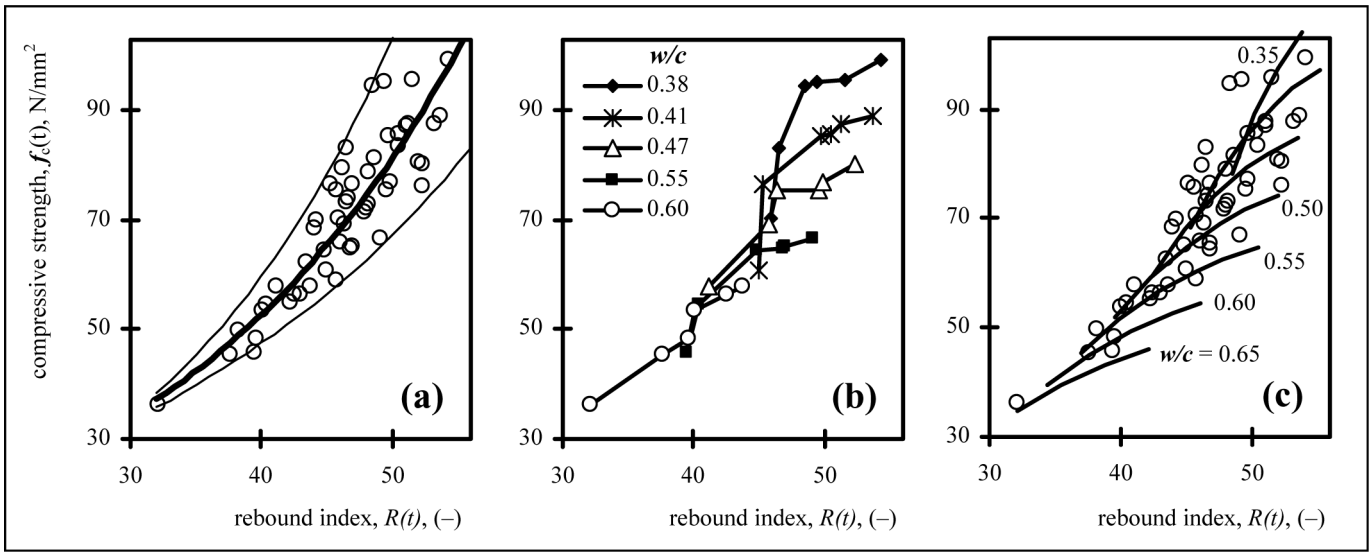

Fig. 6. Experimental verification of the SBZ-model on concrete cube specimens prepared with CEM I 42.5 N cement.
a) data not separated b) data separated by the applied water-cement ratios c) data separated by the fitted SBZ-model

function is also indicated. The correlation coefficient was found to be $r^2 = 0.84$ of this false relationship.

2) An apparent heteroscedastic behaviour of the rebound index vs. compressive strength data pairs is realized if one does not differentiate water-cement ratios and ages of concrete in the graphical representation of test data (*Fig. 6a.*). It can be studied in *Fig. 6a.* that the distance between the lower and upper limit curves corresponding to the increasing rebound index values is increasing that can result the apparent heteroscedasticity (i.e. increasing standard deviation in strength for increasing rebound index).

3) The real performance appears only if one separates the rebound index vs. compressive strength data pairs according to the water-cement ratio (*Fig. 6b.*). For the sake of better visualisation only 5 curves are represented in *Fig. 6b.* from the 9 different water-cement ratios studied. It can be realized that the apparently coherent family of data comes loose to separate monotonic curves for the different water-cement ratios.

4) It can be seen in the real performance that rebound index vs. compressive strength relationships are sensitive (but not uniformly) to the water-cement ratio applied (*Fig. 6b.*). The gradients and directions of the responses clearly indicate the influence of the capillary pores of different water-cement ratios on the strength development and carbonation depth development differences. It can be postulated that the water-cement ratio dependent strength development and carbonation depth development behaviour of concretes gives the complete explanation of the observed results.

5) The application of the SBZ-model is reasonable for the rebound index vs. compressive strength data (*Fig. 6c.*). A suitable fit of the empirical parameters of the SBZ-model can result an acceptable numerical reproduction of any experimental data. The detailed verification study demonstrated the applicability of the SBZ-model for CEM I 42.5 N, CEM II/A-V 42.5 N and CEM III/B 32.5 N cements on a wide range of water-cement ratios and ages of concrete at testing. The SBZ-model provides a clear understanding of the rebound surface hardness of concrete as a time dependent material property. Based on its composition the SBZ-model is deemed to be a unique phenomenological constitutive model available now for the rebound surface hardness of concrete.

7. CONCLUSIONS

Rebound surface hardness testing of concrete is one of the most widespread NDT methods for in-situ strength estimation of concrete structures. Rebound surface hardness methods are available in the civil engineering testing practice for more than 50 years. However, understanding and modelling of the rebound surface hardness of concrete as a time dependent material property is not available in the technical literature.

Present paper introduces the *SBZ-model* developed by the authors of the paper which is a phenomenological constitutive model for the rebound surface hardness of concrete as a time dependent material property, as a function of known concrete technological data. Origination of the SBZ-model is based on the time dependent development of the capillary pore system of the hardened cement paste in concretes that is characterised by the water-cement ratio as a practical simplification. The model covers the following empirical material laws: relationship between the water-cement ratio and the compressive strength of concrete at the age of 28 days; development of the concrete compressive strength with time; relationship between the compressive strength of concrete and the rebound index at the age of 28 days; the development of carbonation depth of concrete with time; the influence of carbonation depth of concrete on the rebound index.

Parametric simulation and an extensive experimental verification of the SBZ-model clearly demonstrated its reasonable application possibilities. The transparency of the SBZ-model offers further promising development, however, provides also in its present form the long time missing fill to the gap of knowledge appeared in the last 50 years.

8. ACKNOWLEDGEMENTS

The authors gratefully acknowledge the support of the Bolyai János research scholarship by the Hungarian Academy of Sciences (MTA). Special thanks to Ms. Beáta *Horváth*, Mr. Tamás *Kasza* and Mr. Tamás *Póka* for their valuable help during the laboratory tests. The authors appreciate very much the detailed discussion of the manuscript by Dr. Attila *Erdélyi*.

9. NOTATIONS

a_1 to a_{12}	non-dimensional empirical parameters in the general SBZ-model, –
a/c	aggregate-to-cement ratio, m/m
C_R	coefficient of restitution, –
$f_{c,28}$	compressive strength at 28 days of age, N/mm^2
$f_c(t)$	compressive strength at t days of age, N/mm^2
R_{28}	rebound index at 28 days of age, –
R(t)	rebound index at t days of age, –
RH	relative humidity, %
Q	square of coefficient of restitution, –
t	time, days
w/c	water-cement ratio, m/m
x_c	carbonation depth, mm
ρ_a	density of aggregate, kg/m^3
ρ_c	density of cement, kg/m^3
ψ	uncertainty factor in the model by Papadakis *et al*, –

10. REFERENCES

Abrams, D. A. (1918) „Effect of Time of Mixing on the Strength and Wear of Concrete", *ACI Journal Proceedings*, Vol. 14., Issue 6., pp. 22-92.

CEB (1993) „CEB-FIP Model Code 1990 – Design Code", Comité Euro-International du Béton, *Thomas Telford*, London, 1993 (CEB Bulletin d'Information No. 213/214.)

EN 13791 (2007) „Assessment of in-situ compressive strength in structures and precast concrete components", *European Standard*

Feret, R. (1892) „The compaction of hydraulic mortars (Sur la compacité des mortiers hydrauliques)", *Annales des Ponts et Chaussees*, Mem Doc, Serie 7, 4, 1892, pp. 5-164. (in French)

Gaede, K. (1934) „A new method of strength testing of concrete in structures (Ein neues Verfahren zur Festigkeitsprüfung des Betons im Bauwerk)", *Bauingenieur*, 1934/15, Vol. 35-36., pp. 356-357. (in German)

Gaede, K., Schmidt, E. (1964) „Rebound testing of hardened concrete (Rückprallprüfung von Beton mit dichtem Gefüge)", *Deutscher Ausschusses für Stahlbeton*, Heft 158, p. 37. (in German)

Hertz, H. (1881) „About the contact of elastic solid bodies (Über die Berührung fester elastischer Körper)", *Journal für die reine und angewandte Mathematik*, 1881/5, p. 12-23. (in German)

Matoušek, M. (1977) „Effects of some environmental factors on structures", *PhD Thesis,* Technical University of Brno, Czech Republic, 1977 (in Czech)

Mindess, S., Young, J. F. (1981) „Concrete", *Prentice Hall,* Englewood Cliffs, 671 p.

Neville, A. M. (1995) „Properties of Concrete", *Prentice Hall,* Essex, 844 p.

Papadakis, V. G., Fardis, M. N., Vayenas, C. G. (1992) „Hydration and Carbonation of Pozzolanic Cements", *ACI Materials Journal*, V. 89, No. 2, March-April 1992, pp. 119-130.

Powers, T. C., Brownyard, T. L. (1947) „Studies of the Physical Properties of Hardened Portland Cement Paste", *Journal of the American Concrete Institute*, April 1947, Vol. 18 (Proceedings Vol. 43), No. 8, pp. 933-992.

Proceq SA (2003) „Concrete Test Hammer N/NR,L/LR and DIGI SCHMIDT ND/LD – Rebound Measurement and Carbonation”, *Info sheet*
Schmidt, E. (1950) „The concrete testing hammer (Der Beton-Prüfhammer)”, *Schweizerische Bauzeitung*, 15. Juli 1950, 68. Jahrgang, Nr. 28, pp. 378-379. (in German)
Shore, A. T. (1911) „Property of Hardness in Metals and Materials”, *Proceedings*, ASTM, Vol. 11., 1911, pp. 733-739.
Skramtajew, B. G. (1938) „Determining Concrete Strength in Control for Concrete in Structures”, *Journal of the American Concrete Institute*, January-February 1938, Vol. 9 (Proceedings Vol. 34), No. 3, pp. 285-303.
Szilágyi, K., Borosnyói, A. (2009) „50 years of experience with the Schmidt rebound hammer”, *Concrete Structures*, Vol. 10, 2009, pp. 46-56.
Ujhelyi, J. (2005) „Concrete knowledge (Betonismeretek)”, *BME University Press*, 346 p. (in Hungarian)
Ujhelyi, J., Popovics, S. (2006) „Improvements in accuracy of the relationship between concrete strength and water-cement ratio (A betonszilárdság és a víz-cement tényező közötti összefüggés megbízhatóságának javítása)”, *Vasbetonépítés*, Vol. VIII., Issue 1., pp. 2-9. (in Hungarian)
Wesche, K. (1967) „Strength testing of concrete in structures (Die Prüfung der Betonfestigkeit im Bauwerk)”, *Betonstein-Zeitung*, Heft 6/1967, pp. 267-277. (in German)
Williams, J. F. (1936) „A Method for the Estimation of Compressive Strength of Concrete in the Field”, *The Structural Engineer* (London), Vol. 14., No. 7., July 1936, pp. 321-326.
Wood, S. (1991) „Evaluation of the Long-Term Properties of Concrete”, *ACI Materials Journal*, V. 88, No. 6, November-December 1991, pp. 630-643.
Zoldners, N. G. (1957) „Calibration and Use of Impact Test Hammer”, *Journal of the American Concrete Institute*, V. 29, No. 2, August 1957, Proceedings V. 54, pp. 161-165.

Katalin Szilágyi (1981) civil engineer (MSc), PhD candidate at the Department of Construction Materials and Engineering Geology, Budapest University of Technology and Economics. *Main fields of interest:* diagnostics of concrete structures, non-destructive testing of concrete, concrete technology, shrinkage compensation of concretes. Member of the Hungarian Group of *fib*.

Dr. Adorján Borosnyói (1974) civil engineer (MSc), PhD, senior lecturer at the Department of Construction Materials and Engineering Geology, Budapest University of Technology and Economics. *Main fields of interest:* application of non-metallic (FRP) reinforcements for concrete structures, bond in concrete, non-destructive testing of concrete. Member of the Hungarian Group of *fib* and of *fib* TG 4.1 „Serviceability Models”.

Dr. István Zsigovics (1949) civil engineer (MSc), PhD, senior lecturer at the Department of Construction Materials and Engineering Geology, Budapest University of Technology and Economics. *Main fields of interest:* concrete technology, self-compacting concretes, diagnostics of concrete structures, non-destructive testing of concrete. Member of the Hungarian Group of *fib*.

DETERMINATION OF K_{IIC} STRESS INTENSITY FACTOR ON NEW SHAPE CONCRETE SPECIMENS



Sándor Fehérvári – Miklós Gálos – Salem G. Nehme

Under load, the number of fissures in concrete or reinforced concrete increases, and such cracks will be the starting points of failure. In order to understand the failure of such structures, the analysis of the stress state of crack tips is necessary, which is the subject matter of fracture mechanics. Due to material inhomogeneity and different modular coordination, the fracture analysis of concrete is more complex than the original tests devised for metals. While methods and specimens have been developed for tension failure (type I), the mode of examining shear failure (type II) has not yet been unequivocally established. This paper focuses on the analysis and test procedures of a new, compact specimen to study the K_{IIC} strength intensity factor.

Keywords: stress intensity factor, shear, compact specimen

1. INTRODUCTION

By the very nature of concrete and reinforced concrete, cracks, pores, and "defect locations" can be found even without loading. Loading increases the number of these defects. The subject of fracture mechanics is the description and characterization of the stress state around these cracks, as well as the determination of factors related to crack propagation. *Griffith* (1920) determined that the failure of any material begins at the locations of material failures. These defects are all the cracks, micro-cracks, open pores, etc. commonly found in concrete. The characterization of the fracture mechanics of a material is possible by the testing of a specially-shaped test specimen, and the analysis of the propagation of discrete, previously prepared cracks (notches). While relationships have been worked out for several different shapes and sizes of test specimens, there is no clearly standardized testing procedure or determination method for concrete. Earlier research, including those of the referenced literature, used a vast range of shapes and sizes for studying the fracture mechanics factors of concrete and reinforced concrete (and other up to date materials).

2. BASIC PRINCIPLES OF FRACTURE MECHANICS

The analysis and theoretical solution of stress concentrations is the subject of fracture mechanics research. During the evaluation of strength tests, the examiners revealed surprisingly high stress concentrations in the area of sharp notches. Cracks in the material change the distribution of stresses, and failure can and does occur due to the stress concentration in the area of the crack tip.

The theoretical and experimental examination of stresses at the crack tip ran in parallel in the last century. Metals were the primary focus of interest. Numerical methods first approached the problem with the help of linear theories. With the advancement of research and expansion of knowledge, increasingly complex mathematical models were created to describe the phenomenon. From the solution of linearly elastic problems, experiments employing special, complex mathematical tools for the basic equations of fracture mechanics first began to yield success at the beginning of the 20th Century. *Koloszov* (1909), *Inglis* (1913), and *Muszhelisvili* (1953) independently worked out complex stress formulae to describe the stress conditions in the area of holes in a linearly elastic disk. The solutions applied first to circular, later to oval holes, first to single, later to a few (not too many) weakenings (Koloszov, 1909; Inglis, 1913; Muszhelisvili, 1953). For certain special cases, *Westergaard* (1939) gave "simpler" complex stress-dependent solutions. The solution for generalized two-dimensional problems was first published by *Sih and Rice* (1965). *Sneddon* (1969) attempted a three-dimensional analytical solution, however, the results are only applicable to certain special cases.

In 1920, *Griffith* gave an approach based on the principle of energy near the crack tip (Griffith, 1920; Blumenauer and Push, 1987). The stress distribution around the ends of an ellipse narrowed beyond all limits (*Fig. 1*) leads to a singular result (infinite stress) in the mathematical model at the crack tip. The energy principle approach gave an entirely new direction to the development of fracture mechanics.

With his theory and the experiments supporting it, *Griffith* (1920) proved that the tensile strength of glass fiber varies between wide limits, depending upon diameter: 35-85 N/mm^2 (d > 10 mm) and 11500 N/mm^2 (d = atomic) (Griffith, 1920; Ujhelyi, 2005). *Jaeger and Cook* (1978) revealed a similar magnitudal difference in their study of hardened cement paste. Their research indicated that the theoretical strength of

Fig. 1: Crack modell and stress concentration according to Griffith (Blumenauer and Push, 1987; Gálos et al, 1994)

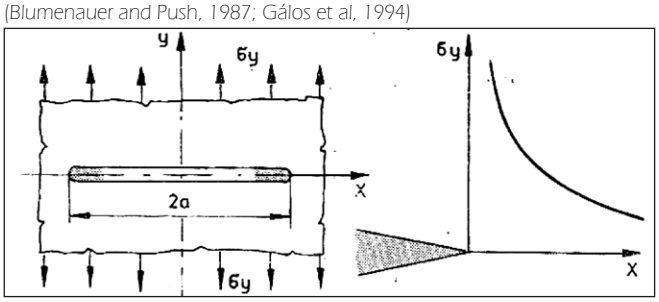

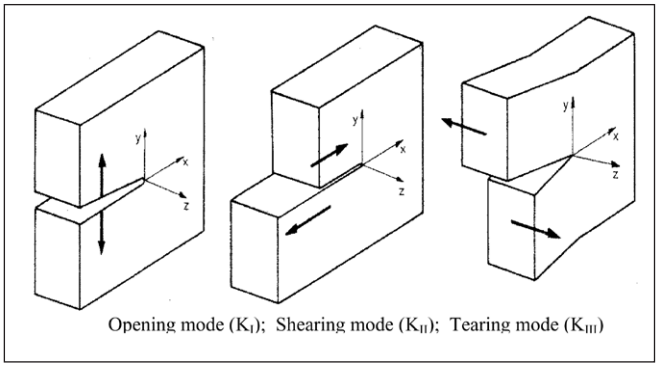

Fig. 2: Three basic modes of crakc tip to Irwin (Blumenauer and Push, 1987)

hardened cement paste can reach a value of 10500 N/mm^2, therefore faults and other practical conditions reduce the material strength to only 1% of that theoretically possible.

On the basis of his analytical stress examinations in the area of crack tips, *Irwin* (1957) suggested that:

- crack types should be typified so that their superposition is valid, assuming a linearly elastic material behavior of the structure;
- new metrics should be introduced for the examination of crack tips by modifying the formulae used to date, which, as a material property, will be a measure of the stress concentrations arising near the tip.

On the basis of *Irwin's* typifications, cracks subjected to tension belong to the first group (type I), shear, the second group (type II), and torsion, the third group (type III) (*Fig. 2*).

Thus, in the case of linear elasticity, with the help of the stress intensity factor considered as a material property, the stress concentrations can be determined near the crack tip of an elliptical hole narrowed beyond all limits (*Fig. 1*), by using the relationships of Equation 1. (Irwin, 1957; Sneddon, 1969)

$$\left.\begin{aligned}\sigma_{ij}(r,\theta) &= \frac{1}{\sqrt{2\pi R}}\left\{K_I f^{I}_{ij}(\theta)+K_{II} f^{II}_{ij}(\theta)+K_{III} f^{III}_{ij}(\theta)\right\}, i,j \Rightarrow x,y,z\\ u_i(r,\theta) &= \frac{1}{2\mu}\sqrt{\frac{R}{2\pi}}\left\{K_I g^{I}_{i}(\theta)+K_{II} g^{II}_{i}(\theta)+K_{III} g^{III}_{i}(\theta)\right\}, i \Rightarrow x,y,z\end{aligned}\right\} \quad (1)$$

The letter for the stress intensity factor, "K", preserves the name of *Kies*, who was *Irwin's* closest colleague and conducted the laboratory measurements. The stress intensity factors are the measure of resistance against quick crack propagation. During stress intensity examinations, the stress intensity factor obtained from calculated results must be compared to the critical stress intensity factor typical for the given material. The units of the stress intensity factor is ***force* × *(length)*$^{-3/2}$** or ***stress* × *(length)*$^{1/2}$.**

This paper deals not with the most commonly studied stress intensity factor of tension K_I, but rather, the shear factor K_{II}, which is more neglected in the case of concrete.

3. EXAMINATION OF FRACTURE MECHANICS OF CONCRETE AND OTHER MODERN MATERIALS

3.1 Determination of tensile stress intensity factor (K_{IC})

It quickly became apparent that test specimens originally specified for metals (such as ASTM E 399-81) were not applicable in the case of modern materials due to their rigid behavior or their coarser grain structure. The typical experimental arrangements, used mainly for the determination of the K_{IC} critical stress intensity factor, arose from increasing the size of proven test specimen shapes and by adapting to the material behavior (*Figs. 3 to 6*). A so-called geometrical function, unique to each experimental arrangement, is used to calculate the stress intensity factor.

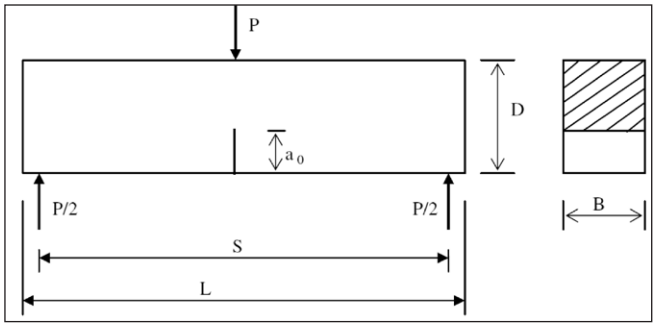

Fig. 3: Three-point bended notched specimen (Xu and Zhang, 2008)

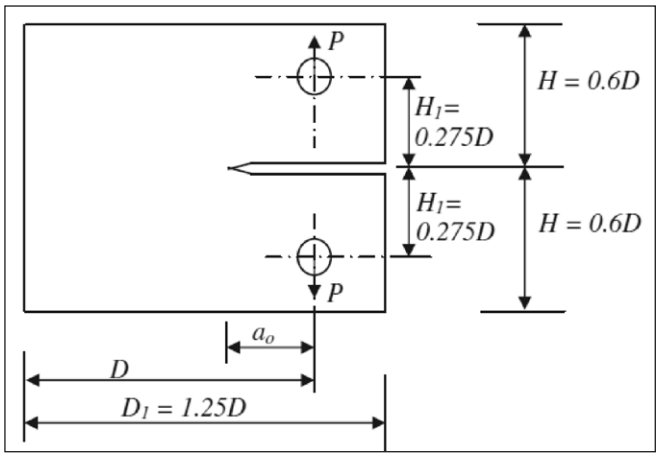

Fig. 4: Compact tension (CT) specimen (Kumar and Barai, 2008)

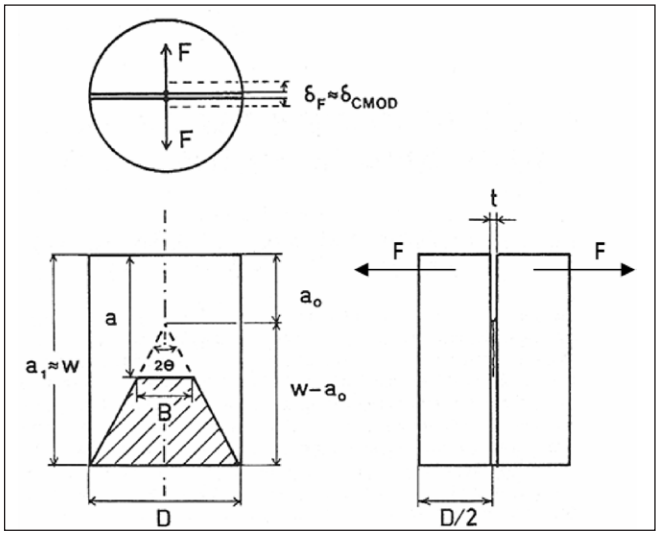

Fig. 5: Specimen (Short Rod) with „negative V" notch (Ouchterlonyi, 1990)

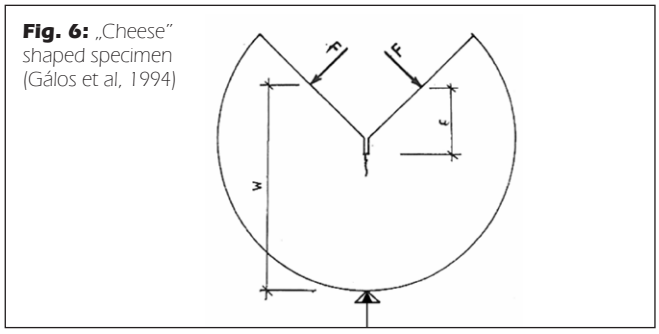

Fig. 6: „Cheese" shaped specimen (Gálos et al, 1994)

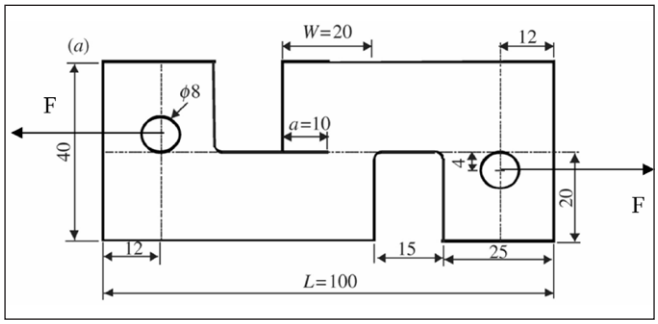

Fig. 7: Pulled polymer specimen for testing K_{IIC} (Williams and Birch, 1976)

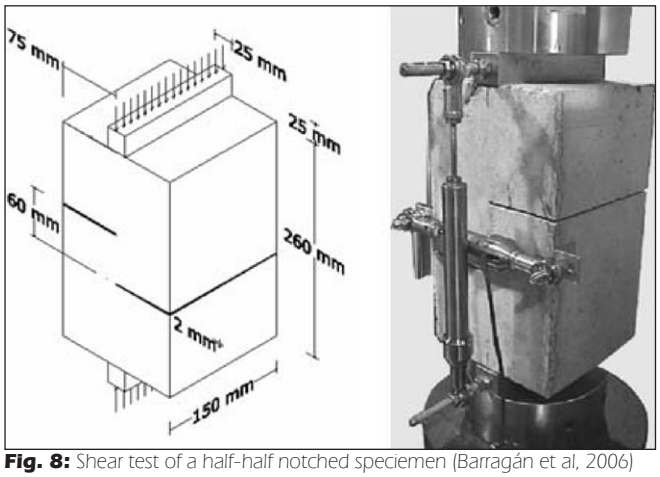

Fig. 8: Shear test of a half-half notched speciemen (Barragán et al, 2006)

3.2 DETERMINATION OF CRITICAL SHEAR STRESS INTENSITY FACTOR (K_{IIC})

New, small-sized test specimens were introduced for determining the critical value (K_{IIC}) of the shear (type II) stress intensity factor. Using the idea of "half-half-notches" in specimens, introduced by *Williams and Birch* (1976) for polymers in tension (*Fig. 7*), as well as the studies on concrete by *Vutukuri* (Vutukuri et al, 1974) and *Barragán et al* (Barragán et al, 2006) (*Figs. 8 and 9*) and the studies on structural stone by *Gálos and Kövesdi* (2006) (*Fig. 10*), squat block and cylinder form test specimens with half-notches were used. In the case of such an arrangement, the K_{IIC} value can be determined from the shearing of the intermediate section.

Because similar arrangements have not been used for test specimens in these types of tests, the geometrical function of influence by loading and boundary conditions was not available.

Their determination was undertaken by parallel (or sometimes outside the laboratory by entirely independent) experiments to study the numerical model, where examination is possible on the full spectrum of shape variables.

Parameters for the geometrical function were also suggested by using the relationships between the results of the K_{IC} and K_{IIC} determination tests which were undertaken in parallel. On the basis of test results *Gálos* (1990), the ratio of K_{IIC}/K_{IC} was chosen to be 1.15.

The change of the critical value (K_{IC}) of the reference tensile (type I) stress intensity factor was examined on notched, three-point bending beam and notched, half-cylinder test specimens. While the notched beam is the most common arrangement for the testing of concrete and stone, the longitudinally cut cylinder is an ideal shape for examining concrete and stone samples extracted by core drilling. The testing of the latter specimens

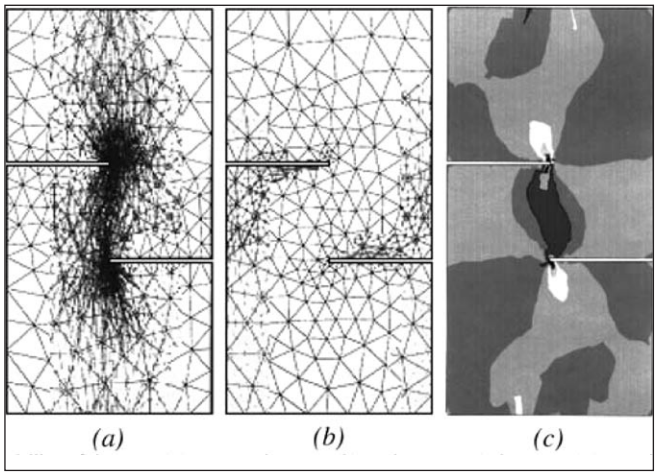

Fig. 9: FE modelling of shear test (a) compressive stress; b) tension stress; c) shear stress) (Barragán et al, 2006)

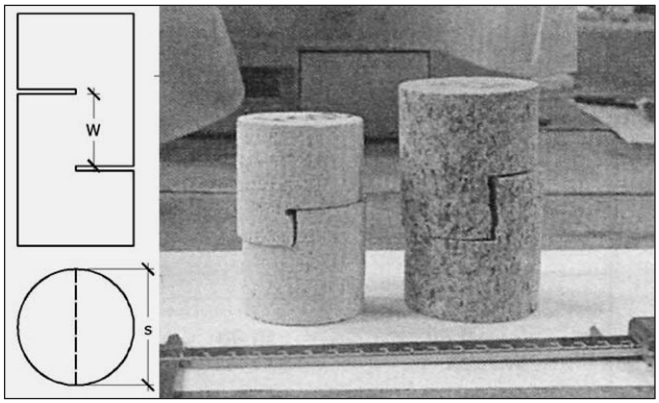

Fig. 10: Shear tests on building stone speciemens (Gálos and Kövesdi, 2006)

was performed and evaluated by *Gálos, Bojtár and Rechtorisz* (Gálos, 1989; Bojtár et al, 1995; Gálos, 2000).

The effect of steel fiber reinforcement was also examined. The test specimens and their notches were formed by cutting. During their research, *Erdélyi and Gálos* (2000) showed amongst other things that the fracture mechanics parameters were nearly identical for steel fiber reinforced test specimens formed by notching and by the use of special formwork (alongside identical arrangement and physical dimensions).

4. EXPERIMENTAL CONCRETE MIX AND EXAMINATION METHODS

4.1 Examination of concrete mix and ready-mix concrete

In the series of experiments, *six* recipes were used to study the effect of changing the usual and special concrete technology parameters and raw materials. During the experiments, the *water-cement ratio* was changed (modified addition of cement alongside constant addition of water), as was the *amount of steel fiber*, and in one case, the *type of aggregate material*. The *cement type (CEM I 42,5 R, Holcim)* was always constant, as was the *maximum size of aggregate (MSA, d_{max} = 16mm)*. The consistency was controlled with the addition of *BASF Glenium 51* super-plasticizer. The constant and variable experimental parameters of the concrete ingredients are shown in *Table 1*.

During the preparation of the aggregate, the endeavor was to keep the modulus of fineness and grading curves of the prepared mix of the two different materials (quartz gravel and

Table 1: Mix design and variables

		Mix No.		
		K1-K3	*K4-K5*	*K6*
Experimental constant	aggregate	quartz gravel and sand d_{max} = 16 mm modulus of fineness m = 6.01		*variable*
	cement	*variable*	400 kg/m³	
	water	~170 ℓ/m³		
	water-cement ratio	*variable*	0.43	
Experimental variable	aggregate	*constant*		basalt (all fractions) d_{max} = 16 mm; m = 6.08
	cement	350-450 kg/m³	*constant*	
	water-cement ratio	0.5-0.43-0.38	*constant*	
	steel fiber	*constant*	0.5-1.0 V/V%	*constant*

sand or basalt) nearly identical. In the mix design, a median curve was targeted between the limit curves *A* and *B* (*Fig. 11*). During mixing, the usual ready-mix measurements were made (bulk density and temperature, slump consistency, air entrainment). For mixes K4 and K5, the air entrainment of the ready-mix increased, from the steel fibers added without the modification of the paste amount, from 20 ℓ/m³ to 28 and 35 ℓ/m³, respectively.

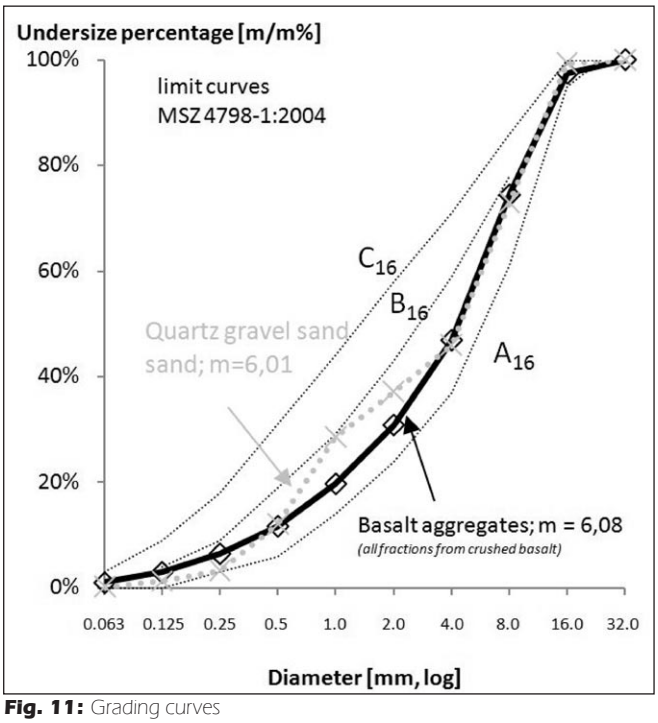

Fig. 11: Grading curves

4.2 TEST SPECIMENS

Figs. 12 and 13 illustrate the theoretical arrangements of the test specimens with cuts and notches. The cuts have a constant width equal to that of the cutting disk. The depth of the cut was always 20% of the greatest thickness of the test specimen measured in the direction of crack propagation in the plane of notching. Figs. 14 to19 show the actual loading arrangements.

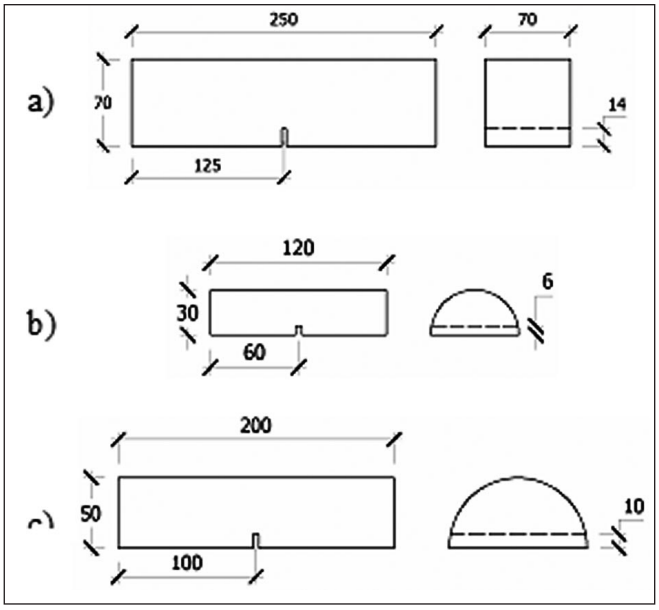

Fig. 12: Schematic shape of a notched beam and halved cylinder

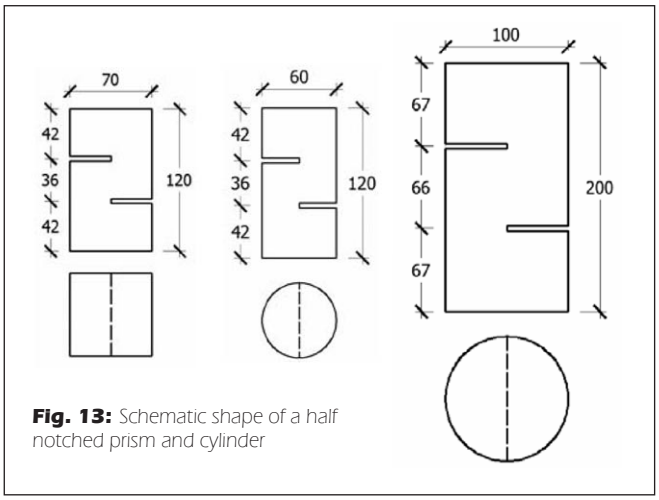

Fig. 13: Schematic shape of a half notched prism and cylinder

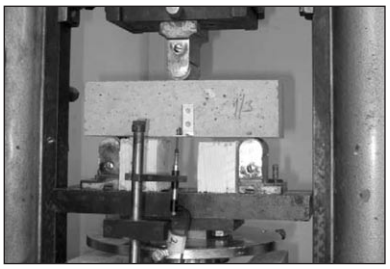

Fig. 14: Bending test of a notched beam, measure 70×70×250 mm, span: 180 mm

Fig. 15: Bending test of a notched, halved cylinder, diamter 100 mm, span: 150 mm

Fig. 16: Shear test of a 70×70 mm excised block

Fig. 17: Sheared specimen

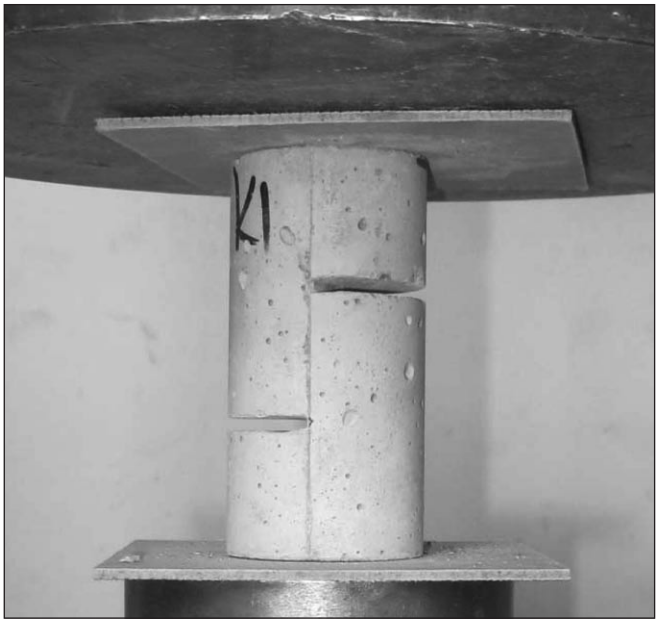

Fig. 18: Shear test of a notched cylinder, diameter 60 mm

5. DETERMINATION OF STRESS INTENSITY FACTOR

The basic formula for the determination of the critical stress intensity factor is derived from Eq. (2) recommended by *Griffith* (1920), and is given as Eq. (3) (Blumenauer and Push, 1987).

$$K_{iC} = \sigma \sqrt{\pi c} f\left(\frac{c}{M}\right) \qquad i = I, II, III \tag{2}$$

and

$$K_{IC} = \sigma \sqrt{c} f\left(\frac{c}{M}\right) \tag{3}$$

It is customary to express the so-called geometrical function, Eq. 4, which describes the relationship of the dimensions of the test specimen and the notch, in the form of an approximative polynomial (Blumenauer and Push, 1987).

$$f\left(\frac{c}{M}\right) = C_1 + C_2\left(\frac{c}{M}\right) + C_3\left(\frac{c}{M}\right)^2 + \tag{4}$$

In the case of test specimens used in a series of experiments.

Eqs. (5) and (6), describing the relationships for notched, bent beams, were given by *Bojtár et al* (1995).

$$K_{IC} = \frac{3FL}{2sM^2}\sqrt{\pi c} f\left(\frac{c}{M}\right) \tag{5}$$

$$f\left(\frac{c}{M}\right) = \frac{1{,}99 - \left(\frac{c}{M}\right)\left(1 - \frac{c}{M}\right)\left(2{,}15 - 3{,}93\left(\frac{c}{M}\right) + 2{,}70\left(\frac{c}{M}\right)^2\right)}{\left(1 + 2\left(\frac{c}{M}\right)\right)\left(1 - \left(\frac{c}{M}\right)\right)^{3/2}} \tag{6}$$

Eqs. (7) and (8) describe the relationships for notched, bent half-cylinders (Bojtár et al, 1995).

$$K_{IC} = \frac{FL}{R^3}\sqrt{4\pi c} f\left(\frac{c}{R}\right) \tag{7}$$

$$f\left(\frac{c}{R}\right) = 1{,}52 - 2{,}20\left(\frac{c}{R}\right) + 7{,}71\left(\frac{c}{R}\right)^2 - 13{,}55\left(\frac{c}{R}\right)^3 + 14.25\left(\frac{c}{R}\right)^4 \tag{8}$$

Geometrical parameters necessary for the calculation of K_{IIC} for test specimens notched half-way have not yet been established. Thus, by the use of Eq. (9), and Eq. (10) by *Gálos* (1990), a recommendation is made on the basis of the compression stresses (*Eq. 11*) acting on the test specimen to fit a curve to the geometrical function from the experimental data (*Eqs. 12 and 13*), where the value of K_{IC} is calculated on the basis of Eq. (5) or (7) for the shape of the given test specimen.

$$K_{IIC} = \sigma \sqrt{\pi r} f\left(\frac{s}{W}\right) \quad (Griffith, 1920) \tag{9}$$

$$K_{IIC} = 1{,}15 K_{IC} \quad (Gálos, 1990) \tag{10}$$

and

$$\sigma = \frac{F}{A} \tag{11}$$

therefore

$$f\left(\frac{s}{W}\right) = \frac{1{,}15 K_{IC}}{\frac{F}{A}\sqrt{\pi r}} \tag{12}$$

$$f\left(\frac{s}{W}\right) = C_1 + C_2\left(\frac{s}{W}\right) + C_3\left(\frac{s}{W}\right)^2 \tag{13}$$

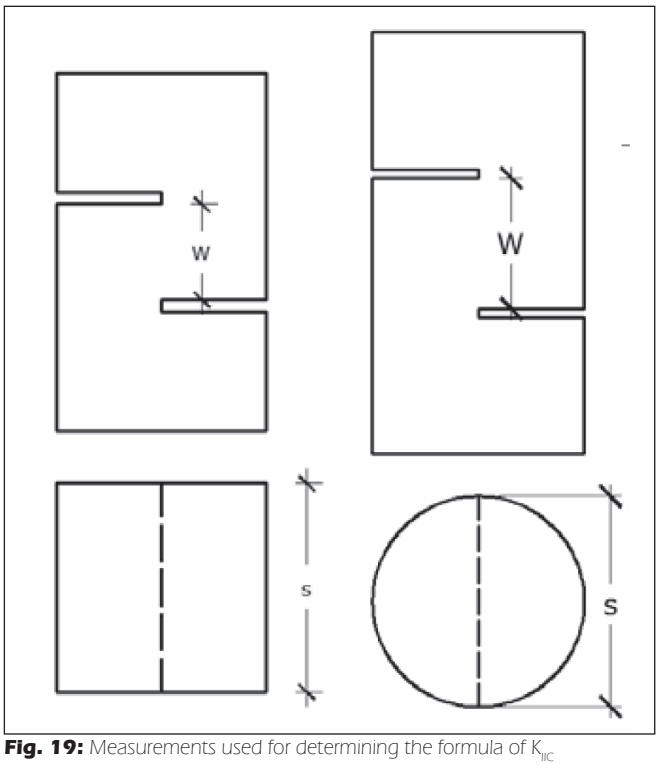

Fig. 19: Measurements used for determining the formula of K_{IIC}

6. EVALUATION OF RESULTS

The elaboration of the determined strength and K_{IC} factor evaluations for cured concrete extend beyond the scope of this paper.

For the determination of the critical value of the K_{IIC} stress intensity factor, the K_{IC} factor determined for the same test specimen shape was used as a basis in every case (beam–beam, dia. 60 mm cylinder–dia. 60 mm cylinder, etc.).

Fig. 20 shows the dependence of the f(s/W) value, calculated on the basis of Eq. (12), on the geometrical parameters (s/W).

Using the quadratic approximation of Eq. (13), the function with the best fit was determined. The square of the *Pearson*-type correlational coefficient of the approximation gave a value of $R^2 = 0.464$. The relationships applied for determining the K_{IIC} stress intensity factor are shown in Eqs. (14) and (15).

$$K_{IIC} = \sigma \sqrt{\pi r} f\left(\frac{s}{W}\right) \tag{14}$$

$$f\left(\frac{s}{W}\right) = 5{,}085 - 0{,}20288\left(\frac{s}{W}\right) + 0{,}9558\left(\frac{s}{W}\right)^2 \tag{15}$$

The dependency on the geometrical parameters of the K_{IIC} stress intensity factor determined in this way is shown in *Fig. 21*. The value of the stress intensity parameter decreases as the geometrical parameter (s/W) increases.

As the first step in evaluating the dependency of the K_{IIC}

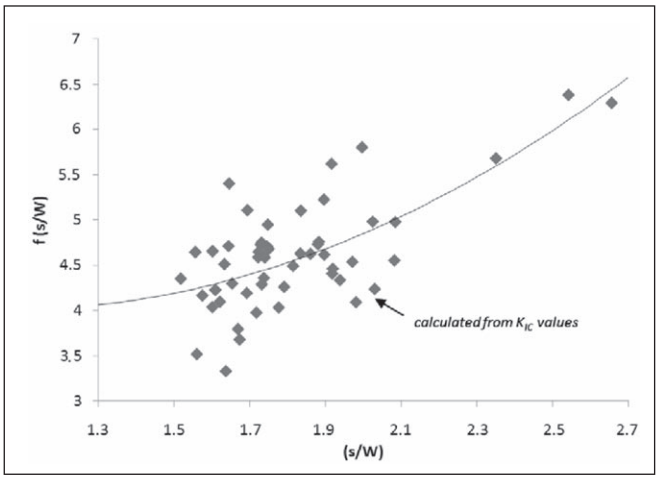

Fig. 20: Coherence of the geometrical data (s/W) and the approximate geometrical function f(s/W)

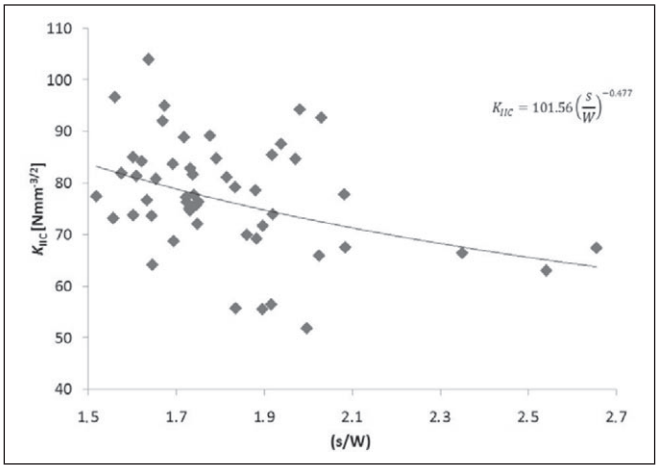

Fig. 21: Coherence of the calculated KIIC stress intensity factor and the geomerical parameter (s/W)

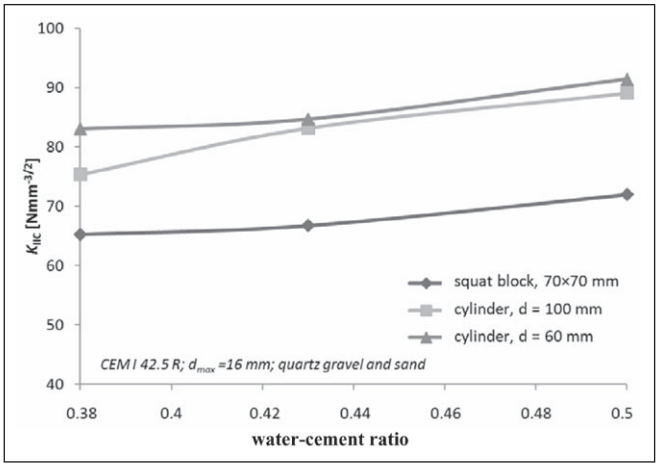

Fig. 22: Effect of the water-cement ratio on the KIIC stress intensity factor

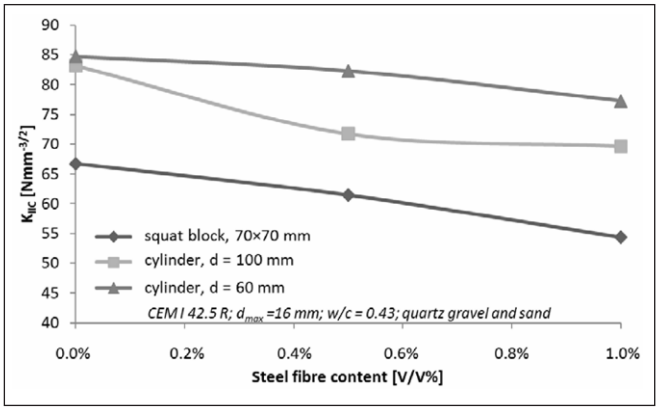

Fig. 23: Effect ot the dosage of steel fibre on the KIIC stress intensity factor

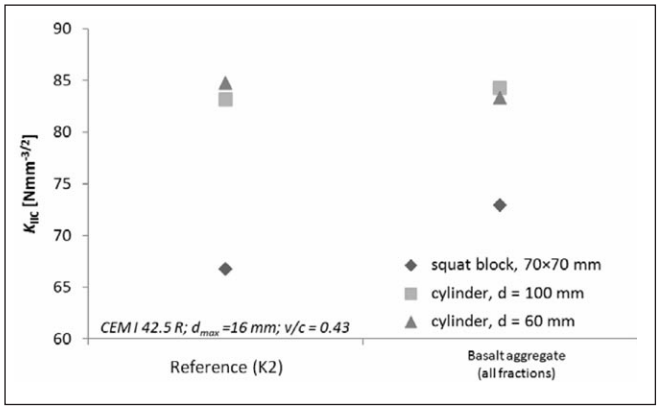

Fig. 24: Effect of the dosage of basalt on the K_{IIC} stress intensity factor

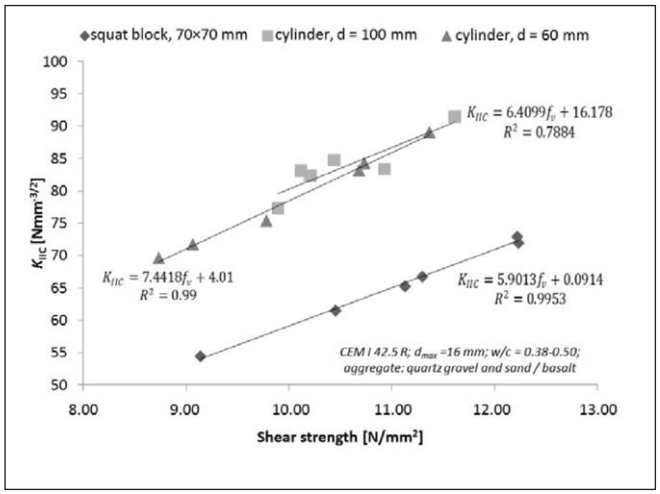

Fig. 25: Coherence of the shear strength ant the K_{IIC} stress intensity factor

value on concrete technology parameters, the variable water-cement ratio was set by increasing the amount of cement while keeping the amount of water constant. Thus, the water-cement ratio decreased while the cement paste content increased (from 286 ℓ/m^3 at w/c = 0.5 to 317 ℓ/m^3 at w/c = 0.38). Due to the increased cement paste content, a minor decrease can be seen in the shear and fissure results, as well as the tensile bending strength, with the decrease of the water-cement ratio. A similar correlation is exhibited by the decrease of paste content and the values of the K_{IIC} factor. *Fig. 22* shows that the greatest difference between the evolving factors is approximately 10%.

The effect of steel fiber amount was evaluated after the effect of the water-cement ratio. Due to the addition of fibers increasing the entrained air (lack of compaction), the value of K_{IIC} decreased in parallel with the increase of fibers, similar to the observations of all the strength tests (*Fig. 23*). The value of the decrease was 10-20% depending on the shape of the test specimen.

Finally, the effect of basalt content on the value of the K_{IIC} factor resulted in differences of ±1 %, within the margin of error, for cylindrical test specimens. A 10% increase was observed in the case of beam test specimens. The results are shown in *Fig. 24*.

In addition to determining the stress intensity factor, the dependency of the parameters on strength was also examined. Naturally, the K_{IIC} value should be compared to the shear strength parameters. The correlation between the shear strength calculated from the test specimens and the K_{IIC} stress intensity factor is very high (*Fig. 25*) despite the fact that in calculating the latter, the normal stress over the entire cross-section was applied for the case of shear (*Eq. 12*). On the basis of the relationship valid for the examined range, the advantageous correlation allows for the estimation of the K_{IIC} value on the basis of the shear strength.

7. CONCLUSIONS

This paper introduces the results of a series of experiments undertaken in the laboratories of the Budapest University of Technology and Economics, Department of Construction Materials and Engineering Geology. The purpose of the experiments was to study the applicability of new, "small-sized", compact concrete test specimens for the examination of fracture mechanics. Various mixes of concrete were also evaluated, as was the effect of changing the concrete technology parameters on the stress intensity parameters, and the relationship between strength and stress intensity parameters.

For the determination of stress concentrations and standardization of the calculations, *Irwin* (1957) introduced the term stress intensity factor (K), which was defined for the case of tension (type I), shear (type II), and torsion (type III). The crack propagates at the critical value of the stress intensity factor (K_{IC}, K_{IIC}, K_{IIIC}).

The new type of test specimen and six different concrete mixes were used in the series of experiments. The effect of the water-cement ratio (increasing cement content beside constant water content) and two steel fiber contents (0.5 and 1.0 V/V%) were examined. Finally, the effect on the studied parameters was determined in the case when all the aggregate was substituted by crushed basalt having an identical grading curve.

For the determination of the parameters, notched beams (70×70×120 mm; 70×70×250 mm), notched cylinders (d/h=1:2, for K_{IIC} value), and longitudinally cut notched cylinders (d = 60 and 100 mm) were prepared.

In the absence of published sources for the test specimens first used by the Authors, the Authors themselves determined the approximative geometrical function, in relation to the values for other test specimen types and other failure modes, calculated on the basis of published data.

On the basis of the results, an approximative geometrical function was given for the geometrical function of the new type of test specimens.

It was determined during the examination of the K_{IIC} stress intensity factor that, within the studied range, the paste content of the ready-mix has a much greater influence than the water-cement ratio. Similarly, the lack of compaction remaining in the concrete due to the addition of steel fibers also has a negative effect on the critical value of the stress intensity factor.

The experiments showed a correlation between the K_{IIC} stress intensity factor and the measured shear strength of the test specimens. With the help of a highly-reliable linear

relationship, the stress intensity factor can be predicted in advance.

With the help of the applied test methods, it was possible to support with the tools of modern fracture mechanics the applicability of the new test specimens with experimental results, and to show a relationship between the concrete technology parameters and the strength and stress intensity results.

8. ACKNOWLEDGEMENTS

The authors of this paper wish to thank *Dávid Diriczi* and *András Eipl* for their assistance in the laboratory examinations. Thanks is also given for the assistance and support of the *Budapest University of Technology and Economics, Department of Construction Materials and Engineering Geology*, *HaNSa Kft.*, and *MetroConsult Ltd.*

9. ABBREVIATIONS

A	cross-sectional area perpendicular to direction of force
c	depth of notch
C_i	experimental constant
f(c/m)	geometrical function
$f^{I}_{ij}, f^{II}_{ij}, f^{III}_{ij}$ and $g^{I}_{i}, g^{II}_{i}, g^{III}_{i}$:	relationship of loading and boundary conditions for the given problem
F	force required for crack propagationK_I, K_{II} és K_{III} stress intensity factor of the given crack type
K_{IC}	critical value of stress intensity factor (tension)
K_{iC}	critical value of stress intensity factor
L	span
M	height of test specimen (dimension in direction of crack propagation)
r	radius at end of notch
R	radius (height) of test specimen
s	width of test specimen and size of shear section perpendicular to crack propagation (according to *Fig. 19*)
W	size of sheared section in direction of crack propagation (according to *Fig. 19*)
λ	*Lamé* type material constant
σ	stress near crack tip, calculated on the basis of strength theory

10. REFERENCES

ASTM E 399-81: „Standard Test Method for Linear-Elastic Plane-Strain Fracture Toughness K_{Ic} of Metallic Materials"; American Society for Testing and Materials

Barragán, B.; Gettu, R.; Agulló, L. and Zerbino, R. (2006): „Shear Failure of Steel Fiber-Reinforced Concrete Based on Push-Off Tests", ACI Materials Journal, Vol. 103, No. 4, pp 251-257.

Blumenauer, H. and Push, G. (1987): „Applied fracture mechanics", Műszaki Könyvkiadó, Budapest (in Hungarian)

Bojtár, I., Gálos, M. and Rechtorisz, Á. (1995): „Determination of fracture mechanical properties on rocks boring core material", Acta Technica Acad. Sci. Hung., Vol. 107/3 4, pp 163-174.

Erdélyi, A. and Gálos, M. (2000): „Evaluation of toughness on steel fiber reinforcement concrete with fracture mechanics methods", OTKA T16683, July 1997 (in Hungarian)

Gálos, M. (1989): „ Mechanical tests to determine rock strength characteristics", Stiller, H. (eds.): „High Pressure Investigations in Geosciences", Akademie-Verlag, Berlin, pp 149-153.

Gálos, M. (1990): „Strength and stress properties of rocks in rocks model system", HAS candidate thesis (in Hungarian)

Gálos, M.; Kürti, I. and Vásárhelyi, B. (1994): „Evaluation of rocks fracture with conventional and fracture mechanics system", Kőolaj és Földgáz, Vol. 27/2, February 1994., pp 44-46; 51-57. (in Hungarian)

Gálos, M. (2000): „Determination of fracture mechanical parameters in rocks speciments"; presentation, VII. Fracture mechanics seminar, Miskolc, appendix CD-Rom; 2000 (in Hungarian)

Gálos, M. and Kövesdi, B. (2006): „Determination of shear strength of rocks on nicked specimens", Török, Á. and Vásárhelyi, B. (eds.): „Mérnökgeológia Kőzetmechanika 2006", Műegyetemi Kiadó, pp 53-58, in Hungary language

Griffith, A. A. (1920): „The phenomena of rapture and flow in solids" Philosophical Transaction, Royal Society of London, Ser. A. Vol. 221, pp 163-198

Inglis, C. E. (1913): „Stresses in Plate Due to the Presence of Cracks and Sharp Corners", Transactions of Institute of Naval Architects, Vol. 55, pp 219-241

Irwin, G. R. (1957): „Analysis of Stresses and Strains near the End of a Crack Traversing a Plate", Journal of Applied Mechanics, Vol. 24, 1957, pp 109-114

Jaeger, J. C. and Cook, N. G. W. (1978): „Fundamental of rock mechanism", 2nd ed., Chapman &Hall, London

Koloszov, G. V. (1909): „Application of complex function theory of planar problem of the mathematical elasticity theory", Thesis, University of Juriev in German language

Kumar, S. and Barai, S. V. (2008): „Determining double-K fracture parameters of concrete for compact tension and wedge splitting test using weight function", Engineering Fracture Mechanics, accepted: 26. dec. 2008; p14

Muszhelisvili (1953): „Some basic problems of mathematical theory of elasticity", P. Nordhoff, London

Ouchterlony, F. (1990): „Fracture toughness testing of rock with core based specimens", Rossmanith, H. P. (eds.): „Fracture and damage of concrete and rock", Pergamon Press, Oxford, pp. 355-365.

Sih, G. C. and Rice, J. R. (1965): „Plane Problems of Cracks in Dissimilar Materials", Journal of Applied Mechanics, 32, pp. 418-423.

Sneddon, I. N. (1969): „Crack problems in the classical theory of elasticity", John Wiley & Sons, Hoboken NJ

Ujhelyi J. (2005): „Tenet of Concrete", Print Műegyetemi, Budapest in Hungary language

Vutukuri, V. S.; Lama, R. D. and Saluja, G. S. (1974): „Handbook on mechanical properties of rocks" Volume I; Trans. Tech. Publications, Clausthal

Westergaard, H. M. (1939): „Bearing Pressure and Cracks", Journal of Applied Mechanics, Vol. 6, pp 49-53

Williams J. G., Birch M. W. (1976): „ASTM STP 601" American Society for Testing and Materials, Philadelphia, pp. 125–137.

Xu, S. and Zhang, X. (2008): „Determination of fracture parameters for crack propagation in concrete using an energy approach", Engineering Fracture Mechanics, Vol. 75/2008, pp. 4292-4308.

Dr. Sándor Fehérvári (1981): MSc. Civil engineer (BME 2006), specialization on concrete technology (BME 2009), PhD (BME 2009). Senior lecturer, University of Debrecen, Faculty of Engineering Department of Civil Engineering; project manager, Budapest Transport Closely Held Corporation DBR Metro Project Directorate. Main field of interests are specialities and determination of tunnel fires, effect of tunnel fires on the linings, special building methods of tunnels and underground structures, structural and curtain grouting, building and repairing technologies of underground and tunnel structures. Member of the public law association of the Hungarian Academy of Sciences, the Hung. Group of ***fib***, the Hung. Chamber of Engineers, the Hung. Tunnelling Assoc., the Hung. Sci. Assoc. for Transport, of the Sci. Society of Silicate Industry (Concrete Div.), Hung. Society of Buildings. Activities: ITA WG 6 (Maintenance and repair), ITA COSUF (Safety in tunnels).

Dr. Miklós Gálos (1938): MSc. Civil engineer (ÉKME 1961), specialization on steel structures (BME 1967), university doctor (1971), candidate of science (MTA 1992), PhD (1997), habilitation (BME 1998). Designer (1961-63), detail designer (1963-78) at Wagon and Engine Works at Győr. Head of department (1963-78) at the building departments of VEGYTERV and OLAJTERV. From 1978 until retirement researcher, assoc. professor, university professor at the BME Faculty of Civil Engineering. From 1992, as a ret. univ. professor take part of the educational and research works of the BME Department of Construction Materials and Engineering Geology. Main field of interests are the experimental and analytical determination of the physical and mechanical parameters of structural stones. Qualification of structural stones. Chair of the Stone and gravel division of the Scientific Society of Silicate Industry, member and of the Hung. Group of ***fib***, Hungarian Geological Society.

Dr. Salem Georges Nehme (1963): MSc. Civil Engineer (BME 1992), specialization on reinforced concrete (BME 1996), PhD (BME 2005). Associate professor and leader of the laboratory of the BME Department of Construction Materials and Engineering Geology. Main fields of interest are the investigation of high strength concrete and mortar. Coherence of the porosity and durability of SCC concretes. Usage of SCC for strengthening of RC structures. Specialities of concrete technology: e.g. usage of SCC as mass concrete solving the problem of cracks occurred of the thermal distribution. Quality control of mass concrete, fair face concretes, concretes with high density aggregates, recycled aggregates. Strengthening of reinforced structures with carbon lamellas. Durability of concrete structures. Increase of punching strength of the SFRC slabs. Member of the Hungary Group of ***fib***, and of the Sci. Society of Silicate Industry (Concrete Div.).

EARLY AGE SHRINKAGE CRACKING OF FIBRE REINFORCED CONCRETE


Olivér Fenyvesi - Zsuzsanna Józsa

Conventional steel reinforced concrete is often sensitive to cracking, and these cracks could be the result of early age shrinkage. Cracks can cause the corrosion of steel reinforcements reducing the lifetime of concrete structures. To reduce this problem fibre reinforced concrete (FRC) is one possible solution. Laboratory tests have been carried out according to the Austrian FRC technical specification, in particular with regard to early age shrinkage cracking. Four different relatively thin and short fibre types were used: fabricated from polypropylene, polyacrylnitrile and non alkaline resistant E-glass. In this paper the relationship between the dosage of fibres and early age shrinkage cracking tendency was tested and effectiveness of fibre types are compared. During the laboratory tests compressive strength was also tested. In case of every fibre type, the relationship between dosage and crack tendency were linear. If we test a fibre type again but with a reference mix with higher crack tendency, the two linear curves will approach each other if dosage is increased. Finally, further possibilities are described with testing more fibre types and higher dosages in the future.

Keywords: shrinkage, shrinkage cracking, early age shrinkage, FRC, polymeric fibres, glass fibres

1. INTRODUCTION

In concrete, mortar and cement paste shrinkage takes place from the very beginning. This is caused by water movement in the porous and rigid body. During the hydration of cement, while the cement paste is plastic, it undergoes a volumetric contraction (autogenous shrinkage) which magnitude is of the order of one per cent of the absolute volume of dry cement. However, the extent of hydration prior to setting is small, and once a certain rigidity of the system has developed, the contraction induced by the loss of water by hydration is greatly restrained (Neville, 1995). Withdrawal of water from concrete or mortar or cement paste stored in unsaturated air causes drying shrinkage. A part of this drying shrinkage is irreversible and should be distinguished from the reversible moisture movement caused by alternating storage under wet and dry condition (Neville, 1995; Grube, 2003).

Influencing factors of shrinkage in mix design:

- cement content of paste
- specific surface area of cement
- fine aggregate content (under 0.125 particle size)
- specific surface area of fine aggregate
- water-cement ratio
- total aggregate content
- type of aggregate
- water absorption capacity/water content of aggregate
- applied admixtures
- compacting rate of paste
- porosity
- other added components e.g. fibres.

Shrinkage of concrete depends on the temperature of concrete and its surroundings, on relative humidity and on the velocity of air movement as well as the curing and composition of the concrete.

The importance of shrinkage in structures is largely related to cracking. Time has a two-fold effect from this point of view: the strength increases, thereby reducing the probability of cracking, but on the other hand, the stress induced by shrinkage also increases. If stress reaches the tensile strength of concrete, cracks appear on the structure or specimen (CEB, 1992; Neville, 1995).

Fibre reinforced concrete (FRC) is a possible solution to avoid early age shrinkage cracking (Balázs, Lublóy, 2007). Earlier in Hungary, asbestos and celluloid fibres were used to produce fibre reinforced cementitious products (mainly roofing elements and pipes) under the trademark “Eternit”. These products have disappeared from the market, but they can be found in old buildings. Asbestos fibres have very small diameter, often smaller than 10 μm, and provide very high strength, but may cause serious health problems (e.g. lung cancer on inhalation). That is the reason why, from a medical point of view, the smallest allowed diameter of fibres is 7 μm, and on the market there are fibres with a diameter between 9 and 500 μm. Nowadays there are fibres made from steel, stainless steel, AR-glass (alkaline resistant), E-glass (non alkaline resistant), polypropylene, polyacrylnitrile, nylon, carbon, etc. (Józsa et al., 2005).

To study crack tendency of different cement types Balázs et al. (1979) have made ring tests, where the time of cracking was measured. Crack tendency of FRCs was investigated by Shah, Weiss, in 2006, Aly, Sanjayan and Collins in 2008 and Aly and Sanjayan in 2009. Restrained shrinkage was also studied by Salah and Lange in 2001. Recently another test method is used to evaluate restrained early age shrinkage according to the Austrian fibre-concrete technical specification described in Faserbeton Richtlinie (2002, 2008). This method was used by Józsa et al. in 2005, and by Schmidt in 2005 and also in

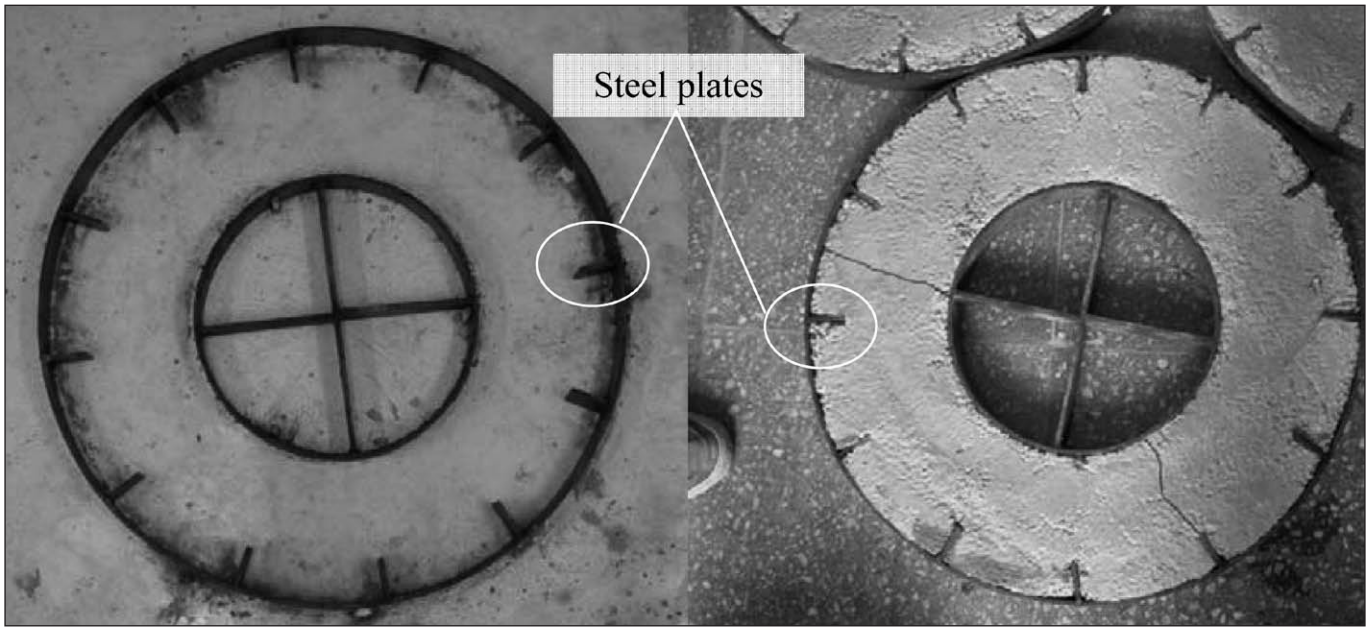

Fig. 1: Empty and filled formworks for ring tests

our present experiments. Also this method was followed to measure early age shrinkage cracks of lightweight aggregate concrete by Fenyvesi in 2006.

2. EXPERIMENTAL STUDY ACCORDING TO THE AUSTRIAN FIBRE-CONCRETE TECHNICAL SPECIFICATION

The effectiveness of fibres in early age shrinkage crack tendency (caused by autogenous and drying shrinkage) can be determined by testing concrete mixtures described in Faserbeton Richtlinie (2002, 2008). The Austrian technical specification gives a mixture recipe which is very sensitive to early age shrinkage cracking. This mixture contains a high volume of fine particle size under 0.125 (500 kg/m^3 cement is 360 kg/m^3 from it). The water-cement ratio is 0.61.

The technical specification describes a test method for which special ring specimens are needed. The outer diameter of the ring is 60 cm, the inner is 30 cm. The height of the ring is 4 cm. To the inner side of the outer formwork steel plates are welded, to increase crack tendency of the specimen (*Fig. 1*). The formworks are fixed in a wind tunnel (*Fig. 2*). The wind tunnel has movable upper covering. Just after mixing, fresh concrete must be put into and compacted in the fixed formworks. Two hours after the mixing the wind tunnel has to be stopped. The experiment goes on for five hours, and has to be carried out in a climatic room at 65 % relative humidity and 20 °C. At the Department of Construction Materials and Engineering Geology of Budapest University of Technology and Economics

Fig. 2: Wind tunnel with four formworks after compacting concrete

we have the opportunity to carry out experiments which need these conditions in a climatic room equipped with an air conditioner and a moisturizing device.

3. MIXTURES, TESTS PARAMETERS

All mixtures contained 66 V% normal sand and gravel aggregate and 140 kg/m^3 limestone dust was added to improve crack tendency of the concrete. The pure Portland cement is the least favorable with regard to early age shrinkage cracks. That was the reason for applying CEM I 42.5 N (normal) pure Portland cement in our experiments. The water-cement ratio was relatively high: 0.61 to enhance early age shrinkage in the concrete. Plasticizer admixture was applied to set up to the same level of consistency in case of every mixture (spread 500

Table 1: Properties of used fibres

Material	Diameter [μm]	Length [mm]	Density [g/cm^3]	Young's modulus [N/mm^2]	Tensile strength [N/mm^2]	Alkali resistance [-]	Melting point [°C]
E-glass	9-20	12	2.6	70 000	2000	poor	840
E-glass	9-20	6	2.6	70 000	2000	poor	840
PAN	12-15	12	1.2	7 000	400	excellent	230
PP	15	6	0.9	1 000	200	excellent	160

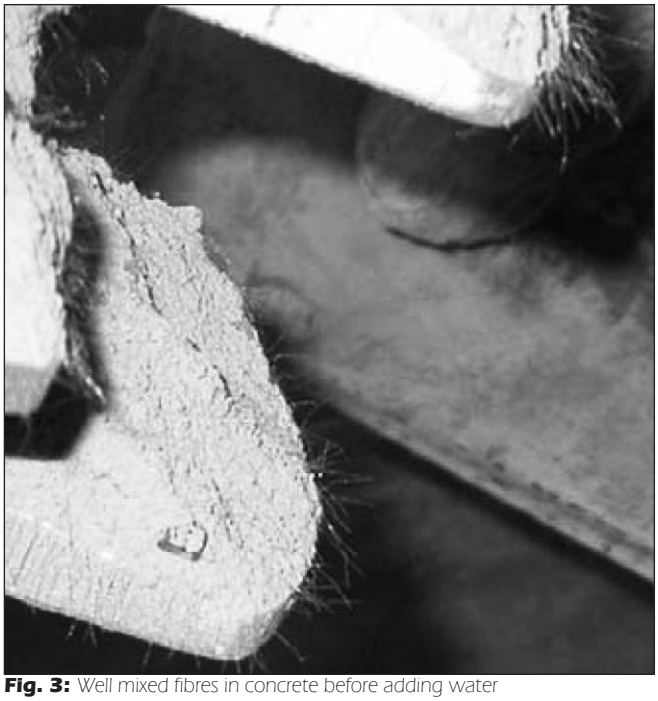

Fig. 3: *Well mixed fibres in concrete before adding water*

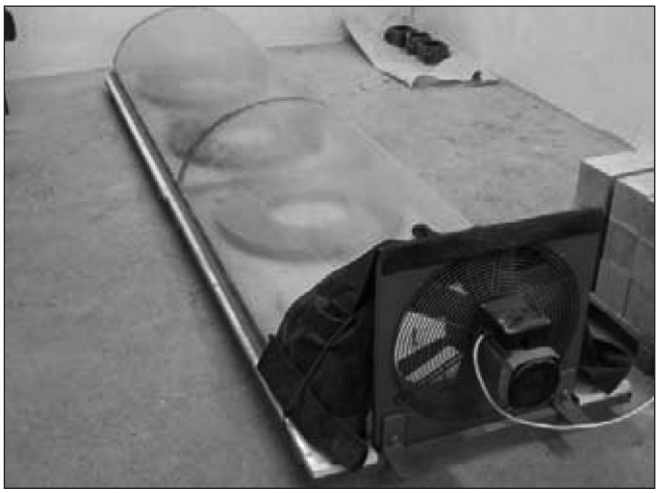

Fig. 4: *Wind tunnel*

Fig. 5: *Wind tunnel with ring specimens*

to 550 mm). Fibres were added to the mixture before the water for better mixing of fibres, it was checked before adding water as *Fig. 3* shows. Variable parameters were dosage and the type of fibres. We used four types of fibres, two of them were made from glass, one is the most commonly used polypropylene (PP) and one is a newly developed polyakrylnitrile (PAN) fabricated with a special method. The main parameters of these fibres are described in *Table 1*.

Consistency of the fresh concrete was measured by flow table test, right after the mixing according to EN 206-1. The density of fresh concrete was measured by weighing both empty and filled formworks. Compressive strength of concrete was tested on standard cube specimens (with dimensions 150×150×150 mm) at the age of 28 days according to EN 206-1.

For early age shrinkage tests, ring specimens were prepared according to the instructions of the Austrian "Fibre-concrete" technical specification (Faserbeton Richtlinie, 2002, 2008 *Table 2*). We prepared four ring specimens for every combination of the mixture. Two hours after mixing, the specimens were placed in a wind tunnel for five hours (*Figs. 4 and 5*). After keeping them for five hours in the wind tunnel, we registered and summarized the lengths of every crack, which indicates the early age shrinkage cracking tendency of the mixture (*see Figs. 6 to 8*). Beside the tests according to the specification of the Austrian technical specification (Fibre-concrete, 2002, 2008) the ring specimens were stored in a tumbler-drier for two further days at a temperature 60 °C to achieve improved drying, after which additional cracks were registered on the specimens.

To evaluate early age shrinkage cracking tendency of every mixture we summarized the length of every crack for each specimen. The average of the summarized crack length of the four ring specimens indicates the crack tendency of mixtures. To evaluate the effectiveness of the different dosages of different fibres, before every sequence we prepared a reference

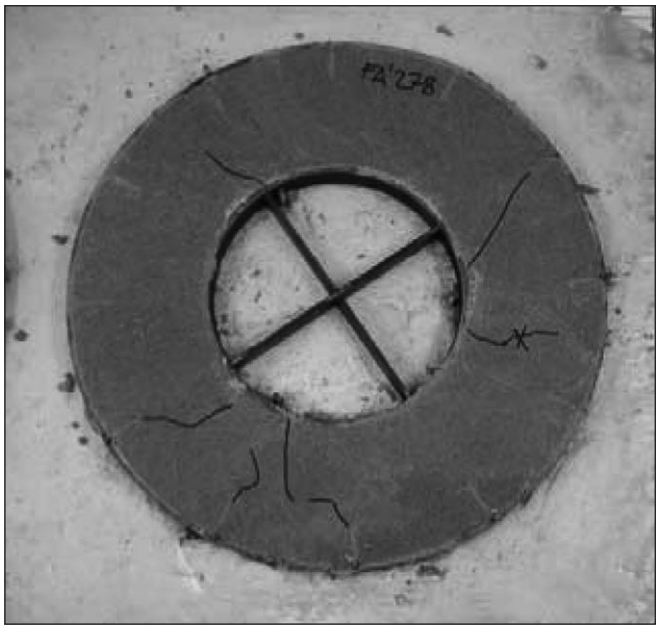

Fig. 6: *Ring specimen after testing with fibre reinforcement*

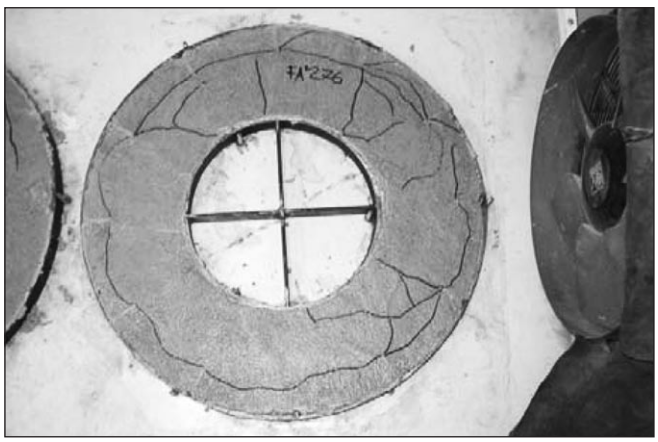

Fig. 7: *Ring specimen after testing without fibre reinforcement*

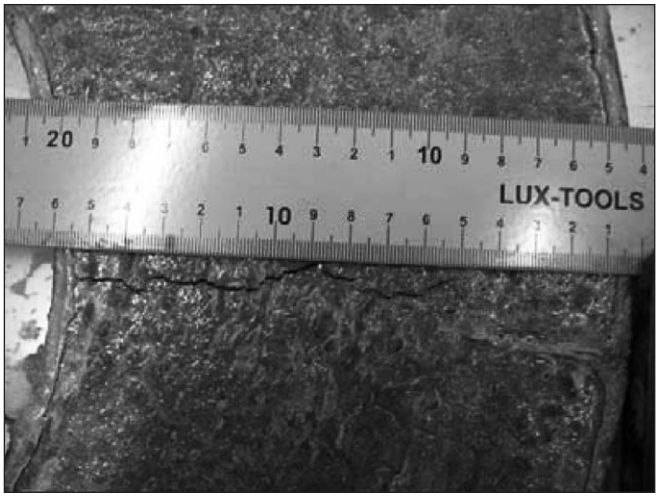

Fig. 8: Crack through the specimen

mixture without fibres. The Faserbeton Richtlinie (2002, 2008) define different classes to evaluate crack tendency according to these reference mixtures (*Table 3*).

4. EXPERIMENTAL RESULTS

In the application of FRC the most important question of concrete mix design is the minimum effective fibre dosage. The industrial experience shows that, for example in case of the PP fibres 0.5 kg/m^3 dosage is enough to avoid early age cracks in industrial concrete pavements (Schmidt, 2005), in case of 12 mm long glass fibres 1.0 kg/m^3 is mostly used. To study this question, we tested many different dosages (0.3 to 1.0 kg/m^3) of each fibre type and created a fibre dosage vs. average summarized crack length diagram (*Figs. 9 and 10*).

In case of every tested type of fibre the relationship was found to be linear. So theoretically very low dosage of fibres reduces effectively the probability of crack growth in the specimen or in the structure. From an other point of view there is no minimum effective dosage or optimal dosage in case of the tested types of fibres, but the higher dosage is applied, the lower crack tendency is reached. Further investigations are needed to decide if this linearity is true at higher dosages than 1.0 kg/m^3.

The shorter (6 mm length) types of fibres (both PP and glass fibres) did not reduce the average summarized crack length of the concrete, but did reduce the crack width. This can be the reason why these fibres are effectively applied in the industry, but the lower applied dosage is not preferred, because if only crack width is reduced, water and other corrosive chemicals can penetrate into the structure and reach steel reinforcements causing corrosion. The reason for the lower effectiveness of short glass fibres can be the lower anchorage length. In case of the PP fibres, according to Wongtanakitcharoen and Naaman (2006) PP fibres (also with higher length) do not reduce crack length in concretes. The reason can be that PP fibres have very low Young's modulus (*see Table 1*), so when shrinkage is increasing, in the fibres there is only very low tensile stress, and the fibres can effectively work just after shrinkage cracks

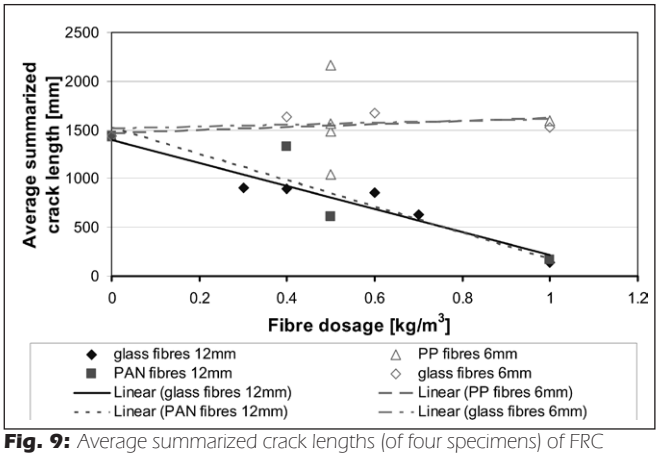

Fig. 9: Average summarized crack lengths (of four specimens) of FRC made with all tested types of fibres after curing in wind tunnel

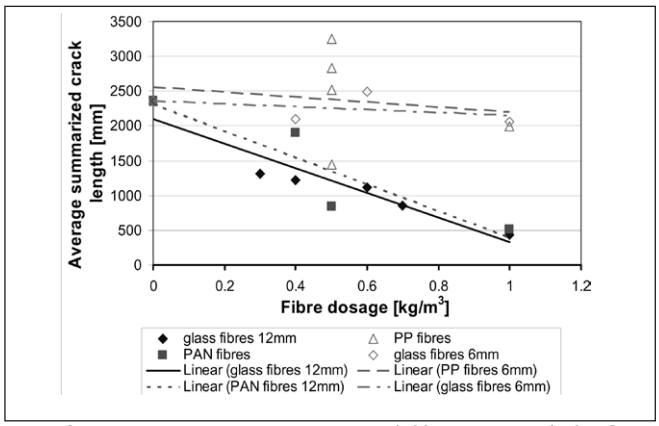

Fig. 10: Average summarized crack lengths (of four specimens) of FRC made with all tested types of fibres after curing in tumbler-drier

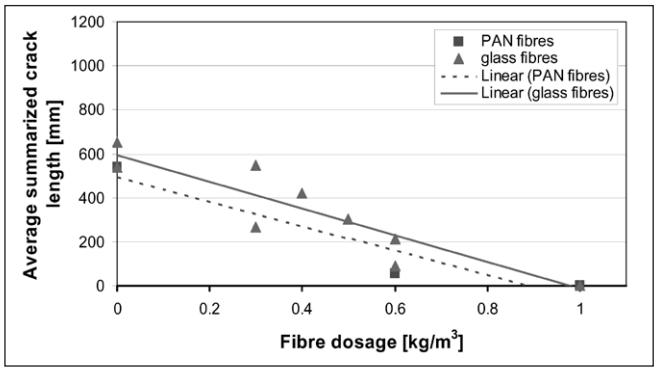

Fig. 11: Average summarized crack lengths (of four specimens) of FRC made with glass and PAN fibres of 12 mm length after curing in wind tunnel

appeared. Therefore crack length is not reduced by fibres that have low Young's modulus, only the crack width. Another important question is the real effectiveness of a fibre type. If we present the results on the diagram, where the fibre dosage is given in volumetric percent and the geometry of fibres is the same, we can see the effectiveness of the fibre. We can see in *Figs. 11 to 14* that from this point of view, glass fibres are better than PAN fibres, but if we apply the dosage in kg/m^3, the difference disappears. In the construction industry fibres are added to the mixture by kg/m^3 so practically we can say that

Table 2: Applied test methods

Measured property	Type of specimen	Duration	Method
Fresh concrete body density	Cube 150×150×150 mm	30 minutes	Mass weighting
Consistency	-	10 minutes	Flow table test
Compressive strength	Cube 150×150×150 mm	28 days	Compression test
Early age crack tendency	Ring ø600/300×40 mm	5 hours	Wind drying
Early age crack tendency	Ring ø600/300×40 mm	2 days	Ordinary drying

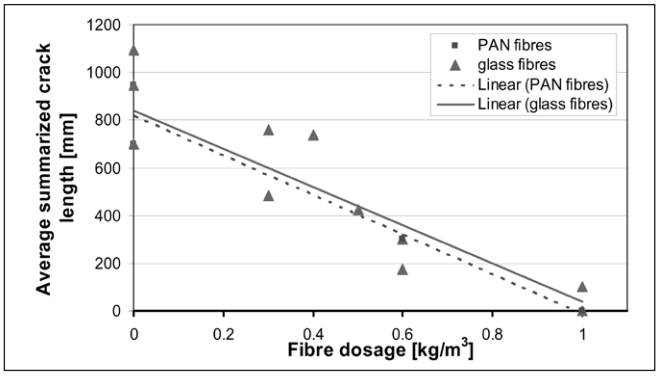

Fig. 12: *Average summarized crack lengths (of four specimens) of FRC made with glass and PAN fibres of 12 mm length after curing in tumbler-drier*

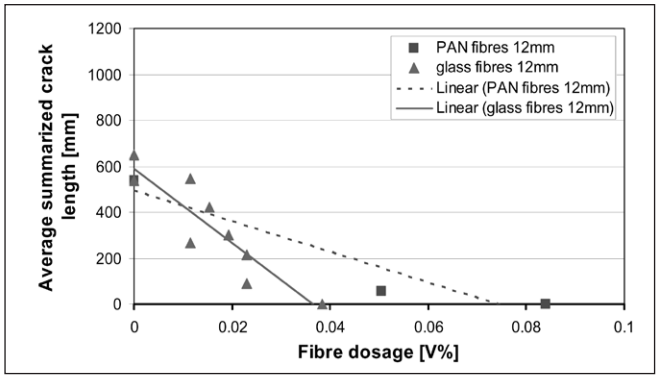

Fig. 13: *Average summarized crack lengths (of four specimens) of FRC made with glass and PAN fibres of 12 mm length after curing in wind tunnel*

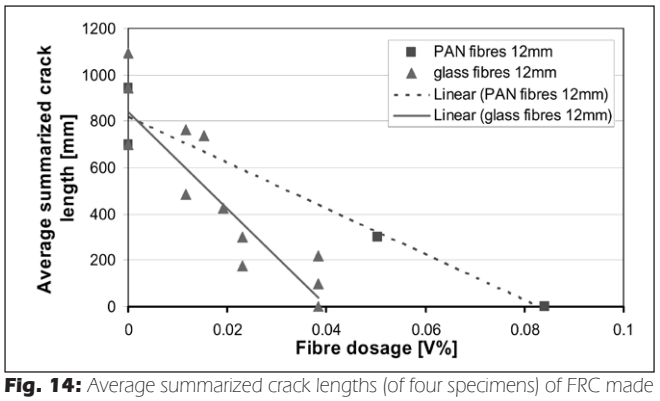

Fig. 14: *Average summarized crack lengths (of four specimens) of FRC made with glass and PAN fibres of 12 mm length after curing in tumbler-drier*

the tested PAN fibre is as effective as the glass fibre, because in one kg there are more pieces of fibre, but if we study real fibre effectiveness, glass fibre is better. The reason of this effect is the higher Young's modulus of glass fibres.

The specialty of the applied experimental method is that if we change the cement type or the aggregate, crack tendency is changing, so we can not compare our experimental results with findings that others measured in other laboratory with a different reference mix. If we repeat an experiment sequence of one fibre type with different mixture with different crack tendency and compare with the first sequence, the results will be different, as shown in *Figs. 15 and 16.* In these curves one point represents the average summarized crack length of

Table 3: *Classes of crack tendency according to Faserbeton Richtlinie (2002, 2008)*

Year	Classes	Average crack length [%]	
		Reference mixture	FRC mixture
2002	FS 1	100	60
	FS 2	100	20
2008	FS	100	20

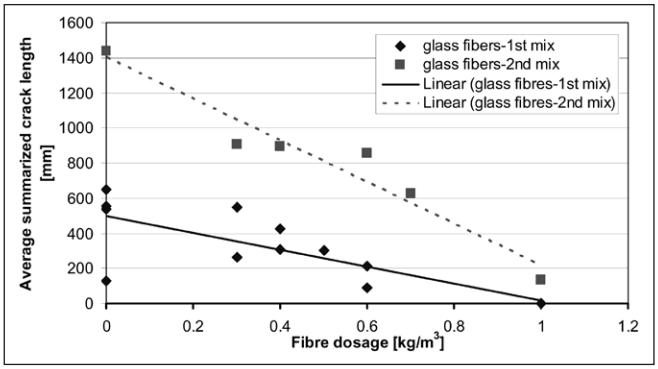

Fig. 15: *Average summarized crack lengths (of four specimens) of two mixes of FRC made glass fibres of with 12 mm length after curing in wind tunnel*

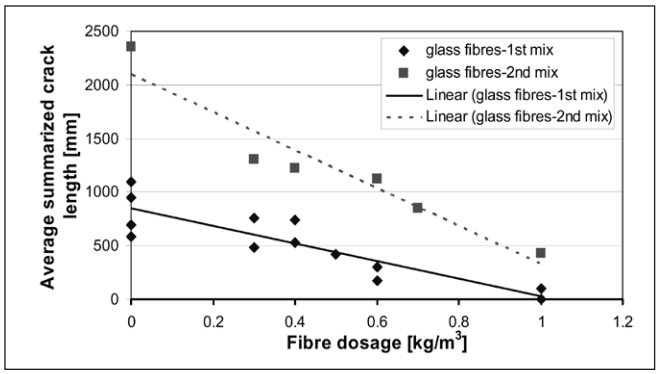

Fig. 16: *Average summarized crack lengths (of four specimens) of two mixes of FRC made with glass fibres of 12 mm length after curing in tumbler-drier*

four ring specimens. The reference mixtures (made without fibre reinforcement) have different crack tendency as the other sequence's reference mix had. If we compare the results of the two sequences, we can see that the two linear curves approach each other. This means that theoretically there is a significant point where the two lines are meeting. In our experiences we could not reach this point, because one of our lines had already reached the horizontal axis before crossing, so there were no cracks registered in case of the first mix, at the highest 1.0 kg/m^3 dosage of fibres. Further investigations are needed with a reference mix with higher crack tendency to reach this point where the lines are meeting. It could happen that we cannot reach this point, because the higher porosity of concrete caused by the higher fibre dosage will deform the linear curves or before this point every mixture will reach the zero crack length.

5. CONCLUSIONS

In this paper early age shrinkage cracking (caused by autogenous and drying shrinkage) of different fibre reinforced concretes (FRC) were investigated. Variable parameters were the type and the dosage of fibres. Four types of fibres were tested fabricated from glass, PAN and PP. To evaluate effectiveness of different types of fibres, a reference mix was produced without fibre reinforcement. To measure the early age shrinkage crack tendency ring test was used according to the Austrian fibre reinforced concrete technical specification described in Faserbeton Richtlinie (2002, 2008). For the ring test special specimens were fabricated and cured in wind tunnel in a climatic room according to the Austrian technical specification. The length of every crack caused by early age shrinkage was registered after the test. Further investigations were carried out by testing the specimens in standard tumbler-drier at 60 °C. Afterwards crack lengths were also registered.

– The relationship between fibre dosage and early age shrinkage crack tendency was found to be linear in case of every tested type of fibres. This means that if we apply a higher dosage of glass or polymer fibres in concrete, a lower crack tendency is reached.
– There is a significant difference between evaluating the results by dosage in kg/m^3 or in V%. If we evaluate the early age shrinkage crack tendency by V% (and the geometry of fibres is the same e.g. the tested PAN and glass fibres) we can see the real effectiveness of a fibre type. Estimating the dosages in V%, glass fibres are better than polymer fibres. But glass has higher density at the same time, so if we evaluate by the dosage of fibres in kg/m^3 that means more pieces of PAN fibres are compared with a few glass fibres.
– If we repeat our experiments with an other reference mix which has higher early age shrinkage crack tendency and compare the two resulted linear curves will be registered, they approach each other by ascendant dosage of fibres.
– As an additional result of our tests further investigations are needed by testing other types of fibres and higher dosages of the tested fibres to evaluate further relationships between early age shrinkage crack tendency and fibre reinforcement.

6. ACKNOWLEDGEMENTS

Authors wish to express their gratitude to Avers Ltd. and Baumbach Metall GmbH for giving free run of materials for present research; and to Csaba *Gyömbér (Djember)* for the important help in the laboratory works.

7. REFERENCES

Aly, T., Sanjayan, J. G., Collins F. (2008), "Effect of polypropylene fibers on shrinkage and cracking of concretes" *Materials and Structures* 22 January 2008 41:1741-1753

Aly, T., Sanjayan, J. G. (2009), "Shrinkage cracking of OPC-fiber concrete at early age" *Materials and Structures* 13 July 2009

Balázs, Gy., Borján, J., Cary Silva, J., Liptay, A., Zimonyi, Gy. (1979), "Crack tendency of cement" (A cement repedésérzékenysége) *Sci. publications* (Tudományos közlemények) in Hungarian, 1979 Budapest, HU ISSN 0324-3575

Balázs, Gy. L. – Lublóy, É., „Residual compressive strength of fire exposed fibre reinforced concrete" *Concrete Stuctures* 2007, ISSN 14196441

CEB (1992), CEB No. 183 „Durable Concrete Structures" - *Design Guide*; ISBN 978-0-7277-1620-0

EN 206-1 – **"**Concrete part 1.: specifications, performance, production and comformity" *European Code*

Faserbeton Richtlinie (2002), **„**Austrian fibre-concrete technical specification" 2002 March (in German) *Österreichische Vereinigung für Beton- und Bautechnik,* 63 p.

Faserbeton Richtlinie (2008), **„**Austrian fibre-concrete technical specification" 2008 (in German) *Österreichische Vereinigung für Beton- und Bautechnik,* 97 p.

Fenyvesi, O. (2006), „Early Age Shrinkage Cracking of Fibre Reinforced Lightweight Aggregate Concrete" Proceedings of 6th International PhD Symposium in Civil Engineering (Eds. T. Vogel, N. Mojsilovic, P. Marti), Zürich 23-26 August, 2006 pp. 1-8.

Grube, H. (2003), „Definitions of different types of shrinkage – concrete" (Definition der verschiedenen Schwindarten) – Beton, 2003/12 pp. 603

Józsa, Zs., Djember, C, Für Kovács, I., Seidl, Á. (2005), "Use of Glass and Synthetic Fibres Preventing Early Age Cracking of Normal and Lightweight Concrete" *Proc. 1st Central European Congress on Concrete Engineering,* 2006 Graz, Austria pp. 125-130.

Neville, A. M. (1995), "Properties of concrete" 1995 ISBN: 0-582-23070-5

Salah, A., Lange, D. A. (2001), "Creep, Shrinkage and Cracking of Restrained Concrete at Early Age" *ACI Materials Journal,* July-August 2001. pp. 323-331

Schmidt, M. (2005), „Baumbach Metall GmbH Product informations for PP fibers" (in German), BAUMBACH METALL GMBH

Shah, H. R., Weiss, J. (2006), "Quantifying shrinkage cracking in fiber reinforced concrete using the ring test" *Materials and Structures* RILEM online 20 September 2006 39:887-899

Wongtanakitcharoen, T., Naaman, A. E. (2006), "Unrestrained early age shrinkage of concrete with polypropylene, PVA, and carbon fibers" *Materials and Structures* RILEM online 10 November 2006 40:289-300

Olivér Fenyvesi (1981), MSc. in civil engineering (BME 2005). PhD Student at Budapest University of Technology and Economics Department of Construction Materials and Engineering Geology. Main fields of interest are the early age (autogenous and drying) shrinkage and early age shrinkage cracking in normal- and lightweight concretes, the FRC, fiber reinforced lightweight concretes, self compacting lightweight concretes, building diagnostics, building heritage. Member of Scientific Society of Silicate Industry (Concrete Division).

Zsuzsanna Józsa (1950) PhD, associate professor at the Department of Construction Material and Engineering Geology at Budapest University of Technology and Economics, architect, postgraduate diploma in building reconstruction. Her main fields of activities are lightweight aggregate concrete, non-destructive concrete testing, concrete corrosion and repair, thermal and moisture properties of materials, thermal insulation and water-proofing, roof tiles, wall construction, bricks and tiles, aerated concrete, environmental compatible building materials. She is member of IASS WG 18 "Environmental Compatible Structures and Structural Materials", Association for Building Biology, Hungarian Scientific Society of Building, Scientific Society of Silicate Industry, Hungarian Group of ***fib*****,** and is member of ***fib*** Commission 8 and earlier of TG 8.1: Lightweight aggregate concrete.

POTENTIALS IN CONCRETE MIX DESIGN TO IMPROVE FIRE RESISTANCE



György L. Balázs – Éva Lublóy – Sándor Mezei

Recent fire cases in tunnels (Mont Blanc, 20 March 1999, Gotthard 24 October 2001) and in highrise buildings indicated again the importance of fire research. Constructions materials suffer in fire. Deterioration of material characteristics and structural performance highly depends on the constituents and on the temperature history. Design for high temperatures requires additional aspects of material composition and material characteristics compared to design for ULS and for SLS. Purpose of our experimental study was to improve fire resistance of a typical thin-webbed-prestressed concrete roof girder. We carried out both material and beam tests to improve fire resistance. Test results all together indicated that modification of concrete compositions resulted in very considerable increase of fire resistance.

Keywords: fire, reinforced concrete, beam, slag, polypropylene fibres, fire test

1. INTRODUCTION

Concrete properties may be considerably influenced in case of high temperatures (Ingberg, et al. 1921; Hull, Ingberg, 1925). Modification of properties is a function of the maximum temperature and the composition of concrete: w/c, type of cement, type of aggregate, porosity (Schneider, 1986; Hinrichsmeyer, 1987; Bazant, Kaplan, 1996; Thielen, 1994; Gambarova, 2004; Hietanen, 2004; Balázs, Lublóy, 2009; Lublóy, Balázs, 2009).

Effects of high temperatures on the mechanical properties of concrete have been investigated as early as the 1940s (Schneider, 1986). In the 1960s and 1970s fire research was mainly directed to study the behaviour of concrete structural elements (Kordina, 1997). There was relatively little information on the concrete properties during and after fire (Waubke, 1997).

2. CONCRETE

Concrete is a composite material that consists mainly of mineral aggregates bound by a matrix of hydrated cement paste. The matrix is highly porous and contains a relatively large amount of free water unless artificially dried. When exposed it to high temperatures, concrete undergoes changes in its chemical composition, physical structure and water content. These changes occur primarily in the hardened cement paste in unsealed conditions. Such changes are reflected by changes in the physical and the mechanical properties of concrete that are associated with temperature increase.

Deterioration of concrete at high temperatures may appear in two forms: (1) local damage in the material itself (*Fig. 1*) and global damage resulting in the failure of the elements (*Fig. 2*).

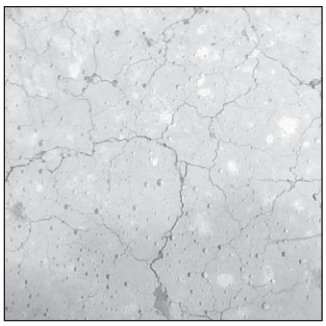

Fig. 1: Surface cracking after subjected to high temperatures

Fig. 2: Structural failure (http://www.polizia.ti.ch)

2.1 Deterioration of the material

Chemical changes in the structure of concrete can be studied with thermo-gravimetrical analyses (TG/DTG/DTA). The following chemical transformations can be observed by the increase of temperature. At around 100°C the weight loss indicates water evaporation from the micro pores. Dehydration of ettringite ($3CaOAl_2O_3 \cdot 3CaSO_4 \cdot 31H_2O$) occurs between 50°C and 110°C (Kopecskó, 2006). At 200°C further dehydration takes place which causes small weight loss in case of various moisture contents. The weight loss was different until the local pore water and the chemically bound water were gone. Further weight loss was not perceptible at around 250-300°C (Schneider, Weiss, 1977; Khoury, Grainger, Sullivan, 1985). During heating the endothermic dehydration of $Ca(OH)_2$ occurs between 450°C and 550°C ($Ca(OH)_2 \rightarrow CaO + H_2O\uparrow$; Schneider, Weiss, 1977). In case of concretes with quartz gravel aggregates another influencing factor is the crystalline conversion of quartz from α formation into β formation at the temperature of 573°C (Waubke, 1997). This transformation is followed by 5.7% volumetric increase. Dehydration of calcium-silicate-hydrates were found at the temperature of 700°C (Hinrichsmeyer, 1987).

The stress-strain relationships in *Fig 3.* shows changes in the ultimate stress and the ultimate strain of compressed fire exposed concrete.

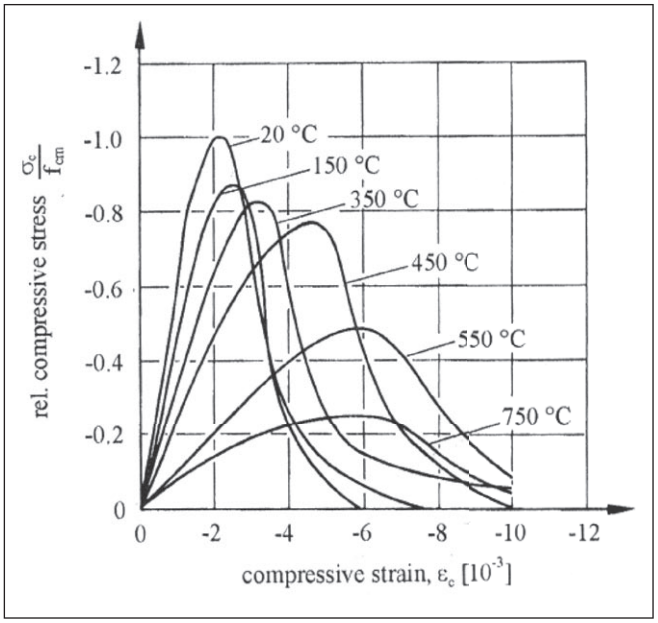

Fig. 3: Stress-strain relationships for concrete with quartz gravel aggregate as a function of temperature (Schneider, 1986)

In case of high strength concrete the strength reduction during and after fire can be different from that of normal strength concrete (Cheng, Kodurz, Wange, 2004; Dehn, 2008; Noumowé, Siddique, Ranc, 2009). As it has been already observed in previous studies, UHPC is more sensitive to fire compared to normal strength concrete (Schneider, 1994; Xiao, Falkner, 2006).

Compressive strength range of C60/70 to C100/115 N/mm^2 is generally considered as high strength (HSC) and strength above C100/115 N/mm^2 is considered as ultra high strength (UHSC). High strength concrete has a higher rate of reduction in residual compressive strength than normal strength concrete after being exposed to temperatures up to 400°C (Horiguchi, 2005). Test results by Khoury (1999) indicated that the residual strength of HSC concrete after thermal exposure is lower than its hot strength (*Fig. 4*).

Residual strength of steel fibre reinforced ultra high strength concrete (e.g. RPC) was found to be completely different (*Fig. 5*) (Khoury, 1999; fib, 2007). Reduction of hot strength was more pronounced compared to the post heating strength.

2.2 Deterioration of the structural performance

In case of fire in tunnels, in addition to the reduction of load bearing capacity, explosive spalling of concrete cover causes further difficulties. The probability of spalling of concrete cover increases by increasing the strength of concrete (Janson and Boström, 2004).

Spalling of concrete surfaces may have two reasons: (1) increased internal vapour pressure (mainly for normal strength concretes) and (2) overloading of concrete compressed zones (mainly for high strength concretes). The spalling mechanism of concrete cover is visualized in *Fig. 6*.

Special care is needed to avoid spalling of concrete cover. A group of experiments extended also to normal strength concrete suggested that the application of polymeric fibres considerably reduced the probability of spalling of concrete cover (Wille, Schneider, 2002; Dehn, Wille, 2004; Janson, Boström, 2004; Dehn, Werther, 2006).

Experiments with tunnel segments (span 11 m, height 2 m) carried out by Mörth, Haberland, Horvath and Mayer (2005)

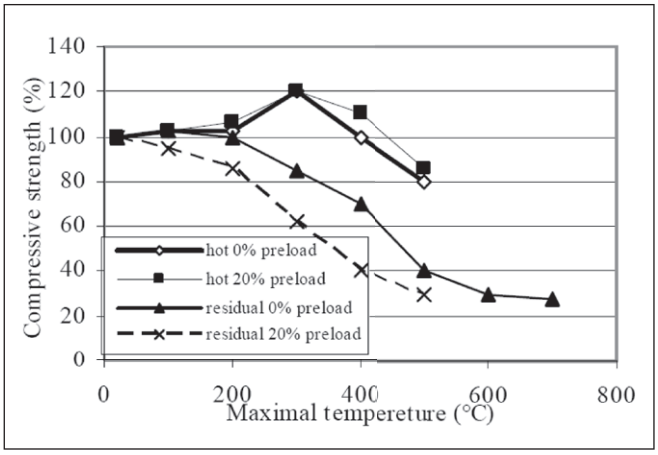

Fig. 4: Modification of strength of high strength concrete subjected to high temperatures (fib, 2007)

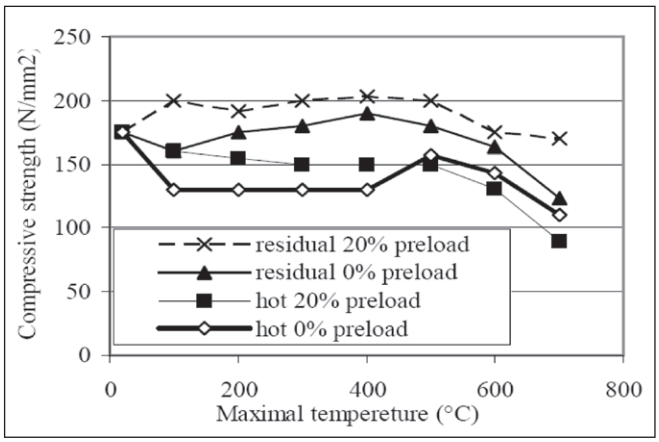

Fig. 5: Modification of strength of steel fibre reinforced ultra high strength concrete subjected to high temperatures (fib, 2007)

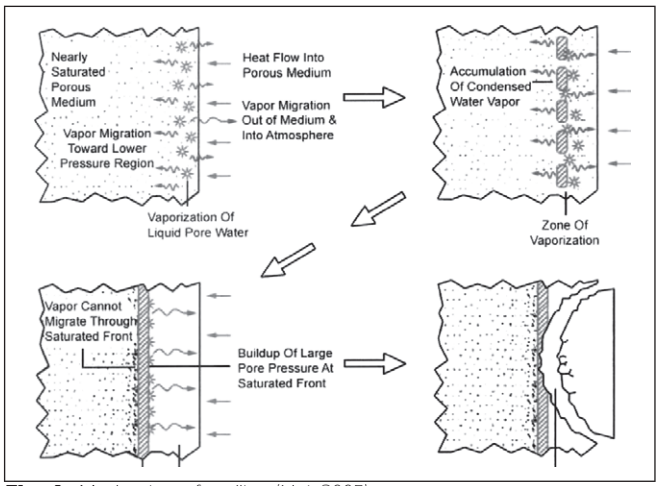

Fig. 6: Mechanism of spalling (Høj, 2005)

indicated that the cover the polypropylene fibre reinforced concrete with 2 kg/m^3 synthetic fibres did not spall up to 1200°C temperature. In Austria a group of researchers (Walter et al., 2005) had the same findings (*Fig. 7*).

The tested reinforced concrete slabs were loaded in their planes. Spalling of concrete cover developed in case of the conventional reinforced concrete slabs without polymeric fibres. However, spalling was not observed in slabs made with 1 to 3 V% polypropylene fibres. Silfwerbrand (2005) suggested that application of polypropylene fibres is preferable also for high strength concrete.

Utilisation of polypropylene fibres does not only reduce the probability of spalling of concrete cover but it may reduce the residual compressive strength (Dehn, König, 2003). Horiguchi,

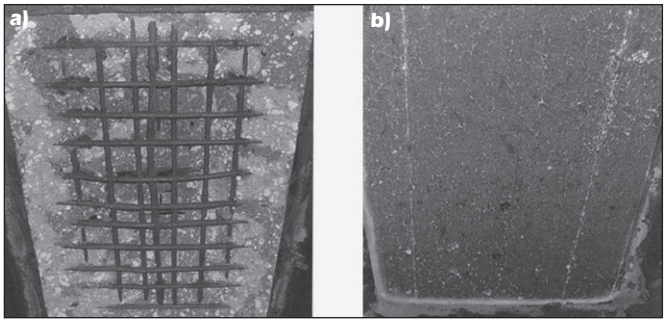

Fig. 7: Surface of the slabs after 2-hour fire exposure (Walter, Kari, Kutserle, Lindlbauer, 2005)
a) without fibre reinforcement
b) with 2 kg/m³ synthetic fibre reinforcement

(2004; 2005) experimentally proved on cylinders (∅=100 mm, ℓ=200 mm) that the addition of polymeric fibres increased the residual compressive strength. Specimens were heated by 10°C/minute rate up to 200°C or 400°C, then kept for 1 hour at high temperature, and finally tested at room temperature

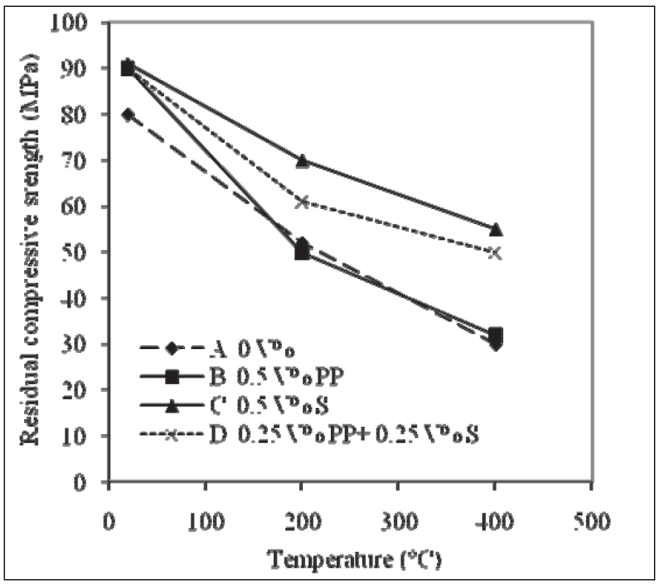

Fig. 8: Residual compressive strength of high strength concrete with or without fibres (Horiguchi, 2005)

(Fig. 8). The water to cement ratio was 0.3 (with 583 kg/m³ cement and with 175 ℓ water). Mix A: prepared without fibres, Mix B: with 0.5 V% polypropylene fibres, Mix C: with 0.5 V% steel fibres, Mix D: with 0.25 V% polypropylene and 0.25 V% steel fibres.

3. OUR EXPERIMENTAL STUDIES

Purpose of our experimental study was to improve fire resistance of a typical thin-webbed prestressed concrete roof girder. Owing to the small thickness of the web (*Fig. 11),* special considerations were needed to modify the composition of the concrete mix. The reference concrete grade was C50/60.

3.1 Testing of material properties

Preliminary fire tests indicated inadequate fire resistance of the typical thin-webbed (60 mm, thickness), prestressed roof girder. The self-compacting concrete (SCC) mix included limestone as filling material. Cement type was CEM I 42.5 N. The applied composition and the very low thickness of the web resulted in early spalling of concrete cover.

In order to be able to improve the fire resistance of the concrete mix as well as that of the girder, our intention was directed to optimize the concrete mix without changing the geometry of the girder. Therefore, we decided to modify the concrete composition in two steps as follows:

1. changing the filling material from limestone to slag,
2. adding polypropylene fibres to the mix (1 kg/m³ or 2 kg/m³ (*Table 1*).

Table 1: Test parameters (all other parameters were the same for the mixes)

Concrete mix	filling material	PP fibres	material test 20°C, 600°C, 800°C	beam test
Mix 1 (reference)	limestone	0 kg/m³	+	+
Mix 2	limestone	1 kg/m³	+	-
Mix 3	limestone	2 kg/m³	+	+
Mix 4	slag	1 kg/m³	+	+

Material tests were carried out on 150 mm cube specimens kept for two hours on 600°C or 800°C then cooled down to room temperature. The material tests were carried out at the Department of Construction Materials and Engineering Geology of Budapest University of Technology and Economics.

3.1.1 Tests with the reference mix

In case of our reference mix (Mix 1) a special type of failure occurred during the heating process within the temperature range of 600 to 800°C (*Fig. 9. a*). Some corners of the cube specimens cracked off. This phenomenon could be explained by the stress concentrations in corner regions due to the high temperatures. Stress concentrations in the corners may resulted in deterioration of the structural performance of an element or possible spalling of concrete cover.

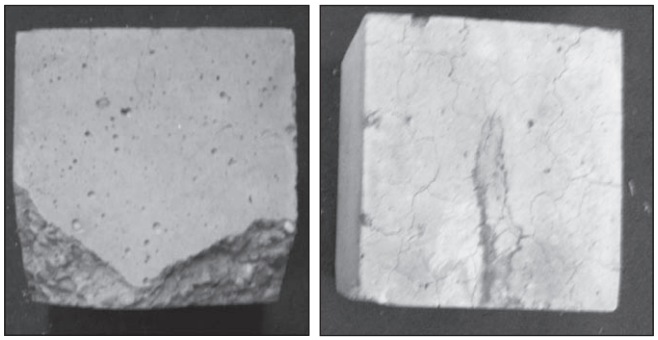

Fig. 9: Concrete surfaces kept at 800°C for two hours and then cooled down. a) Reference mix (Mix 1) b) mix with 1 kg/m³ PP fibres (Mix 2)

3.1.2 Tests with mixes containing PP fibres

By addition of 1 kg/m³ polypropylene fibres, failure of the specimen (corner cracking) did not occur, however, surface cracking was observed (*Fig. 9. b*).

By further increase of fibre content up to 2 kg/m³ PP fibres, the relative residual compressive strength decreased by about 8% (*Fig. 10*).

3.1.3 Tests with mixes containing slag as filler

We have observed the highest relative residual compressive strength by changing the filling material from limestone to slag and including 1 kg/m³ polypropylene fibres (*Fig. 10*), subjected to 800°C.

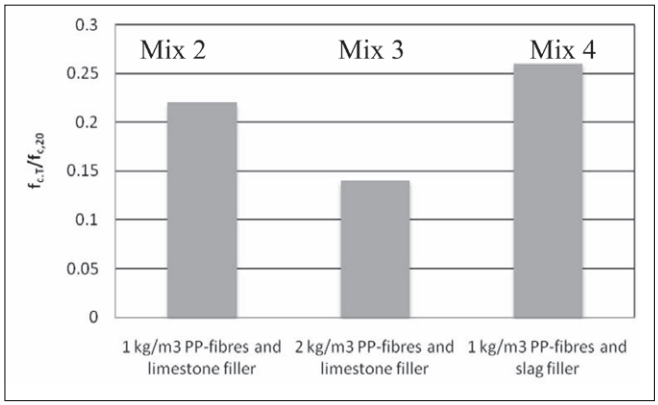

Fig. 10: *Measured relative, residual compressive strengths for tested concrete mixes heated on 800°C for two hours and cooled down (every column is an average of 3 measurements, relative values are related to measured on at 20°C)*

3.2 TESTS WITH BEAMS

Fire tests on prestressed beam specimens were carried out with mixes 1, 2 and 4 (*see Table 1*), in Fire Laboratory of ÉMI Non-Profit Ltd. The heating curve for the furnace was the following:

$$T = 345 \cdot \lg(8t + 1) + 20$$

where
T is the average furnace temperature (°C)
t is the time (min).

The specimens were kept for 90 days in laboratory conditions before testing.

The temperature increase was controlled by thermometer during the heating process.

The length of beams was 3.4 m. The prestressing force was 130 kN. Each beam was loaded with P=2 × 350 kN during the fire test *(Fig. 11.)*.

The test beam with reference mix (Mix 1) failed in 12 minutes owing to the complete spalling of concrete cover of the web (*Fig. 12*).

The test beam with Mix 2 including 1 kg/m^3 polypropylene fibres failed in 42 minutes in shear (without spalling of concrete cover).

Fig. 12: Beam with the reference

Fig. 13: Beam with Mix 4 after failure concrete (Mix 1) after failure

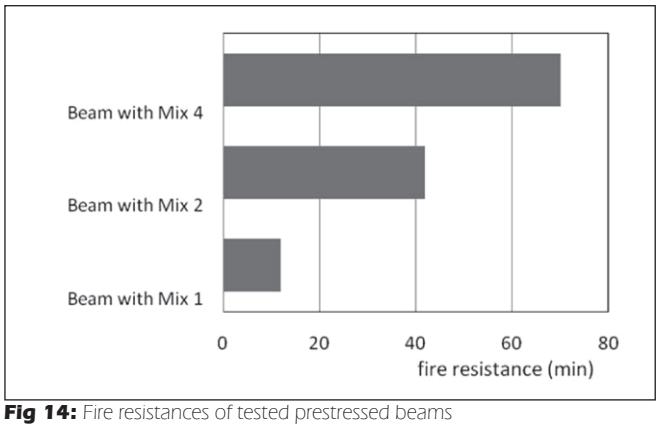

Fig 14: Fire resistances of tested prestressed beams

The test beam with Mix 4 including 1 kg/m^3 polypropylene fibres and slag as filling material instead of limestone failed in 67 minutes in shear (without spalling of concrete cover *Fig. 13*)

Fig. 11: *Tested beam specimens*
a) Cross - section of beams b) Side view of beams

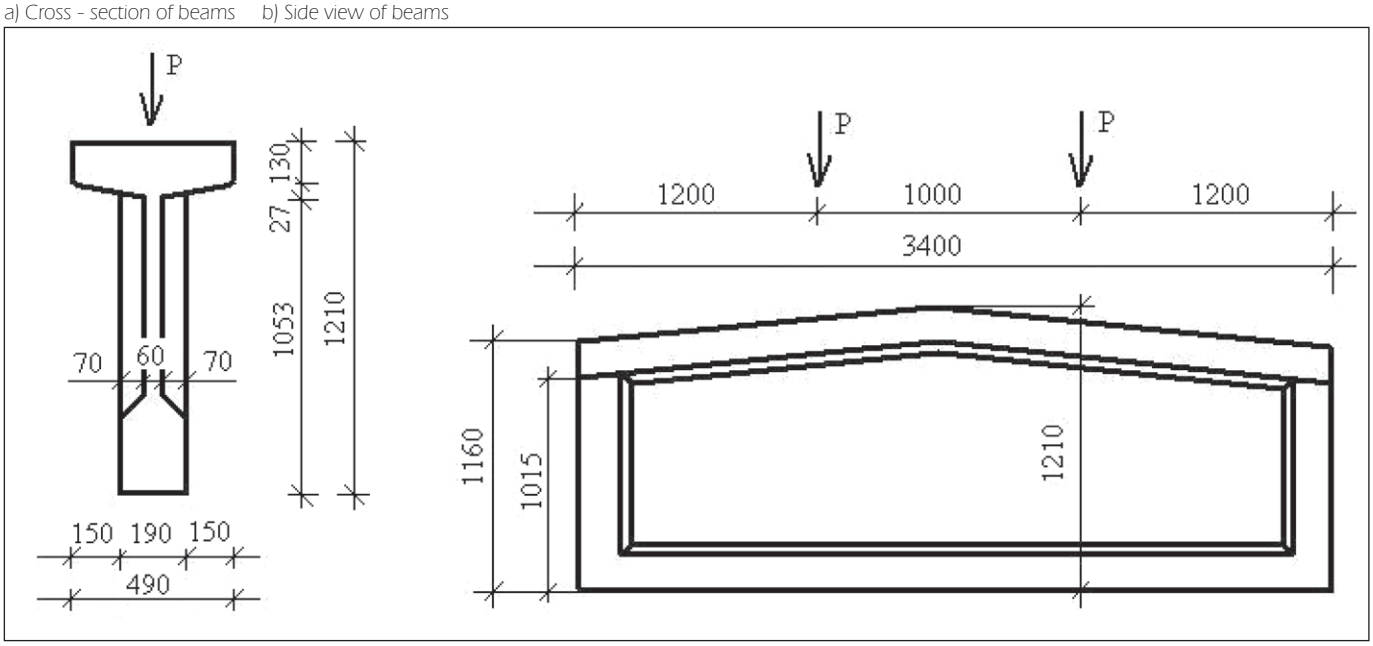

The considerably improving fire resistances for the applied concrete mixes is presented in *Fig. 14.*

4. CONCLUSIONS

Concrete is a composite material, that consists mainly of mineral aggregates bound by a matrix of hydrated cement paste, and may suffer in fire. The matrix is highly porous and contains a relatively large amount of free water unless artificially dried. When exposed it to high temperatures, concrete undergoes changes in its chemical composition, physical structure and water content. These changes occur primarily in the hardened cement paste in unsealed conditions. Such changes are reflected by changes in the physical and the mechanical properties of concrete that are associated with temperature increase. Deterioration of material characteristics and structural performance highly depends on the constituents and the temperature history. In order to understand the complex phenomenon observed in concrete due to high temperatures an extensive test was carried out. We intended to study the effect of different filling materials and various amounts of polypropylene fibers. Our activity induded both material tests and beam tests subjected to high temperatures.

1. Results of material tests

In case of reference mix (Mix 1) cube specimens failed during the heating process within the temperature range of 600 to 800°C. By addition of 1 kg/m^3 polypropylene fibres, failure of the specimen (spalling of corners) did not occur, however, surface cracking was still observed. After two hours of fire exposure at 800°C and a subsequent cooling down process the highest relative residual compressive strength as well as the minimum amount of surface cracking was observed by changing the filling material from limestone to slag and including also 1 kg/m^3 polypropylene fibres, subjected to 800°C.

2. Results of beam tests

Test beam with reference mix (Mix 1) failed in 12 minutes owing to the complete spalling of concrete cover of the web. Test beam with Mix 2 including 1 kg/m^3 polypropylene fibres failed in 42 minutes in shear (without spalling of concrete cover). Test beam with Mix 4 including 1 kg/m^3 polypropylene fibres and slag as filling material failed in 67 minutes in shear (without spalling of concrete cover).

Test results indicated very considerable increase in fire resistance of a structural element just by the modification of the concrete composition.

5. REFERENCES

Balázs L. Gy., Lublóy É. (2009), „*Influence of high temperatures on constituents of concrete structures*" *VASBETONÉPÍTÉS* 2009/2, pp. 48-54

Bazant, P. Z., Kaplan, F. M. (1996), „*Concrete at High temperatures: Material properties and mathematical models*" ISBN: 0-582-08626-4, Longman Group Limited, Harlow

Cheng, F. P., Kodurz, V. K. R, Wange, T. C. (2004), „ *Stress-strain curves for high strength concrete at elevated temperatures*" *Journal of Materials in Civil Engineering* 16 (1) pp. 84-90

Dehn, F. (2008), " *Use of synthetic fibres for fire resistant tunnel concretes– summary of general requirements*", *Proceedings of International RILEM Symposium on Fibre Reinforced Concretes,* BEFIB 2008 17-19 September, Chennai, India (Ed.: Gettu, R.), pp. 631-640

Dehn, F., Wille, K. (2004), " *Micro analytical investigations on the effect of polypropylene fibres in fire exposed high performance concrete (HPC)*", *Proceedings of International RILEM Symposiumon Fibre Reinforced Concretes,* BEFIB 2004 20-22 September, Varenna, Italy (Eds. Prisco, M., Felicetti, R. Plizzari, G. A), pp. 659-678

Dehn, F., Werther, N. (2006), *„Fire tests on tunnel elements for M 30 tunnel in Madrid"* („*Brandversuche an Tunnelinnenschalenbetonen für den M 30- Nordtunnel in Madrid*"), *Beton und Stahlbetonbau*, 101/9, Berlin, ISSN 0005-9900 (in German)

Felicetti, R., Meda, A. (2005), "*Residual behaviuor of reinforcing steel bars after fire*", Proceedings of Keep Concrete Attractive. Hungarian Group of fib, 23 - 25 Mai 2005, Budapest University of Technology and Economics, Budapest,: 2005, pp.: 1148-1156, ISBN 963 420 837 1

fib (2007), "*Fire design of concrete structures- materials, structures and modelling*", fib bulletin 38, ISBN: 978-2-88394-078-9

Gambarova, G. P. (2004). "*Opening Adresses on Some Key Issues Concerning R/C Fire Desing*", *Proceedings for Fire Design of Concrete Structures: What now?, What next?,* December 2-3, 2004, (Eds.: Gambarova, P. G., Felicetti, R., Meda, A., Riva P.), Milano

Hietanen, T. (2004), "*Actuale State of the Codes on Fire Design in Europe*", *Proceedings for Fire Design of Concrete Structures: What now?, What next?*, December 2-3, 2004 (Eds.: Gambarova, P.G., Felicetti, R., Meda, A., and Riva P.), Milano

Hinrichsmeyer, K. (1987), „*Analysis and Modelling of Concrete deterioration due to high temparatures*", („*Strukturorientierte Analyse und Modellbeschreibung der thermischen Schädigung von Beton"),* 74 IBMB, Braunschweig, (in Gerrman)

Høj, N. P.(2005), Keep concrete attractive - Fire design of concrete structures, *Proceedings of fib symposium on Keep concrete attractive*, edited by Gy. L. Balázs, A. Borosnyói , 23-25 May 2005 Budapest, pp.1097-1105

Horiguchi, T. (2004), "*Fire resistance of hybrid fibre reinforced high strength concrete*", *Proceedings of International RILEM Symposiumon Fibre Reinforced Concretes,* (Eds. Prisco, M., Felicetti, R. Plizzari, G. A), pp. 1-18

Horiguchi, T. (2005), "*Combination of Synthetic and Steel Fibres Reinforcement for Fire Resistance of High Strength Concrete*", *Proceedings of Central European Congress on Concrete Engineering* 8-9 Sept. 2005 (Ed.: Pauser, M), Graz, pp. 59-64.

Hull, W. A., Ingberg, S. H. (1925), „*Fire resistance of concrete columns*" *Journal of the Franklin Institute*, Volume 200, Issue 3, September 1925, pp. 379-381

Ingberg, S. H., et al. (1921), *„Fire tests of building columns" Journal of the Franklin Institute*, Volume 191, Issue 6, June, 1921, pp. 823-827

Janson, R., Boström, L. (2004), "*Experimental investigation on concrete spalling in fire*", *Proceedings for Workshop on Fire Design of Concrete Structures: What now?, What next?,* December 2-3, 2004, Milano, (Eds. P.G., Gambarova, R., Felicetti, A., Meda, P., Riva), pp. 2-42

Khoury, G. A. (1999), "*Mechanical behaviour at high temperature in compression*", *HITECO Report*, Imperial College, August, 1999, 72 p.

Khoury, G. A., Grainger, B. N., Sullivan, P. J. E. (1985), "*Transient thermal strain of concrete: literature review, conditions within specimen and behaviour of individual constituents*", Magazine of Concrete Research, Vol. 37, No. 132, 1985 pp. 37-48.

Kopecskó K. (2006), Cementklinkerek és cementek kloridion megkötő képessége, PhD thesis, BME

Kordina, K. (1997), „Fire resistance of reinforced concrete beams" (Über das Brandverhalten punktgeschützter Stahlbetonbalken), Deutscher Ausschuss für Stahlbeton, Heft 479, ISSN 0171-7197, Beuth Verlag GmbH, Berlin, 1997.

Lublóy É., Balázs L. Gy., (2009), *„Influence of high temperatures on concrete structures" VASBETONÉPÍTÉS* 2009/4, pp. 113-119

Mörth, W., Haberland, Ch., Horvath, J. and Mayer, A. (2005), „*Behaviour of Optimized Tunnel Concrete with Special Aggregates at High Temperature*", *Proceedings of Central European Congress on Concrete Engineering,* 8-9 Sept. 2005, (Ed. Michael P.), Graz, pp. 41-50.

Noumowé, A., Siddique, R., Ranc, G. (2009), „ *Thermo-mechanical characteristics of concrete at elevated temperatures up to 310°C*", *Nuclear Engeneering and Desig*n, Vol. 239, pp. 470-476

Schneider, U., (1986), „*Properties of Materials at High Temperatures*" *RILEM Publ*., 2nd Edition, Gesamthochschule Kassel, Universität Kassel

Schneider, U., Lebeda C., (2000), „*Fire protection of engineering structures*", („*Baulicher Brandschutz*"), ISBN 3-17-015266-1 W. Kohlhammer GmbH, Stuttgart

Schneider, U. ,Weiss, R. (1997), „*Kinetische Betrachtungen über den thermischen Abbau zementgebundener Betone und dessen mechanische Auswirkungen*", Cement and Concrete Research, Vol 11, 1997, pp. 22-29

Silfwerbrand, J. (2005), "*Guidelines for preventing explosive spalling in concrete structures exposed to fire*", *Proceedings of Keep Concrete Attractive*, Hungarian Group of ***fib***, 23-25 Mai 2005, (Eds. Balázs, L. Gy; Borosnyói, A.), ISBN 963 420 837. , pp. 1142-1147

Thielen, K. Ch. (1994), „*Strength and Deformation of Concrete Subjected to high Temperature and Biaxial Stress-Test and Modelling*" (Festigkeit und Verformung von Beton bei hoher Temperatur und biaxialer Beanspruchung - Versuche und Modellbildung), *Deutscher Ausschuss für Stahlbeton*, Heft 437 Beuth Verlag GmbH, Berlin

Walter, R., Kari,. H., Kusterle, W., Lindlbauer, W. (2005), „*Analysis of the*

Load-bearing Capacity of Fibre Reinforced Concrete During Fire", *Proceedings of Central European Congress on Concrete Engineering* 8-9 Sept. 2005, (Ed. Michael P.), Graz, pp. 54-59.
Waubke, N. V. (1997), „*Physical analysis of strength reduction of concrete up to 1000 °C*" (Úber einen physikalischen Gesichtspunkt der Festigkeitsverluste von Portlandzement−betonen bei Temperaturen bis 1000 °C−Brandverhalten von Bauteilen), *Dissertation,* TU Braunschweig, 1973
Wille, K., Schneider H. (2002), „Investigation *of fibre reinforced High Strength Concrete (HSC) under fire, particularly with regard to the real behaviour of polypropylene fibers"* Lacer Nr. 7 pp. 61-70
Xiao, J., Falkner, H., (2006), „*On residual strength of high-performance concrete with and without polypropilene fibres at elevated temperatures*" *Fire Safety Journal*, 41, pp. 115-121

György L. Balázs, professor in structural engineering, at the Budapest University of Technology and Economics. His main fields of activities are: experimental and analytical investigations as well as modelling of reinforced and prestressed concrete, fiber reinforced concrete (FRC), fiber reinforced polymers (FRPs) for concrete structures as internal or external reinforcements, bond and cracking in concrete, durability and fire resistance of concrete structures. He is convenor of ***fib*** Task Groups on "Serviceability Models" and "Dissemination of knowledge" as well as he is a member of several other ***fib*** Task Groups or Commissions. He is Deputy-President of ***fib*** for 2010 and 2011 and Head of the Hungarian Group of ***fib***.

Éva Lublóy, professor assistant in structural engineering, at the Budapest University of Technology and Economics. Her main fields of interesting are: fire design, behaviour of constructions materials at elevated temperature. Member of the Hungarian Group of ***fib.***

Sándor Mezei (1979) PhD student at Department of Construction Materials and Engineering Geology at the Budapest University of Technology and Economics. Simultaneously, he is working at the Scientific Department for Fire Protection at the Non-profit Ltd. for Quality Control and Innovation in Building (ÉMI). His main fields of interest are: fire design and behaviour of structures at elevated temperatures. He is a member of the Hungarian Group of ***fib***.